EXAMINATION OF EUKARYOTIC CHAPERONIN-MEDIATED

NASCENT CHAIN FOLDING IN THE CYTOSOL: A

PHOTOCROSSLINKING APPROACH

A Dissertation

by

STEPHANIE ANNE ETCHELLS

Submitted to the Office of Graduate Studies of
Texas A&M University
in partial fulfillment of the requirements for the degree of

DOCTOR OF PHILOSOPHY

August 2003

Major Subject: Biochemistry

EXAMINATION OF EUKARYOTIC CHAPERONIN-MEDIATED

NASCENT CHAIN FOLDING IN THE CYTOSOL: A

PHOTOCROSSLINKING APPROACH

A Dissertation

by

STEPHANIE ANNE ETCHELLS

Submitted to Texas A&M University
in partial fulfillment of the requirements
for the degree of

DOCTOR OF PHILOSOPHY

Approved as to style and content by:

Arthur E. Johnson (Chair of Committee)	Gregory D. Reinhart (Member)
Hagan P. Bayley (Member)	Gregory D. Reinhart (Head of Department)
Ryland F. Young (Member)	

August 2003

Major Subject: Biochemistry

ABSTRACT

Examination of Eukaryotic Chaperonin-Mediated Nascent Chain Folding in
the Cytosol: A Photocrosslinking Approach. (August 2003)

Stephanie Anne Etchells, B.Sc.H., Queen's University

Chair of Advisory Committee: Dr. Arthur E. Johnson

TRiC (TCP-1 ring complex), a type II chaperonin, facilitates protein
folding, and we previously showed that TRiC crosslinks to ribosome-bound
actin and luciferase nascent chains. Here, it was found that actin and
luciferase nascent chains were adjacent to more than one TRiC subunit at
different stages of translation. Six and seven out of the eight TRiC subunits
were photocrosslinked to the luciferase and actin nascent chains,
respectively. Actin nascent chains with widely-spaced, site-specific probe
locations were adjacent to the same three TRiC subunits (α, β and ε) at
different stages of translation. The exposure of other TRiC subunits to
nascent chains varied with the length and identity of the nascent chain. In
addition, the presence or absence of ATP influences the photocrosslinking
yields. This suggests that ATP alters the conformation of the subunits
and/or their affinity for the nascent chain. Photocrosslinking also revealed
that TRiC is in close proximity to the exit site of the ribosomal tunnel,
presumably to create a protected folding environment for the nascent
chain.

Immunoprecipitations under native conditions revealed that prefoldin photocrosslinks to the actin nascent chain and that these prefoldin-containing photoadducts are coimmunoprecipitated with antibodies specific for the TRiC α subunit. This result suggests that prefoldin and TRiC bind simultaneously to the same actin nascent chain. Photocrosslinking studies with probes at position 68 in the actin nascent chain revealed that prefoldin binds to the nascent chain subsequently to TRiC binding.

An unknown protein with an apparent molecular mass of 105 kDa was shown to photocrosslink to the luciferase nascent chain in a length-dependent manner at specific probe locations close to the N-terminus of the nascent chain.

Thus, the nascent chain sees a variety of proteins in its immediate environment as it emerges from the ribosomal tunnel and undergoes its chaperonin-assisted folding.

ACKNOWLEDGMENTS

for teaching me spiritual gifts and sending lots of care packages when I needed to sit down on the road. Megan, I thank you letting me try out my teaching skills on you and for your great encouragement and reminding me that no matter what "I was still your sister". Abner, I thank you for always having an encouraging word to say.

Last but not least I would like to thank all the people whom it was my honor to work with in the Johnson Lab (Yiewi and Yuan the fabulous technicians, Hung, Tina, Michael, Bruce, Alejandro, Andrey, Cheryl, Nora, Nathan, Mingyang, Shuren, Jialing, Brian, Chen, Sub, Kakoli, IngMarie, John, Bixia, Kathy, Heidi, Holly, Peter, Rajesh, Kristen, Lindsey, Judith, Lisa Eubanks, Suraj, and Judit). Thank you Dr. Johnson for not giving up on me, and persevering as I grew as a scientist and person. Thank you for providing excellent scientific criticism so that my work might be "bulletproof" and for developing my teaching and speaking skills. Thank you to my Ph.D. committee members (Dr. Hagan P. Bayley, Dr. Ryland F. Young, and Dr. Gregory D. Reinhart) and to those who helped me through the Graduate Teaching Academy (Dr. Martin Gunn and Dr. James F. Amend).

Thanks to all who have made this seven-year odyssey such a great learning experience.

TABLE OF CONTENTS

CHAPTER   Page

LIST OF FIGURES

FIGURE   Page

LIST OF TABLES

CHAPTER I

INTRODUCTION

Synthesis of Cytosolic Proteins in the Cell

Inside the cell, the information for making a protein is encoded in a gene in double-stranded DNA. The linearly encoded gene is transcribed into a linear strand of RNA, which is processed and becomes messenger RNA (mRNA). The mRNA is translated into a polypeptide chain which is a linear polymer of amino acids. The polypeptide folds to take on a three dimensional shape, as it becomes a functional protein. Cytosolic proteins are translated in an aqueous environment by riboprotein complexes called ribosomes. Newly synthesized polypeptide chains, exit the ribosome through the ribosomal exit tunnel and enter the cytosol, where folding may begin. It is at this early stage of the folding of these cytosolic proteins that will be the focus of this dissertation.

Defining Molecular Chaperones

Lasky et al. first used the term molecular chaperone in 1978 when describing how a protein called nucleoplasmin was necessary for the

_____

This dissertation follows the style and format of Cell.

correct assembly of nucleosome cores from DNA. The nucleoplasmin was shown to bind transiently to reduce the positive charge density of the histones and thus lessen the likelihood of their forming inappropriate aggregates with the negatively charged DNA backbone. Molecular chaperones are defined as " a class of unrelated families of protein that have in common the ability to assist the noncovalent assembly of other protein-containing structures *in vivo*, but which are not permanent components of these structures when they are performing their normal biological functions" (Ellis, 1990a; Ellis, 1990b; Ellis, 1993; Ellis and Hemmingsen, 1989) Another definition is a "protein that binds to and stabilizes an otherwise unstable conformer of another protein, and by controlled binding and release of the substrate protein facilitates its correct fate *in vivo*, be it folding, oligomeric assembly, transport to another subcellular compartment or controlled switching between active and inactive conformations" (Hendrick and Hartl, 1993). Both of these definitions agree about the fact that chaperones assist in getting a protein from a non-functioning structure to a functioning structure. The former definition would have it that protein disulfide isomerase (PDI), which binds to proteins, isomerizes their disulfide bonds and can helping assist folding, would only be considered a chaperone when the protein was doing the later and not the former. Since there are no common structural motifs that all proteins currently called chaperones contain, the definition of a

chaperone is a functional definition and not a structural definition. This is similar to the functional definitions used to classify a protein as an enzyme. Chaperones can also exist in large complexes called chaperonins. It is the chaperonins that we will be defining next and will be the main focus of the remainder of the introduction.

Defining Chaperonins

Chaperonins are multiprotein complexes of related chaperone proteins which have a characteristic bi-toroidal double ring structure and which are involved in the noncovalent folding of proteins into their functional structures.

There are currently two families of chaperonins, referred to as type I and type II. These classifications are based on whether or not a co-chaperonin is needed. Type I chaperonins are found in prokaryotes, mitochondria and chloroplasts and they need a co-chaperonin complex in order to fold native proteins. Examples of type I chaperonins are the heat shock proteins named Hsp60, GroEL, and their respective co-chaperonins Hsp10 and GroES. Type II Chaperonins are found in eukaryotes and are named TRiC (TCP-1 ring complex) or CCT (chaperonin containing TCP-1, where TCP-1 stands for t-complex peptide 1). Archaea also have a type II chaperonin called the thermosome.

History of Chaperonin Discovery

Eight years after Lasky's observation about nucleoplasmin,

Musgrove and Ellis discovered a protein that was needed to help in the

assembly of large subunits of the photosynthetic carbon dioxide-fixing

enzyme ribulose-bisphosphate carboxylase/oxygenase (Rubisco), which is

found in chloroplasts. This new protein was called the Rubisco subunit

binding protein (RSBP) (Barraclough and Ellis, 1980). The idea that RSBP

was a chaperone was not received with enthusiasm by the scientific

community due in large part to its contradiction of one of the key theories at

the time. Since Anfinsen had already shown that proteins could

spontaneously fold (Anfinsen, 1973) and Caspar and Klug (Caspar, 1962)

showed they could self-assemble into functional structures, what would be

the need for molecular chaperones? Over time many more papers were

published observing proteins that needed "helper" proteins to fold correctly

or to form large multimeric complexes. The idea that chaperones might be

a universal phenomenon was strengthened when it was shown that RSBP

was found to have 50% amino acid identity with GroEL, a protein from the

prokaryote *E. coli.* Although the GroEL protein had been found in 1973 as

a common antigen found in many bacterial infections, and was necessary

for the assembly of bacteriophages such as lambda, it was not known to be

a chaperone. GroEL was named for the phage mutation that overcame the

"gro" or growth defect and it was mapped to the E gene. L was for the large

gene, and S as in GroES was for the small gene (Tilly et al., 1981). New experiments done in the presence of GroEL, repeating those seminal ones done by Anfinsen showed that proteins were folded in an ATP dependent manner with more efficiency in the presence of GroEL (Martin et al., 1991). This showed scientists that just because a protein can fold spontaneously *in vitro,* one cannot assume that it will fold spontaneously *in vivo.* After finding GroEL in prokaryotes and the Rubisco binding protein in chloroplasts, a homologous binding protein was found in mitochondria. The focus was then turned to eukaryotes to determine if they also had a protein complex that acted as a chaperone.

The discovery of type II chaperonins was an accident. A massive release of toroidal particles composed of two stacked octameric rings was seen when archaeal *Pyrodictium* cells were accidentally heat shocked and lysed on an electron microscopy grid (Phipps et al., 1991). Upon further investigation it was found that this complex, called the thermosome, was able to hydrolyze ATP. Later in 1991 another discovery of a similar 9-fold toroidal complex of two stacked rings was made in the thermophilic archaea *Sulfolobus shibatae* (Trent et al., 1991). The 55-kDa protein subunit of these rings was named TF55. No significant sequence homology was found between TF55 and GroEL using the program 'Relate' (Trent et al., 1991). These two sequences were then compared to a eukaryotic protein TCP-1 (t-complex polypeptide) of unknown function (Gupta, 1990),

and it was shown that there was significant sequence homology between TRiC and TF55 but not TRiC and GroEL (Trent et al., 1991). In 1979 Silver *et al.* found a mouse TCP-1(Silver et al., 1979). In 1992, two groups simultaneously found that TCP-1 was part of a 970 kDa oligomeric complex (Frydman et al., 1992; Lewis et al., 1992). When the purified TRiC complex was resolved on SDS-PAGE, it was discovered that the complex was composed of many proteins between 52-60 kDa in size (Lewis et al., 1992) and one of the proteins was TCP-1 (Yaffe et al., 1992). Using both rabbit reticulocyte lysate and purified TRiC from bovine testis, it was shown that the 900kDa complexes were composed of eight proteins (Rommelaere et al., 1993). Trypsin digestion and partial sequencing of peptides from each of the eight proteins revealed that one was TCP-1 and the other seven were in a related family (Kubota et al., 1994; Kubota et al., 1995a; Kubota et al., 1995b). These subunits were called TRiC α, TRiC β, TRiC γ, TRiC δ, TRiC ϵ, TRiC θ, TRiC ζ, and TRiC η. Using Northern blot analysis, TRiC $\zeta-1$ (formerly called TRiC ζ) was found to be expressed in all tissues tested, while TRiC $\zeta-2$ was only expressed in testis tissue (Kubota et al., 1997).

GroEL: Structure, Function and Mechanism of Action

The crystal structure of GroEL (figure 1B) revealed a two-ring complex with seven homologous subunits per ring. Each subunit has been

divided into three domains: the apical domain which contains the GroES binding surface, the intermediate domain that acts as a hinge and moves the apical domain upon ATP binding, and the ATPase-containing domain called the equatorial domain for its location at the equator of the complex. The two rings contact one another through their equatorial domains (Braig et al., 1994). The co-chaperonin GroES consists of seven identical 10 kDa subunits and forms a single ring structure that binds to the apical domain of GroEL (figure 1A). Cryo-electron microscopy (cryo-EM) experiments revealed three different shaped structure of the GroEL/ES complex. The first was the open complex with no GroES bound, the second was called a "bullet-shaped structure" and in this structure GroES was bound to one ring of GroEL, and a third structure was called a "football" structure in which GroES was bound to the apical domains of both GroEL rings. It was found that in the ATP bound state of the bullet shaped structure, the cavity of the trans ring was 50 Å in diameter, while in the ADP-bound state the chamber increased to 58 Å in diameter (Rye et al., 1999). The accessibility of hydrophobic surface area of the trans ring was less in the ADP-bound state than in the ATP- bound state (Rye et al., 1999). In another study using the ATP hydrolysis- deficient mutant D398A and cryo-EM, the ATP-bound state of GroEL alone was determined. The interface between
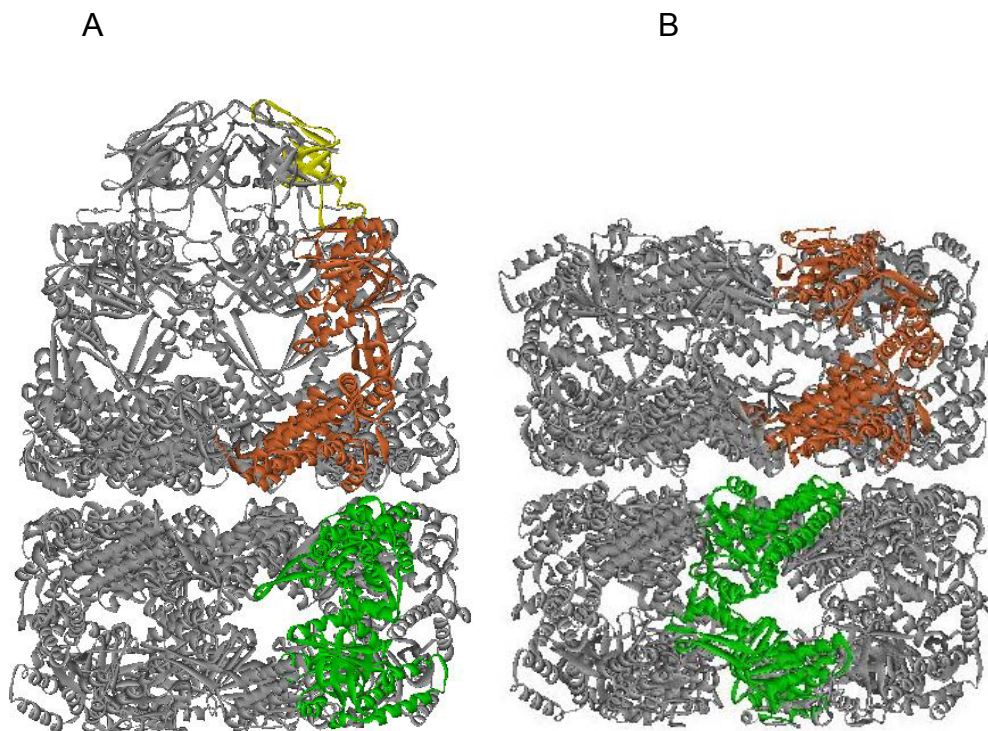
Figure 1. Crystal Structure of GroEL in Complex with Either GroES and ADP or ATP

(A) The crystal structure of GroEL in complex with GroES and bound to ADP. Single subunits of GroEL in the trans and cis ring are green and rust respectively, while a single subunit of GroES is yellow. The same coloring scheme is employed for the ATP-bound GroEL crystal structure (B).

the subunits of the rings was weakened when ATP was bound compared

to the apo state (apo refers to the state in which no nucleotide is bound)

(Ranson et al., 2001). Thus both of these papers suggest that it is ATP

binding that causes large conformational changes in GroEL. Given the

structure of GroEL/ES and its protein folding function, an important issue is

where polypeptide chains bind.

Cryo-EM structures of GroEL/ES with malate dehydrogenase had

shown that the non-native protein bound in the chamber of one of the rings

(Chen et al., 1994). For many years following this finding, the binding

location for nascent chains on the surface of the inner chamber of

GroEL/ES was debated. This question has been answered for the binding

of small peptides to the apical domain. Phage display was used to screen

for a 12mer peptide sequence that had a high binding affinity for GroEL. A

crystal structure of the peptide bound to an apical domain complex showed

that the peptide interacted with helices H and I. A very important finding

was that the two helices that make up the binding site assume a different

conformation when they bind to different peptides (Chen and Sigler, 1999).

Thus this might explain the ability of GroEL to fold a wide variety of

substrates, estimated to be between 10-30% of all newly synthesized

proteins in *E. coli* (Houry et al., 1999).

Biopanning was used to select for peptides that bound to GroEL

with a high-affinity. The K_d for the peptide SBP (the Strongest Binding

Peptide selected from the biopanning process) was determined to be 1.4

μM, 2.0 μM and 6.0 μM at 4°C, 20°C and 37°C, respectively (Chen and

Sigler, 1999). Using the SBP, the first crystal structure of GroEL in complex

with a peptide was solved (Chen and Sigler, 1999). From the crystal

structure, SBP was observed to bind in a hydrophobic pocket between

helices H (residues 230-244) and I (residues 254-268) (Chen and Sigler,

1999). Helices H and I are located in the apical domain of each GroEL

subunit. To further characterize the binding helices of GroEL a mutant

called N229C (which has all the cysteine residues in GroEL changed to

alanines and a new cysteine at position 229) was used to generate a

GroEL-SBP complex (Ashcroft et al., 2002). This complex was titrated with

dansylated HD (Helix D of rhodanese), a peptide known to bind to GroEL.

The relative fluorescence intensity change of HD binding to

GroEL(N229C)-SBP and GroEL(N229C) were very similar, thus leading the

authors to argue that these peptides do not compete for the same binding

site on GroEL (Ashcroft et al., 2002).

Mechanism of Action

As summarized in figure 2A and reviews (Wang and Weissman,

1999; Weissman, 2001) the proposed mechanism for folding of proteins 60

kDa or smaller by GroEL/ES is as follows: the unfolded protein binds to the

open trans ring, then GroES, and ATP bind to the trans ring encapsulating

the protein. The binding of ATP to the trans ring result in a doubling of the volume of the cavity of the trans ring. The conformational change of the GroEL subunits upon ATP binding also hides the previously exposed peptide-binding regions (helices H and I). The interior surfaces of the GroEL subunits, which prior to ATP binding were hydrophobic, became hydrophilic after ATP binding. Next, the substrate folds for 8-10 s before ATP hydrolysis occurs, which primes GroES to dissociate. ATP hydrolysis in the trans ring also affects nucleotide binding in the cis ring, increasing the binding affinity of that ring for ATP (Roseman et al., 1996). GroES, ADP, Pi and the substrate are then released from the trans ring and the process is repeated.

The putative mechanism put forth for folding of proteins such as aconitase that are 82 kDa is different from the mechanism that has just been described. Aconitase binds to the open trans ring that subsequently binds ATP. This binding event causes GroES to be released from the cis ring. Next the trans ring undergoes ATP hydrolysis, the aconitase is released and the cis side of the ring binds GroES and ATP again. Recent

Figure 2. Models for GroEL/GroES Folding of Less Than 60 kDa Proteins and Greater Than 60 kDa Proteins

This figure was adapted from figures in (Chaudhuri et al., 2001; Kusmierczyk, 2001; Weissman, 2001). (A) Model for the folding mechanism of proteins smaller than 60 kDa by GroEL/GroES. The trans and cis rings of GroEL are as labeled. GroES is represented with a purple arch and the non-native folding substrate that represents proteins smaller than 60kDa is drawn in green.
(I) The open trans ring can bind the non-native peptide in the presence of ATP in that ring, while the cis ring has ADP and GroES bound.
(II) The non-native peptide and then GroES binding to the trans ring resulting in a conformational change in GroEL that increases the size of the internal cavity, while ADP and GroES are released from the cis ring.
(III) ATP hydrolysis occurs in about 8-10 seconds and it is thought that the peptide folds during this time. Once ATP hydrolysis is complete, the presence of ADP acts as a trigger for GroES to leave.
(IV) GroES leaves the trans ring since ADP is bound, and ATP binds to the cis ring and it is ready to receive a non-native peptide.
(V) ADP is no longer bound to the trans ring and the peptide leaves as either a native protein (N), an intermediate committed (cN) to reach the native state in the cytosol, or an uncommitted peptide (ucN) that can be rebound by the chaperonin. In the cis ring GroES binds and induces a conformational change and the cycle starts again.
(B) Model for the mechanism of the folding of proteins larger than 60 kDa, such as aconitase.
(1) A non-native protein (red line figure) binds to the open trans ring of GroEL while ADP and GroES are bound the cis ring.
(2) ATP binds to the trans ring and ADP and GroES are then released from the cis ring.
(3) The trans ring undergoes ATP hydrolysis and the cis ring rebinds ATP and GroES causing the polypeptide to be released from the trans ring. If the polypeptide folds into a native structure that can bind its iron-sulfur cluster (blue box) then it will not rebind to GroEL in trans as shown in (4), if not it will rebind to GroEL/ES/ADP as shown in (1).
(4) GroEL bound to the native protein ready to bind to the iron-sulfur cluster.
(5) Released native protein bound to its iron-sulfur cluster, which now acts as a holoenzyme.

A

trans

cis

N or cN

ucN

ATP ATP
ADP ADP

I

ATP ATP

II

T→D T→D

III

ADP ADP
ATP ATP

IV

ATP ATP

V

B

trans

cis

ADP ADP

1

ATP ATP

2

ADP ADP
ATP ATP

3

4

5

Fe-S
Cluster
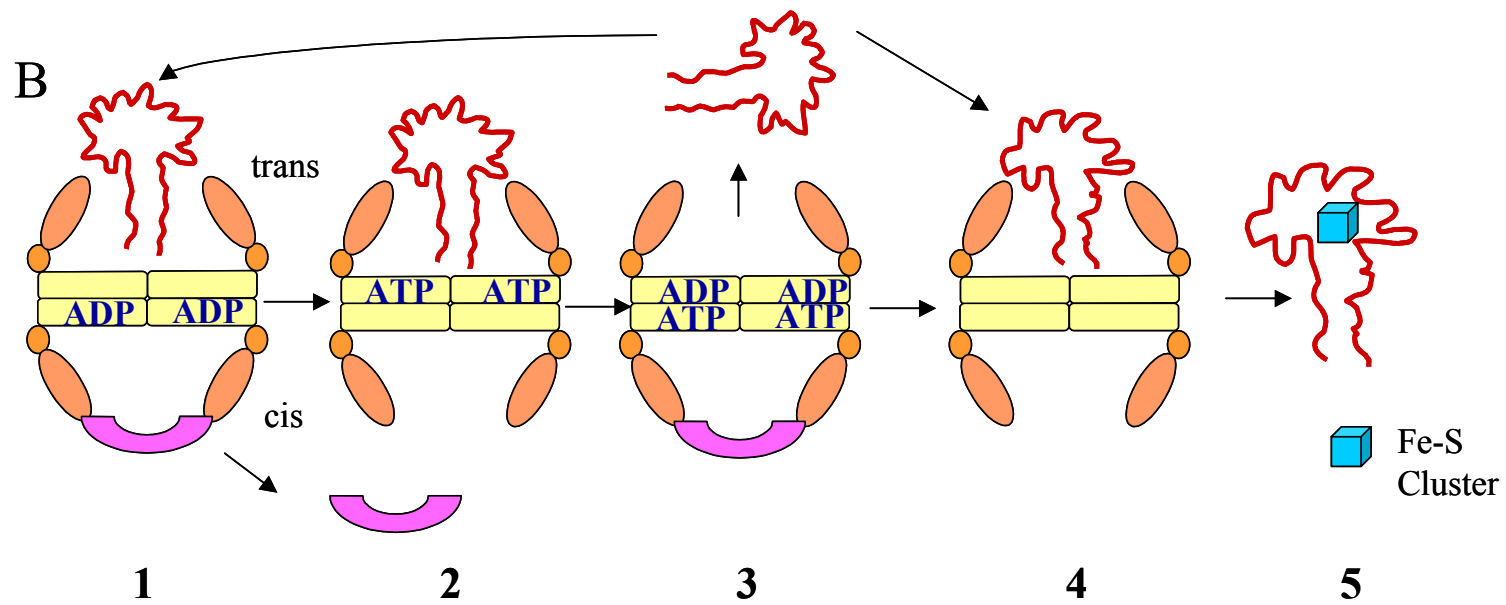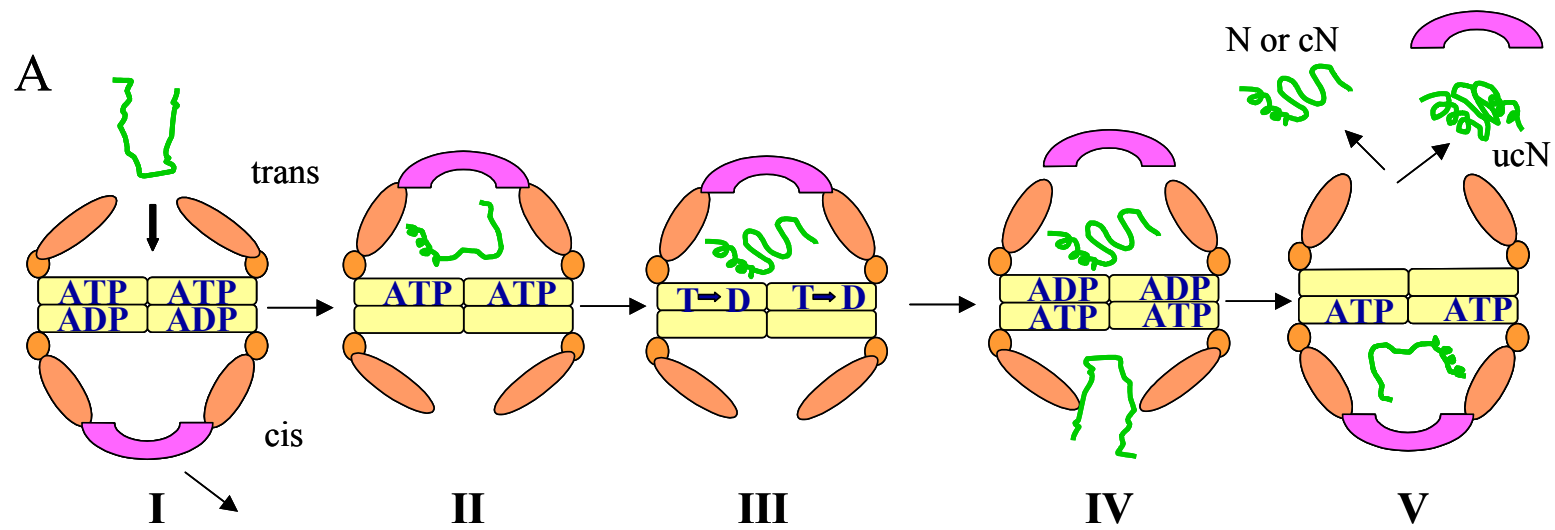
work has shown that aconitase binds to GroEL several times before it is completely folded into its holoenzyme form, which subsequently binds to an iron sulfur cluster (figure 2B) (Chaudhuri et al., 2001).

There has been a great debate for many years about whether a polypeptide folds in one binding event, or whether it needs to bind to GroEL multiple times in order to reach the fully-folded state. As we have just seen above, when folding larger proteins such as aconitase, multiple binding rounds occur. Recent work by Brinker and colleagues (Brinker et al., 2001) in which they used a GroEL streptavidin fusion protein and bound biotin very rapidly in order to block reentry of polypeptide chains smaller than 60 kDa back into the GroEL cavity, protein folding rapidly decreased, back to a rate that was similar to that seen for spontaneous folding (Brinker et al., 2001). Thus the authors concluded that multiple rounds of binding are needed to correctly fold the nascent polypeptide. In a separate experiment using hydrogen exchange, it was found that a single nucleotide provides enough energy for one turnover and that the protein is released at each turnover even if it is not fully folded yet. These authors then suggest that GroEL may function as a mechanical unfolding machine to get the misfolded or molten globule-like protein back on track to correctly fold (Shtilerman et al., 1999). According to Shtilerman and coworkers, GroEL acts to guide the protein back to the correct folding pathway when it gets off course in either a kinetic or a thermodynamic trap.

Another question brought up by scientists in this field was what structural features does GroEL/ES recognize in a protein substrate? To look at the question of whether primary or higher order structures dictate how effective a chaperonin is at refolding an enzyme, experiments using aspartate aminotransferases from eukaryotic mitochondria, cytosol, or prokaryotic cytosol were performed. The tertiary structures of these three proteins are superimposable, but they have only 40% to 47% amino acid identities. *E. coli* aminotransferase shows 50% of its initial enzymatic activity in the absence of any chaperones and/or chaperonins when diluted from 6 M guanidinium hydrochloride, whereas the mitochondrial enzyme increases from 5% up to 25% in the presence of GroEL/ES, DnaJ/K and GrpE, while the cytosolic enzyme increased its enzymatic activity from 25% to 45% in the presence of GroEL/ES, DnaK/J and GrpE (Widmann and Christen, 1995). This led the authors to hypothesize that the primary amino acid sequence might have a great deal to due with chaperone/chaperonin interactions and that the chaperones/chaperonins might be functioning to move the mitochondrial and cytosolic enzymes through different folding intermediates or off pathways than the *E. coli* homologue. It is possible that their results were skewed because they used enzymes that would normally not see GroEL/ES, DnaK/J GrpE, and hence the normal folding pathway that would be performed by TRiC/Hsp70/40 or Hsp60/10 was not available. The conclusions would have been much more

convincing if the authors had used all three aminotransferases with all three chaperone/chaperonin systems.

In a proteomics examination of the structures of the substrates that were bound to GroEL it was suggested that GroEL might be functioning to help fold proteins that have α-helices that are adjacent to β-sheets (Houry et al., 1999). This was an interesting proposal, but was based on only 8 crystal structures of the more than 100 substrates that were found for GroEL. Whether the lack of other protein structures being shown was due to the other proteins not having known crystal structures or to other reasons was not mentioned by the authors. It will be interesting to see if this suggestion holds true when other substrate structures are known because it does not seem to fit with the conclusions from the above study.

To address the question of whether GroEL accelerates an already existing folding pathway or allows for a completely new folding pathway, hen lysozyme refolding was studied (Coyle et al., 1999). In the absence of GroEL, hen egg white lysosyme folds with three intermediate steps. To show that the lysozyme populated all three intermediate states, parallel hydrogen exchange experiments monitored by electrospray ionization mass spectrometry (ESI MS) were performed in the presence and absence of GroEL. The results were identical to the uncatalyzed refolding pathway. However when the rate of the slow phase of lysozyme refolding in the presence of GroEL was examined by observing the increase in tryptophan fluorescence of the lysozyme upon

refolding, a 1.3 fold increase in the refolding rate was observed. Thus the authors concluded that GroEL accelerated the refolding of the enzyme, but did not change its folding mechanism i.e. the intermediate stages that are populated. Since the same intermediates were observed in the presence and absence of GroEL, one conclusion that can be drawn is that GroEL acts like an enzyme to catalyze the natural folding process. However, since this study uses a substrate that folds and does not aggregate in the absence of GroEL, these conclusions cannot necessarily be extended to substrates that are known to require GroEL for proper folding, like aconitase (Chaudhuri et al., 2001).

With a basic understanding of the structure, function and mechanism of the chaperonin GroEL/ES, great interest was now given to the archaeal and eukaryotic chaperonins. Since the archaeal chaperonin called the thermosome is far less complex than the eukaryotic analogs having fewer subunits per ring, more work has been done on its structure, function and mechanism of action than that of the eukaryotic chaperonin TRiC. Consequently a discussion about the thermosome can elucidate the important questions that will pertain to TRiC.

Thermosome: Structure, Function and Mechanism of Action

The thermosome, unlike its prokaryotic homologue GroEL, has been found to contain anywhere between one and three subunits per complex. It is challenging to come to definite conclusions regarding the structure and function of the thermosome because each investigator has used a different organism in

which to perform their experiments, without regard to whether the thermosome from that archaea has one, two or three types of subunits in the complex.

A relevant example is the thermosome from *T. acidophilus,* a species that has two genes for the thermosome. Using cryo-EM studies, two populations of structures were observed. The first was an α only structure containing nine subunits per ring, and the other was an α–β alternating structure in both rings with eight subunits per ring (Nitsch et al., 1997). When the crystal structure of the complete (α, β) thermosome from *T. acidophilus* was solved (Ditzel et al., 1998), there was good agreement with the cryo-electron microscopy data of the same complex. It is interesting that there is little sequence homology with GroEL at the amino acid level, except for the Walker ATPase motif, because the equatorial and intermediate domains are similar in tertiary structure to the equatorial and intermediate domains of GroEL. A difference in three-dimensional structure was observed in the apical domains where a long loop was found in the thermosome (figure 3A) that is not present in the apical domain of GroEL (figure 3B) (Ditzel et al., 1998). The data suggest that the loop in the thermosome might act like a lid, in a similar manner to how GroES acts like a lid for GroEL. An independent group that solved the solution structure of the apical domain of the α subunit of the thermosome found that there was good agreement between the crystal structure of this domain and the solution structure of the whole subunit (Klumpp et al., 1997).

In order to determine if the thermosome from *T. acidophilus* changes its conformation upon nucleotide binding, as GroEL does, purified (α, β) thermosomes were examined using cryo-EM (Gutsche et al., 2000a). Four different structures were found: an apo structure with no nucleotide present, an ATP bound structure, an ADP bound structure and an intermediate structure where the authors argue that the ATP had been hydrolyzed, but the γ-phosphate had not been released. A smaller central cavity was observed for the apo versus ATP and ADP-bound states. The "ATP hydrolysis state" had the largest central cavity (Gutsche et al., 2000b). The crystal structure of the (α, β) thermosome was determined in the presence and absence of ATP by soaking the crystal with nucleotide. When ATP was bound, the thermosome was in a closed state that was very similar to the cis-ring of the GroEL/ES crystal structure. The authors do not see much of a conformational change occurring in the structure of the apical domain when the crystals were soaked with either ATP, ADP or no nucleotide. It is possible that the reason for seeing only the closed thermosome state is the high salt conditions under which the crystal was grown. High salt would not favor the open state, which is suspected to have more hydrophobic residues exposed in the loops of the apical domain.

Another difference between the GroEL and thermosome crystal structures was observed in the inter-ring contacts that occur through the equatorial domains. While one GroEL subunit in the cis ring makes contact with
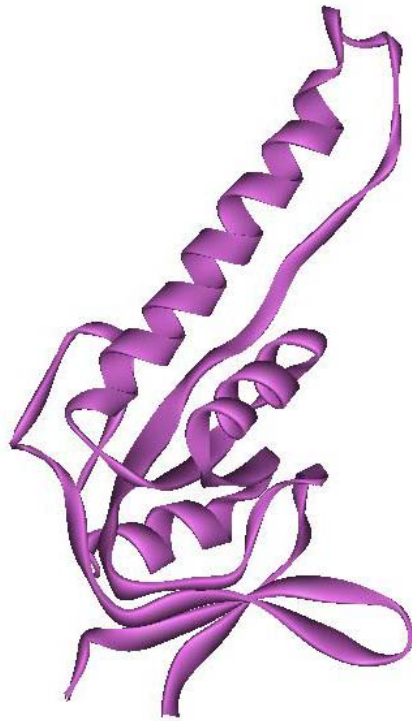
A   B
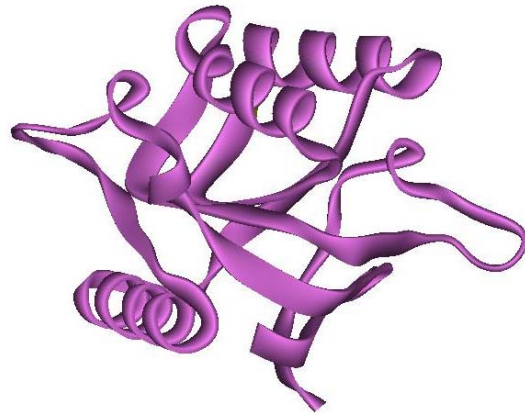
Figure 3. Crystal Structure of the Apical Domains of the Thermosome and GroEL

A side on view of the apical domain and the long loop structure are shown (A) which the apical domain of a GroEL subunit does not have (B).

two GroEL subunits in the trans ring, in the thermosome one α subunit in the cis ring was found to make contact with only one α subunit in the trans ring. However the intra-ring contacts between subunits were conserved. The three-dimensional structures of the α and β subunits of the thermosome were found to be almost identical in this crystal structure (Ditzel et al., 1998). In a cryo-EM study done on the α subunit only complex, three distinct structures of the thermosome were revealed (Schoehn et al., 2000b). The structures were an open, a closed, and an asymmetrically shaped complex. The volume of the cavity for the open ring was determined to be 130 000 Å^3, while the closed ring was 90 000 Å^3. When these cavities are compared to the cavities for the open and closed structure of GroEL and GroEL/ES which are 130 000 Å^3 and 85 000 Å^3 respectively, there is no difference in the open state, and only 5 000 Å^3 in the closed state (Schoehn et al., 2000a). Thus the capacities of the cavities of these two chaperonins seem to be very similar, moreover, the similarities of the structures suggest that the apical loop domain of the thermosome is acting as a lid, just as GroES is a lid for GroEL. No conclusive study to date has been done to address this question.

A structural study of the thermosome from *Sulfolobus solfatericus* showed a nine-membered ring structure of alternating $\alpha-\beta$ subunits, with each α and β subunit in the top ring touching its corresponding α or β subunit in the bottom ring in a equatorial-equatorial domain fashion (Ellis et al., 1998). This structure was determined using two-dimensional crystallization. Since there are

nine subunits per ring, one of the two subunits must be adjacent to another of the same type. This was determined to be the α subunit. The α subunit has been shown to be able to form a homogeneous ring (Ellis et al., 1998), while no such homogeneous ring has been observed for the β subunit. Thus it seems that the α subunit has an intra-ring surface that is compatible with itself and the β subunit.

When the *Haloferax volcanii* strain that has three thermosome genes was examined, all three genes were found to be heat shock inducible (Large et al., 2002). Surprisingly the expression levels of each protein were not similar, although all three proteins were co-purified in a high molecular weight complex like other thermosome structures (Large et al., 2002).

Prefoldin

In 1998, two groups found a new chaperonin which they independently named GIM (genes involved in microtubule biogenesis) (Geissler et al., 1998) and prefoldin (Geissler et al., 1998; Vainberg et al., 1998). GIM genes were found in *Saccharomyces cerevisiae* in a screen designed to find synthetic lethals for a mutant of the γ-tubulin gene. These genes were named gim1 through 5 (Geissler et al., 1998). The discovery of prefoldin was accomplished using a more classical biochemical approach of purifying a protein complex that was shown to associate with unfolded actin on native gels. The complex was purified and shown to contain at least six proteins of molecular weights between

14 and 31 kDa. Partial peptide sequencing was done and the appropriate genes were found in the human and mouse data bases. Further characterization showed that prefoldin transfers its unfolded substrate (actin or tubulin) to TRiC in an ATP-independent manner (Vainberg et al., 1998). It was also found that prefoldin bound to TRiC but not to GroEL. Finally a prefoldin 5 deletion was made in yeast and it was found to grow slowly at 30°C, be cold sensitive, high salt sensitive (KCl) and the actin cytoskeleton was not well developed (Vainberg et al., 1998).

Using one of the prefoldin substrates, actin, it was found that after *in vitro* synthesis of only 145 amino acids of the actin nascent chain, the prefoldin complex was associated with the ribosome-bound nascent chain complex, as determined by native gel analysis (Hansen et al., 1999). C-terminally truncated actin (1-336 aa) was used in similar experiments, and was shown not to fold but to associate mostly with prefoldin on native gels (Hansen et al., 1999). By co-sedimentation experiments and subsequent immunoblots, prefoldin was found to associate with ribosome-bound nascent chains (Hansen et al., 1999). Another group doing similar experiments in *Saccharomyces cerevisiae* were able to overexpress a mutant of GroEL, D78K, that could bind substrate as well as wild type, but could not hydrolyze ATP and hence release bound substrate (Siegers et al., 1999). If actin was released into the cytosol after translation, but before it folded into its native structure, then $GroEL_{D78K}$ would compete with TRiC for actin binding. However, little actin was found associated with GroEL

D78K. When this same experiment was performed in a TRiC temperature sensitive yeast cell line, actin still did not associate with GroEL D78K even though TRiC was not functional. Thus the authors argued that newly-made nascent chains are in a sequestered environment until they are folded (Siegers et al., 1999). This proposal is different from models in which multiple rounds of GroEL binding and release are seen before a protein substrate is completely folded (Brinker et al., 2001). Since prefoldin interacts with actin, what happens to the folding rates of actin in the absence of prefoldin? It was found that actin folded five times more slowly in the *S. cerevisiae* Δ prefoldin deletion strains than in wild-type strains (Siegers et al., 1999). Further experiments led these authors to argue against prefoldin transferring non-native actin to TRiC, but instead concluded that prefoldin may help accelerate actin folding on TRiC or may have some type of "proof-reading ability" to sense when a protein that is not correctly folded is trying to release from TRiC (Siegers et al., 1999). Actin sequences that were necessary and sufficient to bind prefoldin were shown to be residues 50-60 and 184-194 and showed 90-219% and 128-144% binding, respectively. Residues 236-250 in tubulin showed 132-152% binding to prefoldin (Rommelaere et al., 2001). Using a peptide competitor, the association of actin to prefoldin was effectively competed away (Rommelaere et al., 2001). No special motifs were found in any of these three regions. Thus, it is not known what prefoldin specifically recognizes in the nascent chains of unfolded polypeptides.

Two homologous genes encoding prefoldin α and β (aka MtGimC α and β) were found in the archaea *Methanobacterium thermoautotrophicum.* The two proteins were found to be in a hexamer-like prefoldin in eukaryotes, but the hexamer was composed of 2 α subunits and 4 β subunits (Leroux et al., 1999). The α and β genes were found to complement the growth defect of yeast strains lacking prefoldin 5 and prefoldin 6 (Leroux et al., 1999).

In order to look at the function of the archaeal prefoldin, the following experiments were performed. Purified archaeal prefoldin formed a complex with purified actin that had been rapidly diluted from denaturant (Leroux et al., 1999). This agrees with previous data in yeast and reticulocyte lysate that actin interacts with prefoldin (Vainberg et al., 1998). Further experimentation to show that prefoldin was a general chaperone in archaea revealed that prefoldin reduced aggregation of D-lysozyme and D-rhodanese in a concentration-dependent manner (Leroux et al., 1999). It was also shown to increase the percentage of folded rhodanese compared to just GroEL/ES alone (Leroux et al., 1999).

When the crystal structure of the archaeal prefoldin was solved, it was found to be composed of two α and four β subunits (Siegert et al., 2000) , as observed earlier (Leroux et al., 1999). The subunits were held together by β sheets that form a β−barrel platform in which the four β subunits contributed two β-sheets each and the two α subunits contributed four β-sheets (figure 4). The authors described this structure as similar to a "jelly fish" (Siegert et al., 2000).

The tips of the α-helical coiled-coils of prefoldin were shown to contain hydrophobic patches (figure 4B) (Siegert et al., 2000). To test whether these hydrophobic patches were involved in folding the tips of the β subunit's coiled coils were removed. This tip cleaved version of prefoldin was used in rhodanese aggregation assay as noted above (Leroux et al., 1999). The result was a marked reduction in the ability of prefoldin to decrease rhodanese aggregation when compared to the wild type prefoldin (Siegert et al., 2000). Second, in a native gel assay, luciferase was found in complex with prefoldin only when the coiled coils of the β subunit were present. This suggests that the coiled coils of the β subunit are important for functionality (Siegert et al., 2000). Since luciferase is one of the substrates used in experiments performed in this thesis, this fact should be kept in mind. It will be interesting to see if the tips of β subunits of the eukaryotic prefoldin are also essential for substrate binding and chaperone activity.
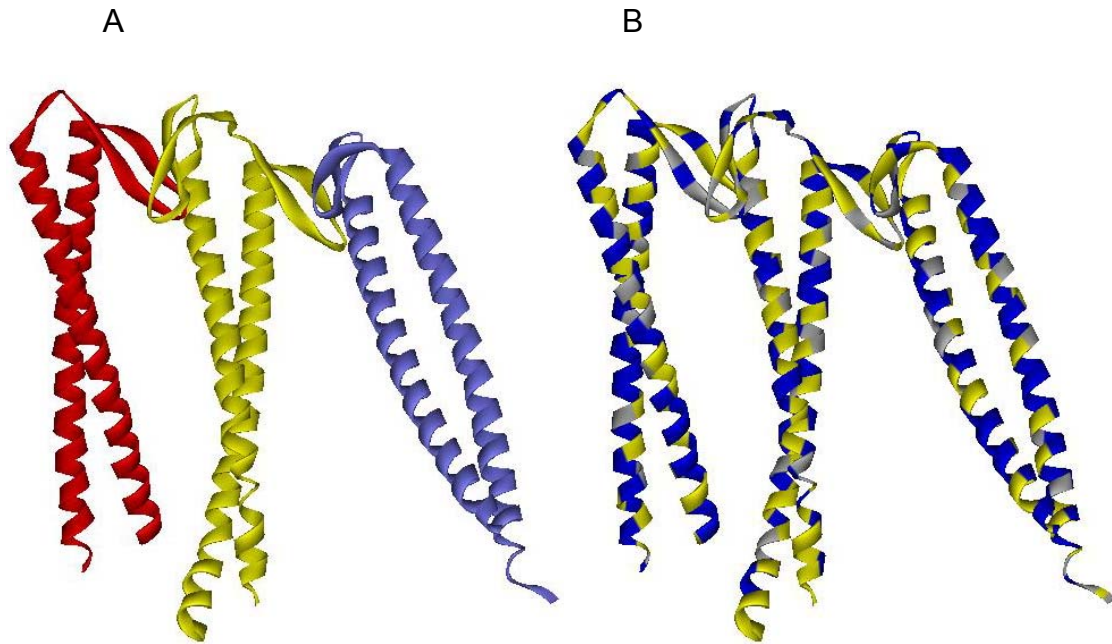
Figure 4. Crystal Structure of One Unit Cell of Archaeal Prefoldin

(A) The α subunits are colored red and blue and the β subunit is yellow.
(B) The same structure as in (A) with the hydrophobic residues colored in yellow, and the hydrophilic residues in blue all other residues are gray.

TRiC

TRiC and its genes have been associated with a wide variety of diseases. In autoimmune diseases (such as rheumatoid arthritis), TRiC α subunit was found at higher levels that in control patients (Yokota et al., 2000). In Parkinson's disease, the TRiC δ gene was found to be up regulated in neurons, and, when antisense mRNA against TRiC δ was present, there was a decrease in dopamine-induced apoptosis (Barzilai et al., 2000). Some of TRiC's folding substrates have been implicated in cancers or viruses when missfolded. A few examples are the von Hippel-Lindau protein which leads to renal carcinomas (Feldman et al., 1999; Ivan and Kaelin, 2001), the Gag protein from Mason-Pfizer monkey virus (Hong et al., 2001), hepatitis B capsid protein (Lingappa et al., 1994), and the Epstein-Barr virus-encoding nuclear protein 3 (Kashuba et al., 1999). Understanding the role of TRiC in these diseases will require study of how TRiC folds its substrates.

TRiC Structure and Function

Cryo-EM images of TRiC show that it is composed of two back-to-back rings of eight subunits per ring, and, like the thermosome, the apical domains have long loops (Gao et al., 1992). TRiC assumes the same conformation either with ADP bound or with no nucleotide bound. However a large conformational change occurs when an ATP transition state analog is bound (Meyer et al., 2003). The apical and equatorial domains move up and out, and

the apical loops are more separated from one another (Llorca et al., 1999b).

This occurs in only one of the two rings, thus renders the TRiC complex

asymmetrical. When the ATP analog AMP-PNP is bound, the rings are closed,

but the apical domains are still more separated (Llorca et al., 2001). Cryo-EM

studies of purified denatured actin and purified mouse TRiC complexes showed

that actin is in the central cavity and touches the apical domains of two subunits

(Llorca et al., 1999a). Antibodies to the δ subunit showed binding to only one

subunit of the top ring. Moreover the bound subunit was next to one end of the

semi-native actin in the central cavity. The other end of the actin binds to either

the ϵ or β subunit (Llorca et al., 1999a), based on the proposed following

clockwise order of subunits in the ring: $\alpha, \epsilon, \zeta, \beta, \gamma, \theta, \delta,$ and η (Liou, 1997). In

contrast, α-tubulin and β-tubulin were investigated and found to be associated

with 5 of the 8 subunits (Llorca et al., 2000). The crystal structure of a portion of

the apical domain of the γ subunit revealed a highly charged surface at the

putative peptide binding site (Pappenberger et al., 2002). This is not what was

expected since the peptide binding site in GroEL is hydrophobic (Chen and

Sigler, 1999). Also there is disagreement in the field as to where the actual

peptide binding site is in type II chaperonins (Frydman, 2001; Klumpp et al.,

1997). Two allosteric transitions were observed in the ATP hydrolysis catalyzed

by bovine testes TRiC (Kafri et al., 2001). The authors hypothesize on the basis

of in silico modeling that TRiC undergoes negative inter-ring cooperativity and

positive intra-ring cooperativity with respect to ATP hydrolysis (Kafri et al.,

2001). In a study by Kafri, two phases of conformational change in TRiC were observed. The first phase, called the "fast phase", is attributed to the conformational change that occurs upon ATP binding. This fast phase has a rate constant of 17 s^{-1} at 25°C (Kafri and Horovitz, 2003). This is 10-fold slower than the same rate observed for GroEL (Kafri and Horovitz, 2003). The second slower phase is [K$^+$], dependent and is attributed to a conformational change upon ATP hydrolysis, since it was not observed in the presence of ADP or ATPγS (Kafri and Horovitz, 2003). The authors conclude that the mechanism of allosteric transitions for GroEL is not the same as the mechanism for TRiC (Kafri and Horovitz, 2003). This is not surprising since TRiC is not known to interact with a co-chaperonin like GroES. In another study using MALDI–mass spectrometry, TRiC θ was found to undergo two post-translational modifications (Hynes et al., 1996). The first was an acetylation in the region of the putative peptide binding site, and the second was a phosphorylation of another region of the same subunit that contains serine and tyrosine residues (Hynes et al., 1996). These modifications may be the first clue that TRiC is regulated in the cell, but the mechanism of this putative regulation is still unknown.

TRiC and Cytosolic Protein Folding

In order to begin looking at how TRiC refolds proteins, refolding experiments using purified chaperonin and denatured substrate proteins were

performed, like those done with GroEL and the thermosome (Frydman et al.,

1992). TRiC and ATP were shown to refold firefly luciferase and tubulin that had

been denatured in 8 M guanidium HCl (Frydman et al., 1992). When actin or

luciferase were chemically denatured and then refolded in the presence of

TRiC, Hsp70, and Hsp40, it was found that the proteins partitioned between a

chaperone/chaperonin-bound state or an unbound state (Nimmesgern and

Hartl, 1993). At the same time as the Frydman group, Gao and colleagues

found that β-actin was associated with a large complex in rabbit reticulocyte

lysate (Gao et al., 1992). This large complex proved to be TRiC. The authors

went on to show that denatured β-actin was functional after it interacted with

TRiC. Not only was β-actin found in a complex with TRiC, but tubulin also

formed a complex with TRiC. Partial proteolysis studies showed that tubulin

associated with TRiC in the presence of Mg-ATP, a protease-resistant and

presumably folded tubulin emerged (Yaffe et al., 1992). In addition to actin, α-

tubulin, and β-tubulin, Melki and colleagues found that γ-tubulin and

centractin/actin-VRP (vertebrate actin-related protein) were also folded by TRiC

in a nucleotide-dependent manner (Melki et al., 1993). Competition studies

using unlabelled actin or β-tubulin showed that centractin and γ-tubulin compete

for binding to TRiC (Melki et al., 1993). Furthermore, they showed that TRiC

needed to be in its ADP-bound state to bind unfolded actin and tubulin, and that

these proteins were released when TRiC cycled to the ATP-bound state (Melki

and Cowan, 1994).

The sequence specificity of ligand recognition by TRiC is another area of intense study. Three substrates have been the focus of most studies determining which substrate sequences bind to TRiC. These substrates are tubulin (Rommelaere et al., 1999), VHL (von Hippel-Lindau protein) (Feldman et al., 1999) and actin (Rommelaere et al., 1999). In studies using β-tubulin as a model protein, it was found that an in vitro-synthesized nascent chain of the first 83 residues of the protein did not interact with TRiC, as assessed by gel filtration experiments. The remainder of the protein bound to TRiC, with the middle portion of the protein (residues 251-287) found to have the strongest interactions (Dobrzynski et al., 1996). Using polypeptides of β-tubulin residues 251-287 with mutations of hydrophobic residues, it was shown that residues 260, 266, 268, 270, 275 and 277 were important in TRiC binding, but not essential (Dobrzynski et al., 2000). In another study using alanine-scanning mutagenesis of β-tubulin, the following regions were found to bind to TRiC: residues 1-205 bind to either TRiC η/α or TRiC δ/θ, residues 205-257 bind to TRiC γ and ζ, residues 261-274 and 263-384 bind to TRiC β and ε, and residues 398-409 bind to TRiC θ and ε (Ritco-Vonsovici and Willison, 2000). Thus, with reference to TRiC binding sites on β-tubulin, no consensus has been reached. It is unclear how much of a change in structure these mutations and truncations made, on whether the results of the truncated peptides are comparable to the full length.

Feldman and colleagues found that the von Hippel-Lindau (VHL) protein was absent in the disease that bears its name (Feldman et al., 1999). In healthy patients, VHL acts as a tumor suppressor in a complex with elongin B and elongin C and TRiC mediates the formation of this complex (Feldman et al., 1999). Co-immunoprecipitation studies with truncated and/or mutated regions of VHL showed that TRiC is associated with amino acids 100-155 of VHL, a region that corresponds to exon 2 of this gene, where many of the disease-causing mutations have been mapped. A TRiC missense mutant, L158P, was found to stably bind to TRiC and hence not associate with elongin B or elongin C. The mutation causes VHL to lose its tumor suppressor activity (Feldman et al., 1999). Using coimmunoprecipitation techniques, VHL was shown to interact with TRiC γ. No other anti-TRiC antibodies raised against any of the other subunits was tested (Hansen et al., 2002). No known similarities between the putative tubulin binding site and the VHL binding site have been observed.

Most of the studies investigating the binding sites recognized by TRiC have been done with actin. Actin will be examined in detail, as it is one of the substrates that will be focus of the Results section of this dissertation. Using native-PAGE of reticulocyte lysate translations of mutant forms of actin, it was found that actin lacking the first 6 N-terminal amino acids missfolds and binds irreversibly to TRiC (Rommelaere et al., 1999). This was also true to a lesser extent for actin lacking the C-terminal 25 residues. But, according to this paper, with amino acids 1-243, only 8 % of the actin remained bound to TRiC. What is

very interesting is the pattern of the following truncation mutants; residues 25-375 bound 33%, 51-375 bound 78% while 76-375 bound 100%, 100-375 bound 143% while 195-375 bound only 41% of the time. The percentage of relative binding was determined by dividing the quantity of target-bound TRiC by the total amount of actin expressed on the SDS-PAGE, relative to the 7-375 amino acid peptide. With actin peptide mimetics it was found that residues 137-150 and all combinations of 110-150 were not soluble and hence not useful in this study. However peptides containing residues 125-179*, 100-179, 260-285, 244-285*, and 340-375* all had weak binding to TRiC and only three of these (identified with an asterisk) could compete for binding to TRiC (Rommelaere et al., 1999). Moreover using native PAGE, it was shown that species binding TRiC poorly bind efficiently to prefoldin, and vice versa. The authors conclude that there are three sequences in actin that bind TRiC: the N-peptide (residues 125-179), the M-site (residues 244-285), and the C-peptide (residues 340-375); (figure 5) (Rommelaere et al., 1999). The three binding sequences in figure 5 are depicted on the actin crystal structure for ease of viewing and comparison with other figures already published using this format (Rommelaere et al., 1999). However, it must be noted that actin is still folding while it is associated with TRiC and hence these binding sequences may not exist in the conformations depicted in this crystal structure of actin.

A   B
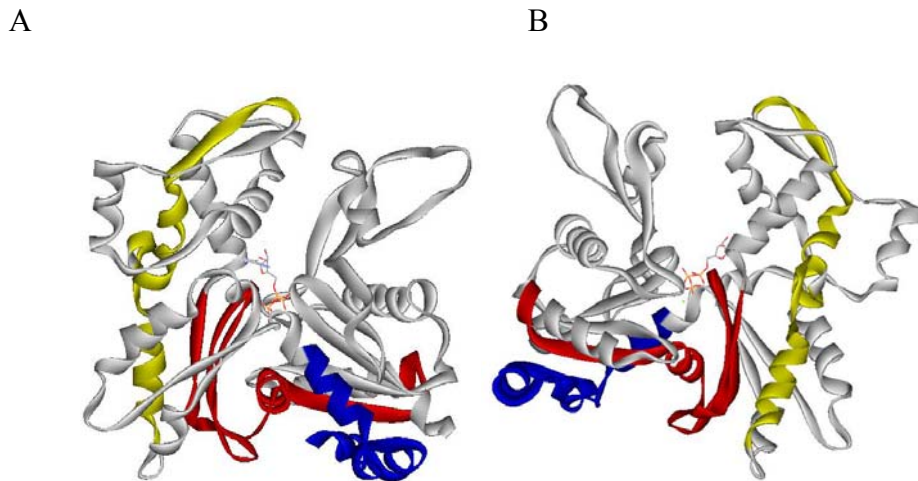
Figure 5. Rommelaere's Model of TRiC Binding Sites on the Actin Crystal
Structure

The N-peptide is shown in red, the M-site is shown in yellow and the C-peptide
is shown in blue. The crystal structure of actin is viewed from the front side (A)
and turned 180° about the vertical axis to view it from the backside (B).

Rommelaere and colleagues noted that both α and β tubulin have a recognition region that has hydrophobic amino acids in the same spatial pattern as the hydrophobic amino acids of the M-site in actin (Rommelaere et al., 1999). In another set of experiments, actin or actin.sub4 (a fusion of the Ha-Ras small GTP-binding protein fused to sub domain 4 of actin, L176-F262, was translated in rabbit reticulocyte lysate, sedimented through a sucrose density gradient, fractionation and finally co-immunoprecipitated with each of the TRiC antibodies (Hynes and Willison, 2000). This showed that actin and actin.sub4 bound to all the subunits of TRiC, although actin.sub4 did so to a much lower extent (Hynes and Willison, 2000). When this experiment was repeated in the presence and absence of ATP, it was found that far less actin co-immunoprecipitated with TRiC when ATP was present. Immobilized actin peptides (15 residues in length covering the entire sequence of actin) were screened for their ability to interact with mouse testis TRiC measured by ELISA (Hynes and Willison, 2000). Peptides of actin that interacted were amino acids 26-40, 31-45, 36-50, 56-70, 126-140, 136-150, 171-185, 191-205, 196-210, 206-220, 231-245, 301-315, 321-335, 331-345, and 346-360. In this type of experiment, the strongest interactions were seen for residues 26-50 and 301-315. Using a peptide containing residues 26 to 70 of actin and performing alanine-scanning mutagenesis, the authors found that mutations of residues 36-40 had the most effect on binding to TRiC. Changing residues 36 or 38 to alanine enhanced binding to TRiC, while changing residue 37 decreased binding. Residues 39

and 40 when changed to alanines showed no change in binding TRiC from the wild type peptide. Finally, when all 5 residues (36-40) were changed to alanines, binding to TRiC was not observed (Hynes and Willison, 2000). Taking all these binding studies into account, the authors propose that there are three sequences in actin that are recognized by TRiC. These sites are called; site 1, 2 and 3 and are shown in red, yellow and blue respectively (figure 6).

Using native PAGE to examine actin interactions with TRiC showed that mutations made in site 1 (figure 6 in red) did not affect TRiC-actin associations. However the change of D244 to alanine, phenylalanine, leucine, proline, serine, or threonine greatly reduced binding to TRiC, as did the double mutation S323A-M325A (McCormack et al., 2001b). Mutation of D11 to anything other than glutamate was not viable in yeast. D11 along with K18, Q137 and D154 all co-ordinate a calcium ion that is involved in ATP binding to actin (McCormack et al., 2001b). Also mutations in actin of G302, T303, M305 and Y306 to alanines all showed an increased interaction with TRiC compared to wild type (McCormack et al., 2001b). These amino acids all line the cleft where ATP
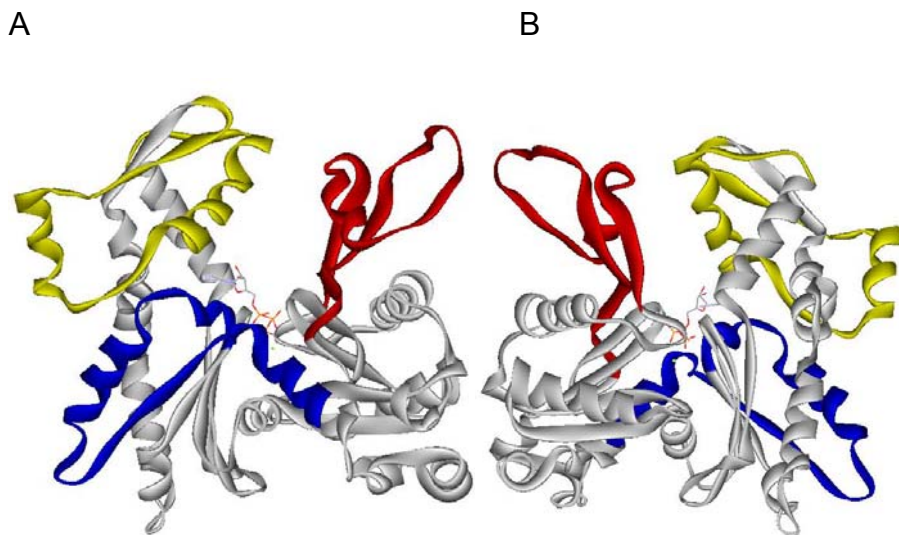
Figure 6. Hynes Model of TRiC Binding Sites on the Actin Crystal Structure

Site 1 is shown in red, site 2 is shown in yellow and site 3 is shown in blue. The front view of actin (A), was rotated 180° about the vertical axis to show the back view (B).

binds. McCormack and colleagues conclude that the three most important TRiC binding sites of actin are amino acids 194-200, 244-247 and 323-325 (McCormack et al., 2001b). These sites are referred to as site Iiii (194-200) shown in red in figure 7, site Iii (244-247) shown in yellow and site IIIii (323-325) shown in blue.

It was found that a point mutation in actin at position 150 (G150P), a location, which is thought to be the hinge region between the small and large domains of actin, caused actin to bind to TRiC for much longer than wild type actin. However in the double mutant of G150P/D244S, the binding affinity for TRiC is the same as the wild-type affinity, but the binding kinetics are slower than for the wild type (McCormack et al., 2001a). Cryo-EM results for the actin (G150P) TRiC complex are very confusing. The authors show the actin G150P mutant in a complex with TRiC and antibodies against the delta subunit; they then label the subunits according to (Liou, 1997). One cryo-EM picture shows actin adjacent to TRiC subunits η and α, while a second cryo-EM picture shows actin adjacent to subunits β, ζ and ε (McCormack et al., 2001a). Nonetheless, the authors conclude that only TRiC subunits β and ε interact with actin G150P (McCormack et al., 2001a). Perhaps their conclusions are drawn from the fact that the TRiC used in these cryo-EM studies to bind actin is apo-TRiC, which means that is has no ATP bound (McCormack et al., 2001b). Thus one is left
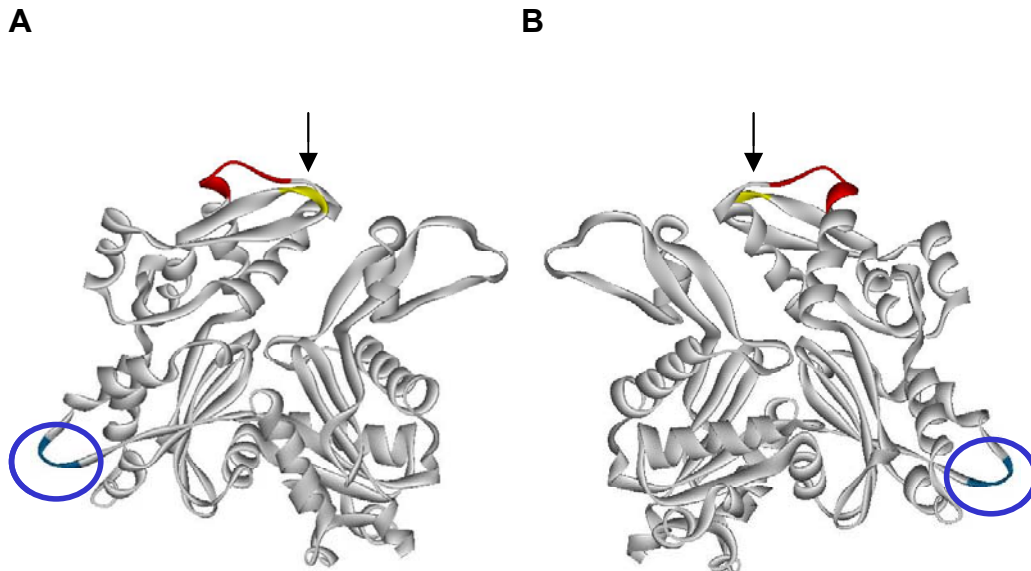
Figure 7. McCormack's Model of TRiC Binding Sites on the Actin Crystal Structure

Site Iiii (amino acids 194-200) is shown in red, site Iii (244-247) is shown in yellow (underneath the black arrow) and site IIIii (323-325) is shown in blue (circled with a blue oval). (A) The front side of the actin crystal structure. (B) The backside of the structure when rotated 180° degrees about the vertical axis.

wondering if the presence of ATP will change the observed cryo-EM structures. In a review article where TRiC binding sites on actin proteins were summarized, the variety of proposed binding sites for TRiC on actin was made clear (Llorca et al., 2001). A sequence alignment was performed between actin and FstA (the prokaryotic homologue of actin). It was observed that the binding sites on actin for TRiC proposed by Hynes and colleagues (Hynes and Willison, 2000) were not present in FtsA (Llorca et al., 2001). Thus, Llorca suggested that the binding sites on actin for TRiC that were not found in FstA, may be biologically important in eukaryotes.

However if one looks at all three studies, the only common region that all three papers agree is important includes residues 244-247 of actin. I would be very surprised if TRiC only recognized 4 amino acids in the whole of actin. Therefore, the biological relevance of each study must be considered. By biological relevance I mean which experiments were performed under conditions that most mimic those found in the cell. By this definition, the studies done by Rommelaere and colleagues were the most biologically relevant of the three studies examined. Nonetheless, even the study by Rommelaere has its limitations. One assumption of the Rommelaere study is the truncated actin behaves in the same manner with regard to binding TRiC as does full length actin.

Although β-tubulin, VHL and actin have all been shown to interact with TRiC, no common sequence that binds TRiC has been identified. One is left

wondering if there is no common primary amino acid sequence that TRiC recognizes, but rather hydrophobic amino acid stretches that might not be exposed in the native protein. This area is still very unsettled.

Co-translational Interactions of Nascent Chains with TRiC

Most of the previously-mentioned studies were done after the substrate such as actin had been fully translated. Recently researchers have examined what happens to such substrates as they emerge from the ribosomal tunnel, thereby raising the possibility of co-translational folding that has not been observed for GroEL or the thermosome. In in vitro translation experiments, it was determined that there was an order in which chaperones and chaperonins interacted with nascent chains. By immunodepletion of either Hsp40, Hsp70 or TRiC from reticulocyte lysate and subsequent co-immunoprecipitation of the ribosome-nascent chains complexes it was found that TRiC did not bind to as many nascent chains when Hsp70 or 40 were depleted (Frydman et al., 1994). Thus the authors concluded that first Hsp40/Hsp70 bound to the nascent chain and then TRiC bound (Frydman et al., 1994). Interactions with Hsp40/Hsp70/TRiC were shown for actin that had been diluted from denaturant or in vitro translated (Frydman and Hartl, 1996). Purified actin diluted from denaturant into a mixture of Hsp40/Hsp70/TRiC/ATP was found to partition freely between the bound and unbound state (Frydman and Hartl, 1996). In contrast, actin translated in vitro in the presence of Hsp40/Hsp70/TRiC/ATP

was found to be in a protected folding environment during the entire folding

process of actin (Frydman and Hartl, 1996). From the crystal structure of firefly

luciferase (Conti et al., 1995) one can see two folding domains with the active

site situated in between. The larger domain is included in the N-terminal amino

acids 1-435, with a sub-domain of amino acids 1-190, while the smaller domain

is in the C-terminal portion of the polypeptide. In vitro translation experiments of

luciferase, treated with mild protease at time points from 5 to 18 min, showed a

protease-protected fragment of 22 kDa that by amino acid sequencing was

determined to be the amino terminal 190 amino acids of luciferase (Frydman et

al., 1999). Thus the authors concluded that luciferase folded in a co-

translational manner.

Since previous studies had shown evidence for TRiC, Hsp40 and Hsp70

binding to ribosome-bound nascent chains using co-immunoprecipitation

protocols, another approach was sought which could independently

demonstrate the association of each chaperone/chaperonin to the ribosome

bound nascent chains, as well as the order of these interactions as a function of

the length of the nascent chain. Using photocrosslinking, with photoprobes site

specifically incorporated at lysine residues in either the actin or luciferase

nascent chains, allows the researcher to "see" what the nascent chain sees as

it is emerging from the ribosome. With this approach, it was demonstrated that

ribosome-bound actin and luciferase nascent chains photocrosslinked (i.e. a

covalent bond was formed between the photoprobe in the nascent chain and a

chaperonin subunit) to a 60 kDa protein which by immunoprecipitation of the photoadduct was shown to be TRiC (McCallum et al., 2000). This result provided direct evidence of the proximity of the nascent chain and TRiC. The photocrosslinking was shown to be dependent on the length of the ribosome-bound nascent chain and on the type of nascent chain (i.e. actin or luciferase). Luciferase nascent chains as short as 77 amino acids photocrosslinked to TRiC, while the shortest actin nascent chains to photocrosslink to TRiC were 133 amino acids long (McCallum et al., 2000). Taking the results of the photocrosslinking studies (McCallum et al., 2000) together with the results of the actin in vitro translations and immunodepletion studies (Frydman et al., 1994), it was established that Hsp40, Hsp70 and TRiC interact with nascent chains in a co-translational manner. Yet what is still not clear is why TRiC has eight heterogeneous subunits per ring in order to fold its substrates while GroEL can fold its substrates with seven homogeneous subunits per ring and the thermosome folds its substrates with one to three different subunits that can be in a heterogeneous or homogeneous complex.

Specific Aims of This Dissertation

The primary goal of this TRiC research project was to examine which subunits of TRiC were involved with or in proximity to the growing ribosome-bound nascent chain during the early stages of translation. Were all the TRiC subunits involved? How close to the ribosomal tunnel exit site is TRiC? What

residues on the nascent chain were recognized by TRiC? Were any other chaperonins adjacent to the nascent chains and if so which residues on the nascent chain did they recognize? To answer these questions, a photocrosslinking approach was used in order to examine the immediate environment of the nascent chain as it emerged from the ribosomal tunnel. This approach involved the co-translational incorporation of a modified lysine into the growing nascent chain. Previously in this lab, the photocrosslinking approach has been successfully employed to examine the environment of nascent chains during translation (McCallum et al., 2000), co-translational translocation (Krieg et al., 1989; Krieg et al., 1986), and co-translational integration (Do et al., 1996; Krieg et al., 1989).

CHAPTER II

EXPERIMENTAL PROCEDURES

Preparing Lys-tRNA^{amb}

Using a plasmid encoding the wild-type *Escherichia coli* (*E.coli*) lysine tRNA gene site-directed mutagenesis was performed to change the anticodon loop to CUA and thus create an amber suppressor tRNA (here termed tRNA^{amb}) that was a generous gift from Dr. Greg Beckler (Promega, Madison, WI). PCR was performed to amplify the region of the plasmid that contained the T7 promoter sequence and the in frame amber suppressor tRNA gene. A typical PCR reaction contained in 100 μl: 1x *Ex Taq*^{TM} polymerase buffer (supplied with *Ex Taq*^{TM} polymerase from Panvera, Madison, WI), 1.5 mM MgCl$_2$, 200 μM dNTPs, 100 pmol upstream primer (1035-YM, see list of primers in table 2) and 100 pmol of downstream primer (1043-YM), and 2.5 units of *Ex Taq*^{TM} polymerase. The reaction started with 2 min at 94°C, followed by 30 cycles denaturing at 94°C for 15 s, annealing at 60°C 15 s, and elongation at 72°C for 15 s. Following these 30 cycles, an elongation step of 5 min at 72°C and a cooling step to 4°C are performed in a PCR machine (Perkin Elymer Applied Biosystems, Gene Amp® PCR system 9700). Next a 10 μl aliquot of the PCR reaction was run on a 1.6% agarose/TBE [90 mM Tris-borate, 2 mM EDTA pH 8.0] gel to confirm that a product of the correct size had been made. The rest of the sample was then extracted with a Qiaex II extraction kit (Qiagen 20021). Elution was in 32.5 μl of elution buffer from the Qiaex II extraction kit. The

sample was then *in vitro* transcribed in a standard 100 μl reaction that

contained 80 mM HEPES (pH 7.5),16 mM $MgCl_2$, 2 mM spermidine,10 mM

DTT, 4 mM ATP, 4 mM CTP, 0.4 mM GTP, 4 mM UTP, 12 μl from the above

purified PCR solution, 0.1 units of pyrophosphatase, 2 units of RNAsin[TM]

(Promega, Madison, WI) and 2.5 μl of T7 RNA polymerase (1.35-1.45 A_{280}

units/ml). The reaction was incubated at 37°C for at least 4 h. Three μl of the

reaction was analyzed on a 1.6% TBE/agarose gel and following confirmation of

the expected product, the rest of the reaction underwent purification by anion

exchange chromatography using a Mono Q HR 10/10 column on an FPLC

(Pharmacia). The tRNA was eluted in 10 mM NaOAc (pH 4.5), 5 mM $MgCl_2$ with

a 115 ml linear gradient of NaCl from 480 mM to 1 M. Aminoacylation was

performed to determine which fractions were enriched in tRNA[amb] as described

previously (Crowley et al., 1993; Johnson et al., 1982; Krieg et al., 1989; Krieg

et al., 1986) with the modification that 6 mM $MgCl_2$ and no KCl was used. The

majority of the tRNA eluted near 550 mM NaCl and the fractions with the

highest functional tRNA[amb] content were aminoacylated with [^{14}C]Lysine and

stored at –80°C until needed (Flanagan et al., 2003).

Chemical Modification of Lys-tRNA[Lys] and Lys-tRNA[amb]

Aminoacylation and purification of yeast tRNA[Lys] were done according to

the methods outlined in (Crowley et al., 1994; Crowley et al., 1993; Johnson et

al., 1976; Krieg et al., 1989; Krieg et al., 1986). Aminoacylation and purification

of *E.coli* tRNA[Lys] and tRNA[amb] were performed as outlined above and in (Flanagan et al., 2003; Johnson et al., 1982; Krieg et al., 1989). The specific activity of an aminoacylated tRNA sample is expressed in pmoles Lys/ A_{260} units of tRNA, with pure Lys-tRNA[Lys] having a specific activity near 1600 pmol Lys/A_{260} unit tRNA. Chromatographically-purified Lys-tRNA[Lys], usually at specific activities of greater than 1000 pmol Lys/A_{260} unit was used for the chemical modification process along with the N-hydroxysuccinimide esters of the photoreactive compounds *N*-5-azido-2-nitrobenzoic acid (ANB-NOS; Pierce Chemicals), trifluoro-diazarinobenzoic acid (TDB-NOS, Photo Probe) and 4-benzoylbenzoic acid (BP-NOS, Molecular Probes). In a typical reaction, ANB-NOS reagent (stored at –20°C) was allowed to come to room temperature in the dark, and 7.5 g of ANB-NOS was added to 1.75 ml of dimethylsulfoxide (DMSO; Gold Label, Aldrich Chemical) for each reaction to be done that day. Fresh solutions of 4 M KOH, 4 M HOAc, 2 M KOAc (pH 5.0), and 500 mM potassium phosphate (pH 7.0) were also prepared. A 3 dram vial and a 2 mm x 7 mm stir bar were washed with ddH$_2$O and acetone to ensure that they were clean and nuclease-free. The 3 dram vial was then set in an ice water bath and held in place by a retort stand and clamp. The ice water bath was set on top of a stir plate so that there was constant stirring during the entire labeling reaction. All of the following steps were performed in the dark room illuminated only with red safety lights, the kind used in photographic dark rooms. [^{14}C]Lys-tRNA[Lys] (5000 pmoles) was added to the vial along with ddH$_2$0 and 0.5 M potassium

phosphate (pH 7.0) to yield a final 50 mM concentration of the latter in a total

volume of 750 μl. Then 1.75 ml of the ANB-NOS/DMSO solution was added

and the stirring speed was quickly reset due to the increased volume of the

solution. Next 15 μl of 4 M KOH were added to the reaction and the reaction

was allowed to proceed for only 14 seconds (absolutely no longer) at which

point 15 μl of 4 M HOAC were added and finally 2.5 ml of 2 M KOAc (pH 5.0)

were added. The KOH was added to deprotonate the ε-amine group of the

lysine residue and initiate the nucleophilic attack of the ANB-NOS reagent. The

HOAc was added to stop the reaction by lowering the pH back to neutral. The

contents of the 3 dram vial were then transferred to an SW-28 polyallomer

centrifuge tube and 26 ml of cold 100% EtOH to precipitate the tRNA. After a

second reaction volume was added to the same SW-28 polyallomer centrifuge

tube (Beckman Instruments), the tubes were wrapped in aluminum foil to

prevent exposure to light and placed at -20°C overnight. The next day the

samples were loaded in the dark in an SW-28 rotor (Beckman Instruments) and

spun at 28,000 rpm for 2.5 hours at 4°C. The supernatant, which contains free

ANB, was removed and discarded, and the pellet was dried under a stream of

nitrogen gas. The dried pellet was resuspended in 300 μl of tRNA buffer [1 mM

KOAc (pH 5.0) and 2 mM MgCl$_2$]. The modified Lys-tRNA$^{Lys/amb}$, N$^{\varepsilon}$-(ANB)-

[^{14}C]Lys-tRNA$^{Lys/amb}$ (termed εANB-Lys-tRNA$^{Lys/amb}$ from here on), was then

dialyzed against 3 volumes of tRNA buffer for 2 h while at 4°C in the dark by

wrapping everything in aluminum foil (figure 8). The tRNA solutions were then

split into 25 μl aliquots in microfuge tubes, wrapped in aluminum foil, frozen in

liquid N_2, and stored at -80°C. An aliquot of the sample was then used in the

characterization of the εANB-Lys-tRNA$^{Lys.}$

Characterization of Modified Lys-tRNA$^{Lys/amb}$

Characterization of εANB-Lys-tRNA$^{Lys/amb}$ and the other chemically

modified Lys-tRNA$^{Lys/amb}$ prior to use in in vitro translation/photocrosslinking

reactions involved taking aliquots of the tRNA sample to determine its A_{260} in a

Mg^{2+}-containing buffer at pH 7.5 and its radioactivity content using liquid

scintillation counting. From these measured numbers, the specific activity of the

Lys-tRNA sample was calculated. The range of specific activities of tRNA

samples used in this dissertation was between 500-1100 pmol Lys/A_{260} unit

tRNA. Lower specific activities were obtained with the amber suppressor tRNA,

both because purification procedures were no as efficient and because

aminoacylation by lysyl synthetase was less efficient than with wild-type tRNA.

Paper electrophoresis was used to determine the extent of lysine

modifications (Johnson et al., 1976). Briefly, freshly prepared 50 mM

triethylamine was added to an aliquot of εANB-Lys-tRNA$^{Lys/amb}$ (~15, 000 dpm)

to hydrolyze the tRNA. This reaction proceeded at 37°C for 90 min, after which

the sample was dried under a stream of nitrogen gas to remove all of the

volatile triethylamine. After resuspension in water, the sample was spotted onto

A
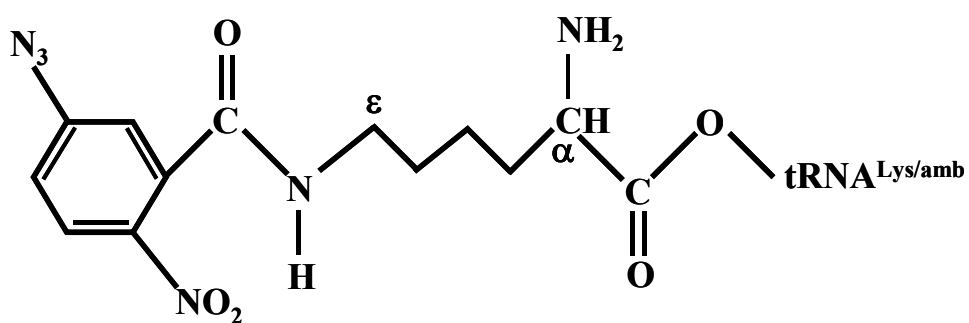
B
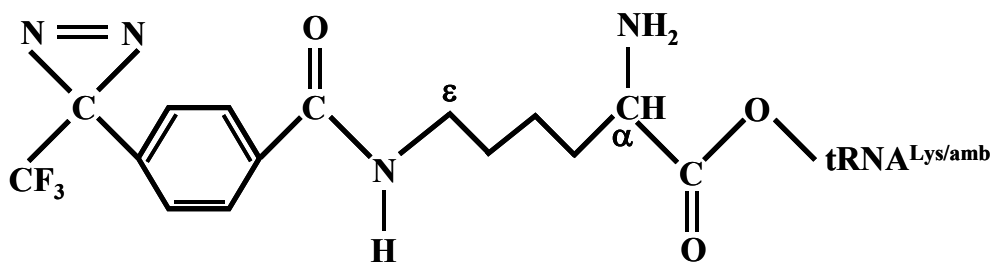
Figure 8. Structures of εANB-Lys-tRNA$^{Lys/amb}$, and εTDB-Lys-tRNA$^{Lys/amb}$

Panels (A) εANB-Lys-tRNA$^{Lys/amb}$, and (B) εTDB-Lys-tRNA$^{Lys/amb}$ represent the structures of all the modified tRNA used in the photocrosslinking experiments in this dissertation.

a 1 m long piece of electrophoresis paper (Whatman[TM] 3 MM) at the origin,

located 20 cm from the anode end of the paper and 80 cm from the

cathode. Unmodified lysine, N$^\alpha$-acetyl-Lys and N$^\epsilon$-acetyl-Lys were spotted at the

origin in different lanes as standards. The paper was then wetted with pH 1.9

buffer Q [8% (v/v) glacial HOAc/1.8% (v/v) formic acid], and placed in a tank so

that each end was in buffer Q (one end in the anode, and the other end in the

cathode), and a 25 V/cm voltage was applied for 3 h. The electrophoresis paper

was then dried overnight, and each lane was cut into 1 cm strips perpendicular

to the electric field and direction of travel before being counted in a liquid

scintillation counter (Beckman LS 6500). The lanes containing the standards

were not cut into 1 cm pieces, but were stained with ninhydrin to establish the

positions of the unlabelled lysine, the α-labeled lysine and the ϵ–labeled lysine

after electrophoresis. Typically, 85-90% of the lysines in a ϵANB-Lys-tRNA prep

were ϵANB-Lys, and most of the remainder was α, ϵ-doubly labeled Lys. The

αANB-Lys content was usually less than 2%, as was the unmodified Lys

content (figure 9). The α-labeled lysine is not incorporated into growing

polypeptide chains, and the unmodified lysine does not have an ANB group and

thus cannot crosslink. Hence, any unmodified Lys-tRNA^{Lys} incorporated into

nascent chains did not interfere with the photocrosslinking or

immunoprecipitation experiments that I performed in this dissertation, aside

from lowering the apparent efficiency of photocrosslinking.
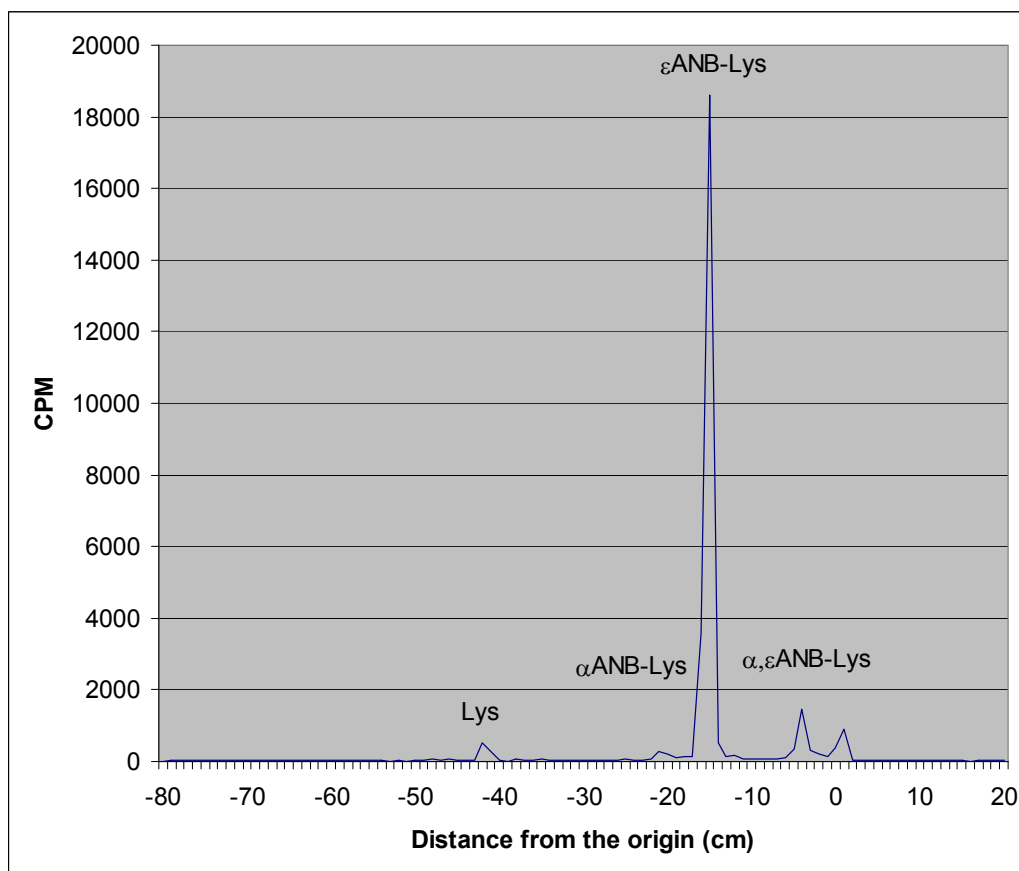
Figure 9. Characterization of an εANB-[^{14}C]Lys-tRNA^{Lys} Sample Using Paper Electrophoresis

The paper electrophoresis analysis shown here demonstrates that in this representative preparation, 87% of the sample is εANB-Lys, 7% is α, ε -(ANB)$_2$-Lys, 2% unmodified lysine and 2% αANB-Lys. The free lysine and the N^ε-acetyl-Lys standards ran (were centered) at –40 and –17 cm, respectively. The data is graphed such that the anode end of the paper is on the left side and the cathode end of the paper is on the right side. The unlabeled peek at the origin (0) represents unhydrolyzed aminoacyl-tRNA.

Preparation of Nuclease-Treated Rabbit Reticulocyte Lysate

The nuclease-treated rabbit reticulocyte lysate (RRL) that was used in most of my experiments was prepared in the laboratory of Dr. William Skach at the Oregon Health Sciences University and was a generous gift to me. Dr. Skach followed the protocol of Hunt and co-workers (Jackson and Hunt, 1983).

Site-Directed Mutagenesis

Desalted and lyophilized DNA primers were ordered and synthesized commercially (IDT and Sigma Genosys). Primers were then resuspended in ddH$_2$O to a final concentration of 50 pmol/μl. A typical PCR contained the following: 1X Pfu buffer which was shipped with the enzyme (Stratagene), 2.5 units Pfu Turbo DNA polymerase (Stratagene), 200 μM dNTPs, 80 pmoles each of upstream and downstream primers, and 20 ng of plasmid DNA, after which the volume was adjusted to 50 μl with ddH$_2$0. The reaction was initially heated to 95°C for 2 min and then 25 cycles of denaturing at 95°C for 30 s, annealing at 55°C for 1 min, and elongation at 69°C for 10 min was performed. This was followed by 7 min at 69°C and finally the reaction was cooled to 4°C before 1 μl of 10 u/μl Dpn1 (New England Biolabs) was added and the reaction was incubated for 1 h at 37°C. Finally 1 μl of Dpn1-treated DNA was added to 100 μl of MC1061 competent *E. coli.* cells and incubated on ice for 1 h. A 30 s heat shock at 42°C was then preformed and the sample was immediately placed back on ice. Next the sample was spread on an LB ampicillin (100 mg/ml) plate

and grown up over night. Colonies were picked, and plasmid DNA was isolated

using a QiaSpin miniprep (Qiagen catalog number 27106). Each mutant

plasmid was then confirmed by DNA sequencing (Gene Technologies Lab,

Texas A&M University). Table 1 lists all of the primers that were used to make

the single-site mutations used in this dissertation. The naming of the primers

follows that adopted by our lab, such that each incoming primer is assigned the

next number in sequence, and this number is followed by the initials of the

person who ordered the oligo.

Table 1. Primers for Site-Directed Mutagenesis

#	Sequence	Template	Mutation	Other Notes
271-SE	GGCTCCGGCATGTGCT AGGCCGGCTTCGCGG GG	pActin	TAG #18	Complements 272-SE
272-SE	CCCCGCGAAGCCGGC CTAGCACATGCCGGAG CC	pActin	TAG #18	Complements 271-SE
273-SE	GTGGGAATGGGTCAGT AGGACTCCTATGTGGG TG	pActin	TAG #50	Complements 274-SE
274-SE	CACCCACATAGGAGTC CTACTGACCCATTCCC AC	pActin	TAG #50	Complements 273-SE
275-SE	GACGAGGCCCAGAGC TAGAGAGGTATCCTGA CC	pActin	TAG #61	Complements 276-SE
276-SE	GGTCAGGATACCTCTC TAGCTCTGGGCCTCGT C	pActin	TAG #61	Complements 275-SE

Table 1. Continued				
#	**Sequence**	**Template**	**Mutation**	**Other Notes**
287-SE	GGTATCCTGACCCTGT AGTACCCCATTGAACA TGGC	pActin	TAG #68	Complements 288-SE
288-SE	GCCATGTTCAATGGGG TACTACAGGGTCAGGA TACC	pActin	TAG #68	Complements 287-SE
289-SE	TGGGACGACATGGAGT AGATCTGGCACCACAC C	pActin	TAG # 84	Complements290-SE
290-SE	GGTGTGGTGCCAGATC TACTCCATGTCGTCCC A	pActin	TAG #84	Complements 289-SE
291-SE	GGCCTTTCTTTATGTTC TAGGCGTCTTCCATTT GG	pLuc	TAG #5	Complements292-SE
292-SE	CCAAATGGAAGACGCC TAGAACATAAAGAAAG GCC	pLuc	TAG #5	Complements291-SE
293-SE	GGCGCCGGGCCTTTCT ATATGTTTTTGGCGTC	pLuc	TAG #8	Complements294-SE
294-SE	GACGCCAAAAACATAT AGAAAGGCCCGGCGC C	pLuc	TAG #8	Complements293-SE
295-SE	CAGGGCGTATCTCTAC ATAGCCTTATGCAG	pLuc	TAG #31	Complements296-SE
296-SE	CTGCATAAGGCTATGT AGAGATACGCCCTG	pLuc	TAG #31	Complements 295-SE
297-SE	GTATTCAGCCCATATC GCTACATAGCTTCTGC C	pLuc	TAG #68	Complements 298-SE
298-SE	GGCAGAAGCTATGTAG CGATATGGGCTGAATA C	pLuc	TAG #68	Complements 297-SE
307-SE	GAATGGCGCCGGGCC CTACTTTATGTTTTTG	pLuc	TAG# 9	Complements 308-SE
308-SE	CAAAAACATAAAGTAG GGCCCGGCGCCATTC	pLuc	TAG#9	Complements 307-SE
309-SE	GTATCTCTTCATAGCCT AATGCAGTTGCTCTCC	pLuc	TAG#28	Complements 310-SE

Table 1. Continued

#	Sequence	Template	Mutation	Other Notes
310-SE	GGAGAGCAACTGCATT AGGCTATGAAGAGATA C	pLuc	TAG#28	Complements 309-SE
359-SE	GGCTCCGGCATGTGCA GAGCCGGCTTCGCGG GC	pActin	ARG#18	Complements 360-SE
360-SE	GCCCGCGAAGCCGGC TCTGCACATGCCGGAG CC	pActin	ARG#18	Complements 359-SE
361-SE	GTGGGAATGGGTCAGA GGGACTCCTATGTGGG TG	pActin	ARG#50	Complements 362-SE
362-SE	CACCCACATAGGAGTC CCTCTGACCCATTCCC AC	pActin	ARG#50	Complements 361-SE
363-SE	GACGAGGCCCAGAGC AGGAGAGGTATCCTGA CC	pActin	ARG#61	Complements 364-SE
364-SE	GGTCAGGATACCTCTC CTGCTCTGGGCCTCGT C	pActin	ARG#61	Complements 363-SE
365-SE	GGTATCCTGACCCTGA GGTACCCCATTGAACA TGGC	pActin	ARG#68	Complements 366-SE
366-SE	GCCATGTTCAATGGGG TACCTCAGGGTCAGGA TACC	pActin	ARG#68	Complements 365-SE
367-SE	CTGGGACGACATGGAG AGGATCTGGCACCACA CC	pActin	ARG#84	Complements 368-SE
368-SE	GGTGTGGTGCCAGATC CTCTCCATGTCGTCCC AG	pActin	ARG#84	Complements 367-SE
369-SE	GCTTTTACAGATGCATA GATCGAGGTGAACATC	pLuc	TAG#46	Complements 370-SE
370-SE	GATGTTCACCTCGATC TATGCATCTGTAAAAG C	pLuc	TAG#46	Complements 369-SE
371-SE	ATCGAGGTGAACATCT AGTACGCGGAATACTT C	pLuc	TAG#52	Complements 372-SE
372-SE	GAAGTATTCCGCGTAC TAGATGTTCACCTCGA T	pLuc	TAG#52	Complements 371-SE
373-SE	CGTACGCGGAATACTA GGAAATGTCCGTT	pLuc	TAG#57	Complements 374-SE
374-SE	AACGGACATTTCCTAG TATTCCGCGTACG	pLuc	TAG#57	Complements 373-SE
504-SE	CCCCCCTGAACCCTTA GGCCAACCGTGAAAAG	pActin	TAG#113	Complements 505-SE

Table 1. Continued

#	Sequence	Template	Mutation	Other Notes
505-SE	CTTTTCACGGTTGGCC TAAGGGTTCAGGGGG G	pActin	TAG#113	Complements 504-SE
506-SE	GCCAACCGTGAATAGA TGACCCAGATCATG	pActin	TAG#118	Complements 507-SE
507-SE	CATGATCTGGGTCATC TATTCACGGTTGGC	pActin	TAG#118	Complements 506-SE
508-SE	GACAGACTACCTCATG TAGATCCTGACCGAGC G	pActin	TAG#191	Complements509-SE
509-SE	CGCTCGGTCAGGATCT ACATGAGGTAGTCTGT C	pActin	TAG#191	Complements 508-SE
534-SE	GTGCGTGACATCTAGG AGAAGCTGTGCTAT	pActin	TAG#213	Complements 535-SE
535-SE	ATAGCACAGCTTCTCC TAGATGTCGCACAC	pActin	TAG#213	Complements 534-SE
536-SE	TGACATCAAAGAGTAG CTGTGCTATGTTGCT	pActin	TAG#215	Complements 537-SE
537-SE	AGCAACATAGCACAGC TACTCTTTGATGTCA	pActin	TAG#215	Complements 536-SE
538-SE	TTCCTCCCTGGAGTAG AGCTATGAGCT	pActin	TAG#238	Complements 539-SE
539-SE	AGCTCATAGCTCTACT CCAGGGAGGAA	pActin	TAG#238	Complements 538-SE
540-SE	TCCTAGCACCATGTAG ATCAAGATCATTGCT	pActin	TAG#326	Complements 541-SE
541-SE	AGCAATGATCTTGATCT ACATGTTGCTAGGA	pActin	TAG#326	Complements 540-SE
542-SE	AGCACCATGAAGATCT AGATCATTGCTCCT	pActin	TAG#328	Complements 543-SE
543-SE	AGGAGCAATTAGCTAG ATCTTCATGGTGCT	pActin	TAG#328	Complements 542-SE
544-SE	CTCCTGAGCGCTAGTA CTCTGTGTGGAT	pActin	TAG#336	Complements 545-SE
545-SE	ATCCACACAGAGTACT AGCGCTCAGGAG	pActin	TAG#336	Complements 544-SE
546-SE	TTCAATTCCATCATGTA GTGTGACGTTGACATC	pActin	TAG#284	Complements 547-SE
547-SE	GATGTCAACGTCACAC TACATGATGGAATTGA A	pActin	TAG#284	Complements 546-SE

Table 1. Continued

#	Sequence	Template	Mutation	Other Notes
548-SE	GTTGACATCCGTTAGG ACCTCTATGCCAAC	pActin	TAG#291	Complements 549-SE
549-SE	GTTGGCATAGAGGTCC TAACGGATGTCAAC	pActin	TAG#291	Complements 548-SE
550-SE	GACAGGATGCAGTAGG AGATTACTGCTCTG	pActin	TAG#315	Complements 551-SE
551-SE	CAGAGCACTAATCTCC TACTGCATCCTGTC	pActin	TAG#315	Complements 550-SE
552-SE	AGATGTGGATCAGCTA GCAGGAGTACGAT	pActin	TAG#359	Complements 553-SE
553-SE	ATCGTACTCCTGCTAG CTGATCCACATCT	pActin	TAG#359	Complements 552-SE
554-SE	ATCGTGCACCGCTAGT GCTTCTAGGC	pActin	TAG#373	Complements 555-SE
555-SE	GCCTAGAAGCACTAGC GGTGCACGAT	pActin	TAG#373	Complements 554-SE

Plasmids

The plasmid pActin, containing the mouse β actin gene under the control of an SP6 promoter, was a gift from Dr. Judith Frydman (Stanford University, Stanford, CA) who obtained it from Dr. Shigeru Sakiyama (Chiba Cancer Center Research Institute, Japan). The pLuc plasmid, containing the gene that encodes firefly luciferase behind an SP6 promoter, was purchased from Promega, (Madison, WI).

The plasmid pActin[18amb] was made by performing site-directed mutagenesis of the plasmid pActin as outlined above such that the lysine codon AAA that encodes amino acid number 18 (numbering is from the N-terminus with the start methionine being amino acid number 1) was changed to TAG that encodes an amber stop codon. The following plasmids were made using the same technique and named accordingly; pActin[50amb], pActin[61amb], pActin[68amb], pActin[84amb], pActin[191amb], pActin[215amb], pActin[238amb], pActin[284amb], pActin[291amb], pActin[315amb], pActin[336amb], pActin[359amb], pActin[373amb]. All of the constructs made and the position of the amber stop codon, are listed in figure 10.
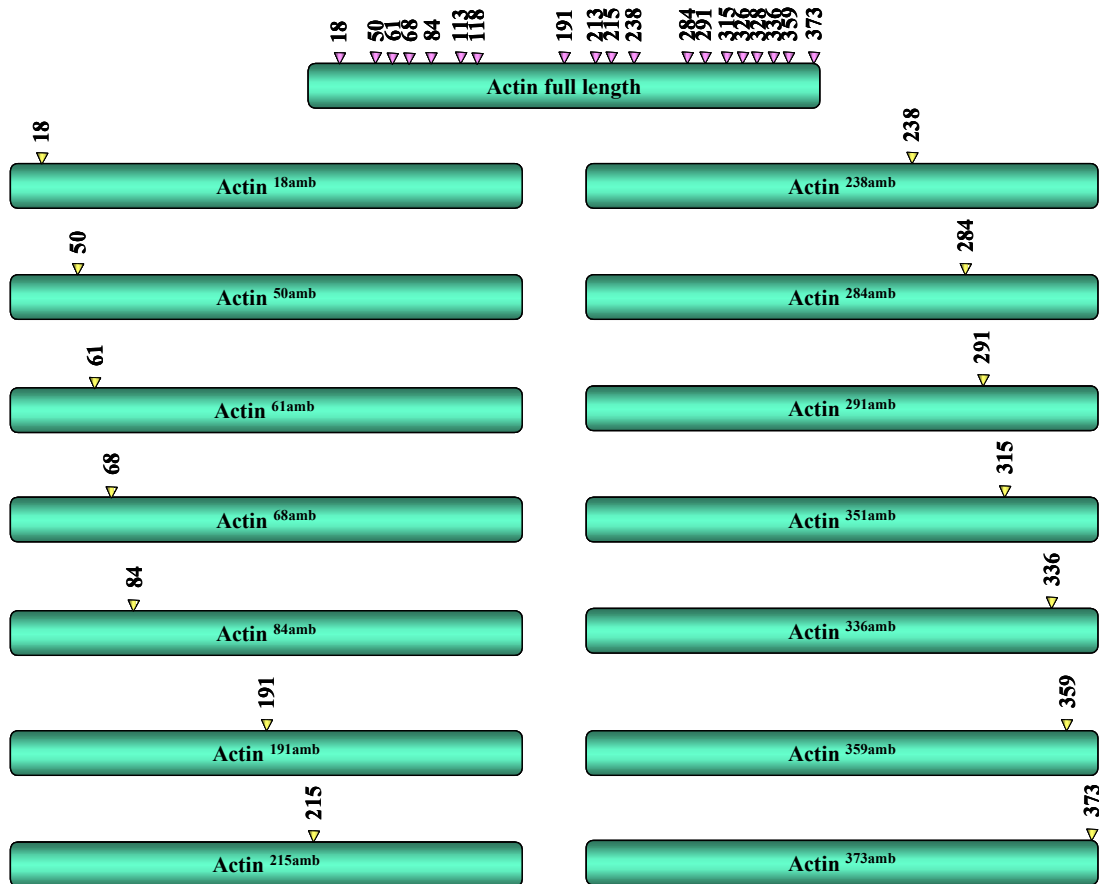
Figure 10. Actin Constructs Used in Photocrosslinking Experiments

The purple arrows and the numbers above each arrow represent the positions of each of the 19 lysines in full-length actin. The yellow arrows represent the position of the amino acid that was changed to an amber stop site. All constructs are shown with the N-terminus on the left.

The pLuc^{5amb} plasmid was made using site-directed mutagenesis to convert at position 5 to an amber stop codon as outlined above. Plasmids pLuc^{8amb}, pLuc^{9amb}, pLuc^{28amb}, pLuc^{31amb}, pLuc^{34amb}, pLuc^{38amb}, pLuc^{46amb}, pLuc^{52amb}, pLuc^{57amb} and pLuc^{68amb} were prepared and named accordingly. These constructs are shown in figure 11.

PCR-Generated Translation Intermediates

Using 5'-primers designed to include the start methionine, and the SP6 polymerase binding site and 3' primers designed to generate DNA products of appropriate lengths, PCR was performed on actin, and luciferase genes. All primers used for these PCR reactions are listed below (table 2). A typical reaction was performed in a total volume of 100 μl and consisted of 1x *Ex Taq*^{TM} polymerase buffer (Takara), 200 μM dNTPs (Takara), 100 pmoles upstream primer (5' end), 100 pmoles of downstream primer (3' end), 10 ng of plasmid DNA, and 5 units of ExTaq DNA polymerase (Takara). The reaction was then put in the PCR machine and the following program was run. A hot start of 95°C for 2 min followed by 25 cycles of denaturing at 95°C for 20 s, annealing at 59-61°C (depending on the primer) for 20 s, and elongation at 72°C for 40 s. A final elongation step of 5 min at 72°C was performed and then the reaction was cooled to 4°C. Following this, 10 μl of the PCR reaction
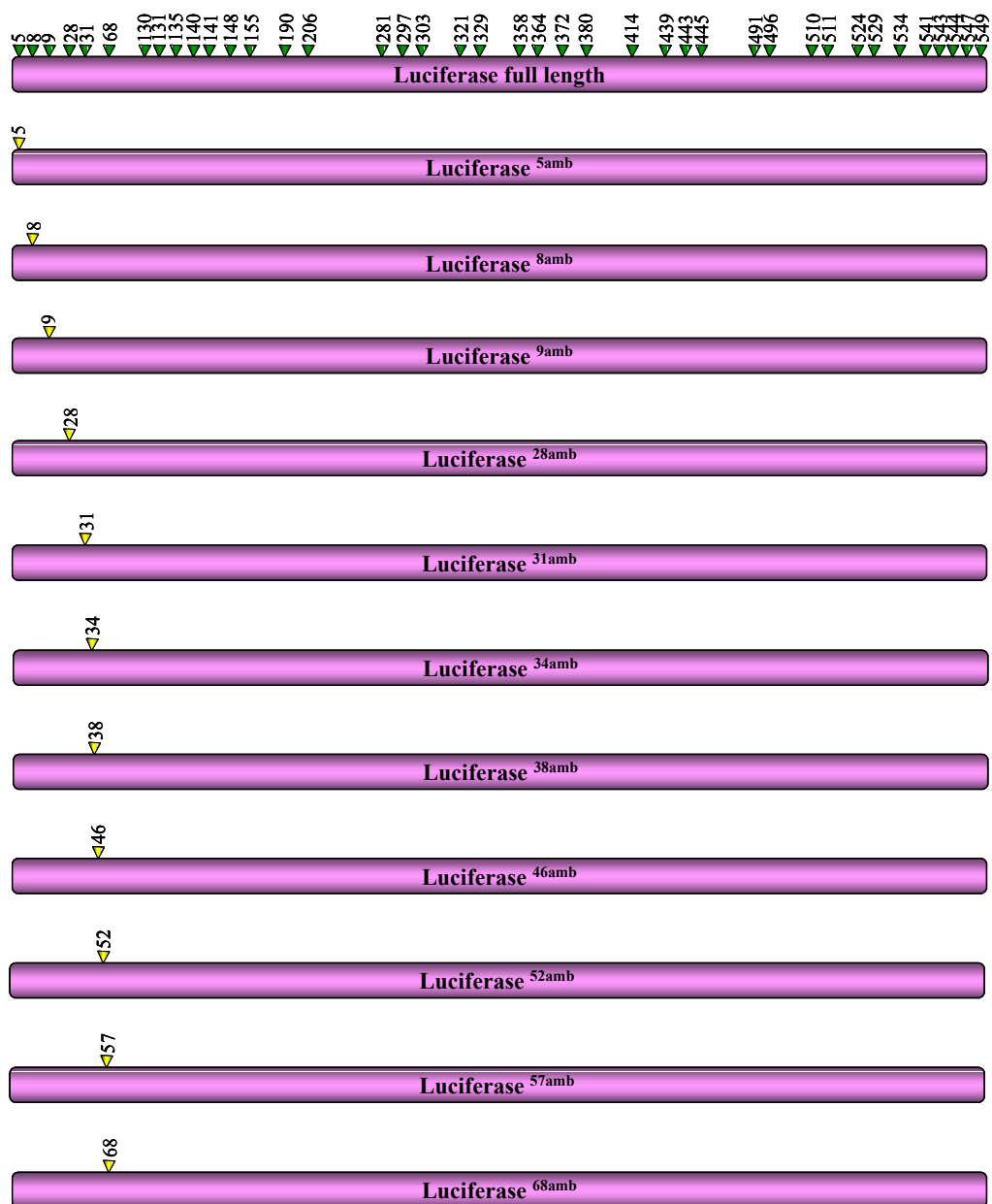
Figure 11. Luciferase Constructs Used in Photocrosslinking Experiments

The green arrows with the numbers above represent the position of each lysine amino acid in each luciferase construct. The yellow arrows represent the position of lysine residue that was changed to an amber stop codon in each construct.

and 2 μl of DNA sample buffer were mixed, and the 12 μl was run on a 1.8%
agarose/TAE (40 mM Tris-acetate and 1 mM EDTA pH 8.0) gel that contained
ethidium bromide (10 mg/ml). Once the length of the PCR product was
confirmed, the sample was purified away from free nucleotides by a QIAquick®
PCR purification kit (Qiagen catalog number 28106). All samples were then
stored at –20°C and used in the *in vitro* run-off transcription reactions.

#	Sequence	Template	Other Primer and Size of Desired Protein	Purpose
1035-YM	GGGAATTCTAATACG ACTCACTATAGGGTC	1:10	1043-YM	Upstream primer
1043-YM	TGGTGGGTCGTGCA GGATTCGAACC	1:10	1035-YM	Amber tRNA down stream primer
1093-SE	GTCTTCTCCATGTCG TCCCAG	pActin	1102-SE	Actin 84mer
1094-SE	CGTACATGGCTGGG GTGTTG	pActin	1102-SE	Actin 133mer
1095-SE	GACGCAGGATGGCG TGA	pActin	1102-SE	Actin 177mer
1096-SE	GAGCAACATAGCACA GCTTCC	pActin	1102-SE	Actin 220mer
1097-SE	GAGCCTCAGGGCAT CGGAAC	pActin	1102-SE	Actin 260mer
1098-SE	GTGGTACCACCAGAC AGCAC	pActin	1102-SE	Actin 303mer
1099-SE	GAGTACTTGCGCTCA GGAGG	pActin	1102-SE	Actin 337mer
1100-SE	CGGTGCACGATGGA GGGG	pActin	1102-SE	Actin 371mer
1101-SE	GTGCTCTGGGCCTC GTCA	pActin	1102-SE	Actin 60mer

Table 2. Primers for PCR-Generated DNA Fragments of Different Lengths

Table 2. Continued

#	Sequence	Template	Other Primer and Size of Desired Protein	Purpose
1102-SE	CTTATGTATCATACA CATACGATTTAG	PActin	Any of 1093-SE to 1101SE	Upstream Primer
1103-SE	CGGACATTTCGAAGT ATTCCG	pLuc	1118-SE	Luc 60mer
1104-SE	GTTCTGTGATTTGTA TTCAGCC	PLuc	1118-SE	Luc 77mer
1105-SE	GACACCGGCATAAAG AATTG	PLuc	1118-SE	Luc 92mer
1106-SE	CTACGGTAGGCTGC GAAATGTTC	PLuc	1118-SE	Luc 125mer
1107-SE	GACATCGACTGAAAT CCCTG	PLuc	1118-SE	Luc 164mer
1108-SE	GAATTCATTATCAGT GCAATTGTTTTG	PLuc	1118-SE	Luc 197mer
1109-SE	GAATGATTTGATTGC CAAAAATAGG	PLuc	1118-SE	Luc 232mer
1110-SE	GTGTAATCCTGAAGG GATCG	pLuc	1118-SE	Luc 280mer
1111-SE	GTCGTATCCCTGGAA GATGGAAG	pLuc	1118-SE	Luc 337mer
1112-SE	GTCGCTTCAAAAAAT GGAACAAC	pLuc	1118-SE	Luc 371mer
1113-SE	CCAGAATGTAGCCAT CCATCCTTG	pLuc	1118-SE	Luc 420mer
1114-SE	CTGCCACGCCCGCG TCGAAG	pLuc	1118-SE	Luc 470mer
1115-SE	CGTCCACAAACACAA CTCCTCC	pLuc	1118-SE	Luc 520mer
1116-SE	GCAATTTGGACTTTC CGCCCTTC	pLuc	1118-SE	Luc 550mer
1117-SE	CGTCATCGCTGAATA CAGTTAC	pLuc	1118-SE	Luc-full length
1118-SE	CCATGATTACGCCAA GCTATTTAGG	pLuc	Any of 1103-1118SE	Upstream primer
1138	GATTTAGGTGACACT ATAGAATACCACCAT GGATGACGATATCGC TG	pActin	Any of 1093-1101-SE	Upstream primer
1268-SE	CGTTGACATCCGTAA AGACC	pActin		Sequencing actin downstream
1269-SE	CATCATTATCAGAAG CACTTGCGGTGCAC GA	pActin	1138-SE	Actin full length

Table 2. Continued

#	Sequence	Template	Other Primer and Size of Desired Protein	Purpose
1294-SE	GATTTAGGTGACACT ATAGAATACCACCAT GGACTCCGGAGACG GG	pActin	177mer-Full length	C-Terminus from aa153 on
1295-SE	GATTTTAGGTGACAC TATAGAATACCACCA TGAAGATCCTGACCG AG	pActin	Lengths 220-Full length	C-Terminus from aa 190 on

In Vitro Run-off Transcription

Typically a 100 μl in vitro run-off transcription reaction consisted of the following: 3 μg of PCR-amplified DNA fragments (see above), 80 mM HEPES (pH 7.5), 16 mM $MgCl_2$, 2 mM spermidine, 10 mM DTT, 0.3 mM GTP, 3 mM each of ATP, UTP, and CTP, 500 μM diguanosine triphosphate [G(5')ppp(5')] (Amersham) which serves as a synthetic mRNA cap, 150 units of RNAsin[TM] an RNAse inhibitor (Promega Biotech) an RNAse inhibitor and 100 units of purified SP6 RNA polymerase. The reaction was incubated at 37°C for 90 min and then 2.7 μl of 100 mM GTP were added and the reaction was continued for another 30 min to complete all transcripts. Following this, a standard ethanol precipitation was performed and then the mRNA was resuspended in 100 μl of Tris-EDTA (pH 7.4) and stored at –80°C. Some mRNAs were purified using the RNeasy® kit (Qiagen catalogue number 74104). The yield and homogeneity of

the in vitro run-off transcription products were confirmed on a 1.8%

agarose/TAE gel.

In Vitro Translations

Using a cell-free protein synthesis system (RRL, see above) and mRNAs

made in the in vitro run-off transcription reaction (see above), in vitro

translations were performed. A typical reaction consisted of a total volume of 25

μl. Translations were performed in 1.5 ml eppendorf tubes for 40 min at 26°C

and contained at least 2.6 mM Mg(OAc)$_2$, 80 mM KOAc, 2 μl of EGS-M/EGS-M-

K (energy generating system with 375 μM of each of the 20 amino acids except

methionine (M) and sometimes lysine (K), 15 mM ATP, 15 mM GTP, 120 mM

creatine phosphate, 90 mM HEPES (pH 7.5), 1.92 mg of creatine

phosphokinase, 0.2 units/μl RNAsin^{TM}, 10 μl of RRL, 3 μl of mRNA, and 0.2

μCi/μl of [^{35}S]methionine (New England Nuclear). The translation product was

routinely examined by SDS-PAGE.

Photoreactions

Translations were done as above with the following modifications; 1.8

μCi/μl [^{35}S]methionine was used and 20 pmoles of modified Lys-tRNA$^{Lys/amb}$ with

the appropriate photoprobe was added. Following the 40 min translations, some

25 μl samples were given 2.5 units of apyrase (Sigma) while others received

water and served as a control; all samples were then incubated for 5 min at

26°C. Translations were stopped by a 10 min incubation in an ice-water bath.

Next, samples were positioned in an ice-water bath in the light beam of a 500 W

mercury arc lamp (Oriel) at a distance of 12 cm through a filter combination

(Oriel 59855 and 66236) that provides a 300-400 nm bandpass. After photolysis

for 15 min, samples were layered over a 100 μl sucrose cushion composed of

120 mM KOAc, 3 mM Mg(OAc)$_2$, 0.5 M sucrose and 25 mM HEPES (pH 7.5)

and spun for 4 min at 100,000 g at 4°C in a TLA 100 rotor in a table top ultra

centrifuge (Beckman). The supernatants were aspirated and discarded, while

the pellets were resuspended in 30 μl of sample buffer with DTT as described

below, and examined by SDS-PAGE.

Immunoprecipitations

Following photolysis as outlined above, samples were removed from the

ice-water bath, and final concentrations of 3 μl of RNAse A (1 mg/ml) (Sigma),

20 mM EDTA (pH 7.4), and 14.4 mM cold methionine were added before the

reactions were incubated for another 10 min at 26°C. Next the reactions were

spun for 10 min at 15, 300 g at 4°C. The supernatants were transferred to new

1.5 ml eppendorf tubes, and ATP was added to a final concentration of 2 mM

then 650 μl of RIPA buffer [containing 140 mM KCl, 0.1% (w/v) SDS, 1% (v/v)

NP-40, 1% (w/v) sodium deoxycholate and 20 mM HEPES (pH 7.5)], and 3-6 μl

of the appropriate antibody were added. Antibodies were a generous gift from

either Dr. Martin J. Carden (Kent University, Kent, England) or Dr. Judith

Frydman, or were purchased from Stressgen (Stressgen, Victoria, BC, Canada) or Sigma (table 3). The tubes were wrapped in parafilm and rocked at 4°C for 2-16 hr. Samples were then spun at 15, 300 g for 15 min at 4°C to remove any aggregates, and the supernatants were transferred to new tubes. To each sample, 10 μl of PAS (protein A-Sepharose) (Sigma) and 10 μl of RIPA buffer containing 10% (w/v) delipidated bovine serum albumin (Sigma) were added, and the reactions were rocked for a minimum of 2 h at 4°C. Next the samples were spun for 1 min to sediment the PAS and washed\d 3 times with 750 μl of RIPA buffer. Finally a flat head syringe was used to remove all of the liquid, leaving only dry beads that were resuspended in 40 μl of sample buffer with DTT. Samples were then heated at 65°C for 30 min. Immunoprecipitated samples were then examined by SDS-PAGE and visualized as described below.

SDS-PAGE

The gels used to resolve our translation, photocrosslinking, and immunoprecipitation samples were 14 cm high x 19 cm wide x 0.8 mm thick. Twenty μl of each sample was loaded into wells that were 2 cm deep and 0.5 cm wide and 0.8 mm thick, and were located in the stacking portion of the gel. The stacking gel was prepared using 4% polyacrylamide, 60 mM Tris-HCl (pH 6.8), 0.1% (w/v) SDS, 360 mM sucrose, 0.05% N, N, N', N'-tetramethyl-ethylenediamine (TEMED), and 0.08% (w/v) ammonium persulfate (APS).

The resolving gel was prepared from 400 mM Tris-HCl (pH 8.8), 0.08% (w/v) SDS, 0.02% TEMED, and 0.08% (w/v) APS that was mixed with a 30% (w/v) acrylamide/0.8% (w/v) bisacrylamide stock solution (BioRad) to form a gel with a 10-15% linear gradient of polyacrylamide (all materials were from Sigma Chemicals unless otherwise specified). Preparation of samples for electrophoresis was done by resuspension of each sample in sample buffer consisting of 120 mM Tris-base, 3.6% (w/v) SDS, 7.5 mM EDTA, 125 mM DTT, 15% (v/v) glycerol, and a small amount of bromophenol blue, followed by either heating the samples for 5 min at 95°C or for 30 min at 65°C to reduce antibody aggregation in immunoprecipitated samples. The running buffer in which the gel was submerged contained 50 mM Tris-HCl (pH 8.8), 400 mM glycine, and 0.1% (w/v) SDS. The gel was then run at a constant current of 17 mA for 30 min while samples moved through the stacking portion of the gel, followed by a constant 32 mA for 2 h and 20 min as samples moved through the resolving portion of the gel. The gel was then placed in a stain solution containing 10% (v/v) glacial acetic acid, 50% (v/v) methanol, and 0.125% (w/v) Coomassie Brilliant Blue (Sigma), which binds to proteins and stains them blue. Following a minimum of 10 min in the staining solution, gels were transferred to a destaining solution containing 10% (v/v) glacial acetic acid and 35% (v/v) methanol until the background was no longer dark blue, but the proteins on the gel were still

_____

Table 3. Immunogenic Sequences Used to Generate Antibodies Against

Specific TRiC Subunits

_____

Subunit	Immunogenic Sequence	Professor/Company
Anti-TRiCα	NH$_2$-CGSYENAVHSGALDD-COOH	M.J.Carden
Anti-TRiCβ	NH$_2$-CAPRKRVPDHHPC-COOH	M.J.Carden
Anti-TRiCβ	NH2-CAPRKRVPDHHPC-COOH	J. Frydman
Anti-TRiCγ	NH$_2$-CGHKKKGDDQTGAPDAGQE-COOH	M.J.Carden
Anti-TRiCδ	NH$_2$-CSILKIDDVVNTR-COOH	M.J.Carden
Anti-TRiCϵ	NH$_2$-CIDDIRKPGESEE-COOH	M.J.Carden
Anti-TRiCϵ	NH$_2$-CIDDIRKPGESEE-COOH	J.Frydman
Anti-TRiCζ	NH$_2$-CEIMRAGMSSLKG-COOH	M.J.Carden
Anti-TRiCθ	NH$_2$-CSGKKDWDDDQND-COOH	M.J.Carden
Anti-TriCα(CTA-123)	NH$_2$-C-Terminal half of the protein	Stressgen
Anti-TRiCγ(CTA-210)	NH$_2$-NRQTGAPDAGQE-COOH	Stressgen
Anti-TRiCδ(CTA-220)	NH$_2$-SILKIDDVVNTR-COOH	Stressgen
Anti-TRiCζ(CTA-250)	NH$_2$-EIMRAGMSSLKG-COOH	Stressgen
Anti-TRiCθ(CTA-260)	NH$_2$-SGKKDWDDDQND-COOH	Stressgen
Anti-TRiCη(CTA-240)	NH$_2$-SAGRGRGQARFH-COOH	Stressgen

bright blue (no less than 20 min). Finally the gel was rinsed with water until no acetic acid odor could be detected. It is important to remove all acetic acid as it can damage the Kodak phosphorimaging screens that are used in the visualization of the gel. Next the gel was submerged in a 2% (v/v) glycerol solution for 1-2 min to reduce the possibility of cracking on the gel dryer (BioRad). The gel was then placed on a piece of 3 mM paper (Whatman) that had been soaked in 2% (v/v) glycerol and placed on the gel dryer to dry for 40 min at 80°C. The dried gel was then taped to a cassette and exposed to a phosphorimaging screen (Kodak) overnight or longer. The image was then visualized using a phosphorimager (Molecular Imager® FX, BioRad) and software package (Quantity One version 4 BioRad).

Preparation of Radiolabeled Cell Lysate

Four 150 mm plates of TSA 201 cells were grown to 60-70% confluence. Cells were starved overnight in DMEM (Dulbecco's Modified Eagle's Media) that lacked methionine and cysteine, but contained pen, strep and glutamine, 7% (v/v) fetal bovine serum (FBS), 5% complete serum [DMEM with 10% FBS (v/v) and pen/strep and glutamine], and radioactive [^{35}S]Met and [^{35}S]Cys at 0.3 mCi/plate. In the morning, the radioactive media was removed and the cells were placed on ice; all subsequent steps were performed with the plates on ice. Each plate was washed with 2-4 ml of cold phosphate-buffered saline (PBS). Next, 2 ml of cold PBS were added to each plate and a rubber policeman was

used to scrape the cells from the plate. The samples were placed in 1.5 ml

Eppendorf tubes and spun for 5 min at 1000 rpm at 4°C. The supernatant was

aspirated and all eight pellets were resuspended and combined in a total of 1.5

to 3 ml of lysis buffer [1% (v/v) Triton X-100, 10% (v/v) glycerol, 0.1 mM PMSF,

1 mM DTT, 0.2 μg/ml aprotinin, 0.5 mM EDTA, 2 mM deoxyglucose, 100 mM

NaCl, 20 mM Tris (pH 7.4) and 1 mM sodium azide]. The samples were

vortexed briefly and incubated on ice for 10 min. Samples were then spun at 14,

000 rpm at 4°C for 20 min. Next, the supernatant from the samples was pooled

and loaded on a Superose 6 size-exclusion column that was equilibrated in

buffer 4 [50 mM NaCl, 10% (v/v) glycerol, 1 mM DTT, 0.1 mM PMSF, 5 mM

MgCl$_2$, 0.1 mM EDTA, 20 mM HEPES-KOH (pH 7.4)]. The flow rate of the

column was maintained at 2 ml per min by the FPLC instrument and 0.5 ml

fractions were collected starting after the first 6 ml had eluted from the column.

After 50 fractions had been collected, the column was washed with buffer 4.

TRiC was eluted from the column at an elution volume near 12.5 ml,

corresponding to fractions 22-27. To confirm that TRiC was in these fractions, a

native immunoprecipitation was performed. Aliquots (50 μl) of fractions 20-28

were added to 25 μl of a 100 mg/ml solution of BSA and then 4 μl of antiserum

raised against the β-subunit of TRiC were added. The samples were then

placed on ice for 40 min. After 15 μl of PGS (Protein G-Sepharose) in 50 μg/ml

of BSA were added [1:1 (v/v) slurry of beads to liquid] the mixtures were rocked

at 4°C for 1 h and then washed 2 times with 500 μl of 1X TBS (Tris-buffered

saline pH 7.5) + 0.05% (v/v) Triton X-100 and 3 times with 500 μl of 1X TBS + 1% (v/v) Triton X-100. Finally, all the supernatants were removed with a syringe and the beads were resuspended in 20 μl each of 4X sample buffer with β-mercaptoethanol at a final concentration of 100 mM. The samples were then heated to 95°C for 5 min and loaded on a 12% gel for SDS-PAGE.

CHAPTER III

RESULTS:PHOTOCROSSLINKING STUDIES OF THE CO-TRANSLATIONAL NASCENT CHAIN PROXIMITY TO SUBUNITS OF THE CYTOSOLIC CHAPERONIN TRiC

Experimental Design

In order to examine which TRiC subunit(s) is/are in proximity to the growing nascent chain as it exits the ribosomal tunnel, a photocrosslinking approach was employed. The rationale for using this technique is detailed below.

A major experimental goal is to examine a homogeneous sample of nascent chains. Currently it is not possible to synchronize the initiation of translation of a population of ribosomes in an in vitro translation system and thus create a homogeneous population of ribosome-bound nascent chain complexes (RNCs). Another approach for generating a homogeneous population of RNCs is to have them all stop at the same point during translation. In the RRL eukaryotic in vitro translation system, when a ribosome translating a truncated mRNA (i.e., one that extends part way into the coding region and does not encode a stop codon) reaches the end of the mRNA, translation ceases and the nascent chain remains covalently attached to a tRNA located in the ribosomal P-site. Thus, by using truncated mRNAs, we can generate a homogeneous population of RNCs.

An advantage of this approach is that by generating truncated mRNAs of differing lengths, nascent chains with different lengths can be examined. This allows the experimenter to take "snap shots" of the nascent chain at different stages of translation and thereby illuminate what happens to the nascent chain after it emerges from the ribosomal tunnel. In order to "see what the nascent chain sees" during in vitro translation, probe-modified lysine residues are incorporated onto the growing polypeptide chain. This approach is advantageous because the probe is then located only in the nascent chain. In contrast, if a probe were simply reacted with RNCs chemically, most of the probes would be attached to the ribosomal proteins or other components since the nascent chains constitute much less than 1% of the total protein in the typical translation reaction. Thus, the modified Lys-tRNA approach allows one to selectively position probes only in the nascent chain.

One modified charged tRNA that our lab has successfully used to incorporate a probe into a growing nascent chain is εANB-Lys-tRNA. The ANB probe is a photoreactive moiety, which is covalently attached to the ε-amino group of the lysine. When εANB-Lys-tRNA is added to an in vitro translation incubation, it can incorporate its probe into the nascent chain wherever an in-frame lysine codon is found in the mRNA sequence. Others in our lab have previously used this approach successfully to examine the environment of the nascent chain during co-translational translocation (Do et al., 1996; Krieg et al., 1986; Liao et al., 1997; Thrift et al., 1991); McCormack et al., paper submitted).

Since my goal was to identify which subunit(s) of TRiC was (were) involved in interacting with a growing nascent chain, I chose to use photocrosslinking as my primary analytical approach. A nascent chain probe will only react covalently with a TRiC subunit if the nascent chain is immediately adjacent to it. Hence, one would expect to crosslink only to TRiC subunits that bound to or otherwise interacted with the nascent chain. By using a photoreactive probe instead of a chemical crosslinking reagent, I can maximize my chances of detecting nascent chain-TRiC subunit proximity because the photoprobe will react covalently with any amino acid (though at different rates), while a chemical crosslinker is limited to reaction with nearby Lys and/or Cys residues. Another advantage of the photocrosslinking approach is that one can completely assemble the nascent chain, including the incorporation of the photoreactive probe into the nascent chain, before initiating the covalent reaction by shining light on the sample.

Work by McCallum and colleagues in our laboratory has demonstrated that actin nascent chains can photocrosslink to TRiC and that TRiC photocrosslinks to ribosome-bound actin nascent chains (McCallum et al., 2000). Full length actin has 19 lysine residues in the nascent chain. The lysine residues are distributed over the length of the chain, as is shown in figure 12. By using actin nascent chains of varying lengths, and multiple probe positions per nascent chain, the environment seen by the nascent chain can be examined. For these reasons, actin was chosen as the nascent chain to use for
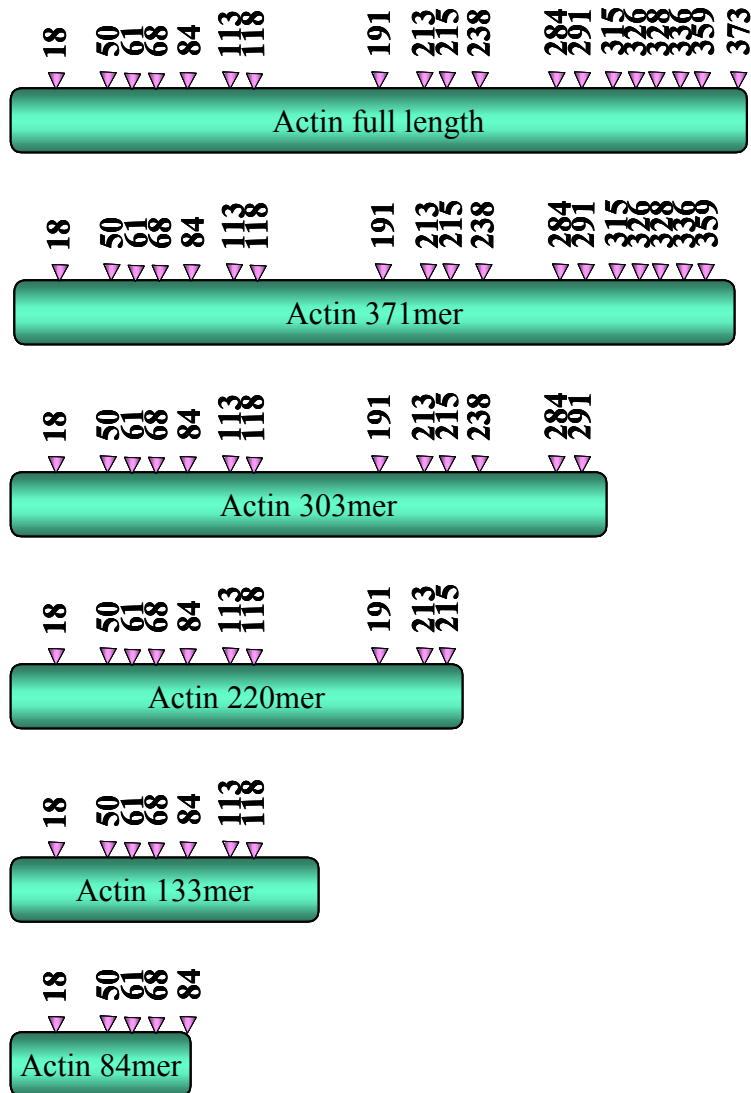
Figure 12. Actin Nascent Chains

Full length actin and actin nascent chains are represented above as green cylinders. The length of the actin nascent chain is indicated in the center of each cylinder. The position of each lysine residue in the actin nascent chains is indicated with a purple arrowhead. The number above the arrowhead represents the position of that lysine residue in actin with the N-terminal methionine being labeled number 1.

the examination of which TRiC subunit(s) are near the nascent chain as it emerges from the ribosomal tunnel.

Immunoprecipitation Conditions and the Specificity of TRiC Antibodies

TRiC is composed of eight unique subunits, and McCallum and co-workers did not identify which of the eight subunits was photocrosslinked to the actin nascent chain (McCallum et al., 2000). Since immunoprecipitations under native conditions would not dissociate the TRiC complex into its subunits, the question of which subunits photocrosslink to actin requires immunoprecipitation conditions that result in the dissociation of the TRiC complex. The two major concerns about this approach are whether the antibody-epitope association would survive denaturing conditions and whether antibodies raised against a particular subunit were cross-reactive with other subunits under these denaturing immunoprecipitation conditions. To address these issues, immunoprecipitations were performed on radiolabeled TRiC complexes.

Human fibroblast TSA 201 cells were pulse labeled with [^{35}S]Met overnight, lysed, and the supernatant was run over a size exclusion column. TRiC containing fractions were identified by native immunoprecipitation with antibodies raised against the β subunit (data not shown). The fractions containing radiolabeled TRiC were then used to determine what conditions dissociated the TRiC subunits. Using antibodies against each of the subunits of TRiC it was determined that radioimmunoprecipitation (RIPA) buffer conditions long used in the denaturing immunoprecipitations from cell lysates allowed for

all eight subunits to be immunoprecipitated. However, other bands representing other TRiC subunits were also found in the immunoprecipitated material, which, suggested that not all the subunits in the complex were fully dissociated (figure 13). However Roobol and colleagues found that addition of 140 mM KCl instead of NaCl and addition of at least 1 mM ATP to the RIPA buffer was sufficient to completely dissociate the TRiC complex such that antibodies against each of the eight subunits could specifically recognize the subunit against which they were raised (Roobol et al., 1999). When these conditions were used, each antibody, except the η antibodies was found to recognize the subunit that it was raised against (figure 14).

A difference in the intensity of some of the immunoprecipitated TRiC subunits is evident in figure 14. The subunits do not contain equal numbers of Met and Cys residues, therefore, this is not surprising. Also, variations in immunoprecipitation efficiencies may result in differences in the antibody-epitope affinities and in the nature of the antibodies themselves. For example the TRiC α antibody is a rat monoclonal, while the other antibodies are rabbit polyclonals. Also, some have been affinity purified, while others that have not. To minimize these concerns, each antibody was titrated to determine it's optimal concentration in samples to maximize the immunoprecipitation of its cognate TRiC subunit (data not shown). Thus, the antibodies shown in figure 14 and the denaturing immunoprecipitation conditions determined (for specific
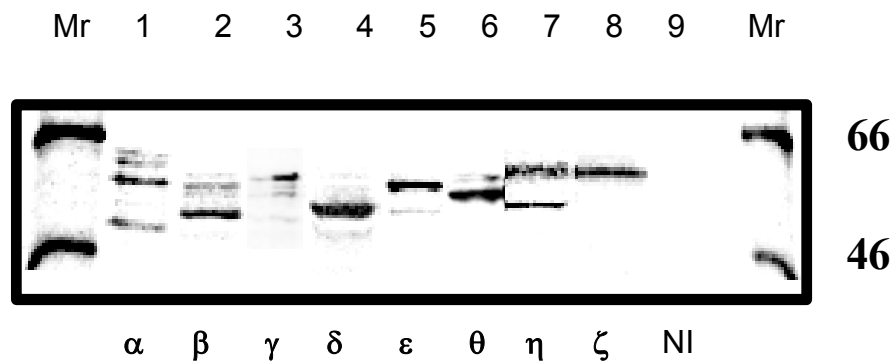
Figure 13. Denaturing Immunoprecipitations of TRiC Subunits

Immunoprecipitation under denaturing conditions of radiolabeled TRiC complexes purified from TSA 201 cells with antibodies raised against specific TRiC subunits: the α subunit (lane 1), the β subunit (lane 2), the γ subunit (lane 3), the δ subunit (lane 4), the ε subunit (lane 5), the θ subunit (lane 6), the η subunit (lane 7), the ζ subunit (lane 8), or non-immune serum (lane 9).
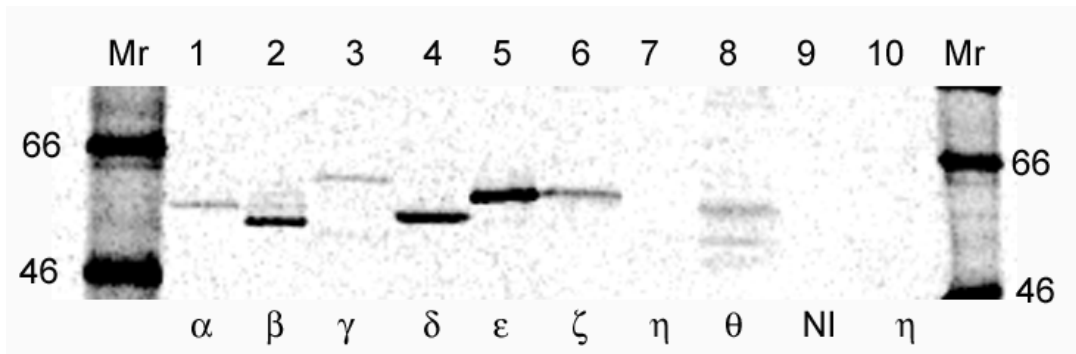
Figure 14. Immunoprecipitations of Radiolabeled TRiC Subunits with Antibodies Against TRiC Subunits α, β, γ, δ, ε, ζ, η and θ

Radiolabeled TRiC was prepared from human fibroblast cells as detailed in the Experimental Procedures. Immunoprecipitations under denaturing conditions were performed with antibodies from two labs. Antibodies used were a generous gift from Dr Judith Frydman (lane 5), were purchased from Stressgen (lanes 1, 3, 4, 6, 7, 8 and 10), or were a generous gift from Dr Martin Carden (lane 2). Lane 9 has twice the amount of antibodies added as lane 7. Non-immune serum was used in lanes 9.

concentrations, see Experimental Procedures in chapter II) were used for subsequent immunoprecipitation experiments done in this dissertation.

Immunoprecipitations against the η subunit were done successfully in the presence of NaCl and not KCl. Thus, these conditions (NaCl) were to access photocrosslinking to the nascent chains in this dissertation.

Photocrosslinking of Actin 220mer to TRiC α, β, δ, ε, ζ and θ Subunits

To ascertain which subunits of TRiC photocrosslinked to actin, denaturing immunoprecipitation experiments with antibodies raised against each of the eight subunits of TRiC were performed. Since it was known that actin nascent chains as short as 133 amino acids and as long as 371 amino acids photocrosslinked to TRiC (McCallum et al., 2000), an intermediate length of actin of 220 amino acids was chosen as a starting point to determine which subunits were in proximity to the nascent chain. Photoadducts containing the actin 220mer nascent chain and six of the different TRiC subunits (α, β, δ, ε, ζ and θ) were observed (figure 15, lanes 1, 2, 4, 5, 6 and 8), and are identified by an arrowhead adjacent to lane 1.

One immediately notices a difference in the apparent molecular mass of these photoadducts. In mouse, the molecular masses of each TRiC subunit ranges from 57 to 60 kDa. The order from largest to smallest of the subunits is as follows: $\gamma > \alpha > \eta > \varepsilon > \theta > \delta > \zeta > \beta$. If one compares the photoadducts observed in figure 15, that the photoadduct to the ε subunit has a higher

apparent mass than do the photoadducts to the δ or θ subunits and a lower apparent mass than the photoadduct containing the smaller ζ subunit. Because the photoadducts to the α and β subunits are so intense and thick on this gel, it is difficult to ascertain their relative masses on this gel. However, data in chapter IV will show that the photoadduct to the α subunit does have a higher molecular mass than that of the β subunit, as expected.

In figure 15, lanes 1, 2, 4 and 8, a higher molecular mass photoadduct that is identified with a double arrowhead observed. Based on the molecular mass of these photoadduct, it would appear to be a crosslink between two TRiC subunits and the actin nascent chain. Since there are 10 lysines coded for in an actin nascent chain of 220 amino acids, there will be multiple probes in most nascent chains. Thus it is very possible that the actin nascent chain could crosslink to two TRiC subunits. One would expect that this photoadduct represents two probes being adjacent to two different subunits since cryo-EM studies have shown there to be only one of each subunit per ring and there is a septum between the rings which would not allow for the nascent chain to see subunits in the other ring. While it is possible that the nascent chain is adjacent to the outside of the TRiC complex and not the inner cavity, this seems highly unlikely given the plethora of cryo-EM structures with GroEL/ES, the thermosome and TRiC all showing the substrate inside the bi-ring structure.
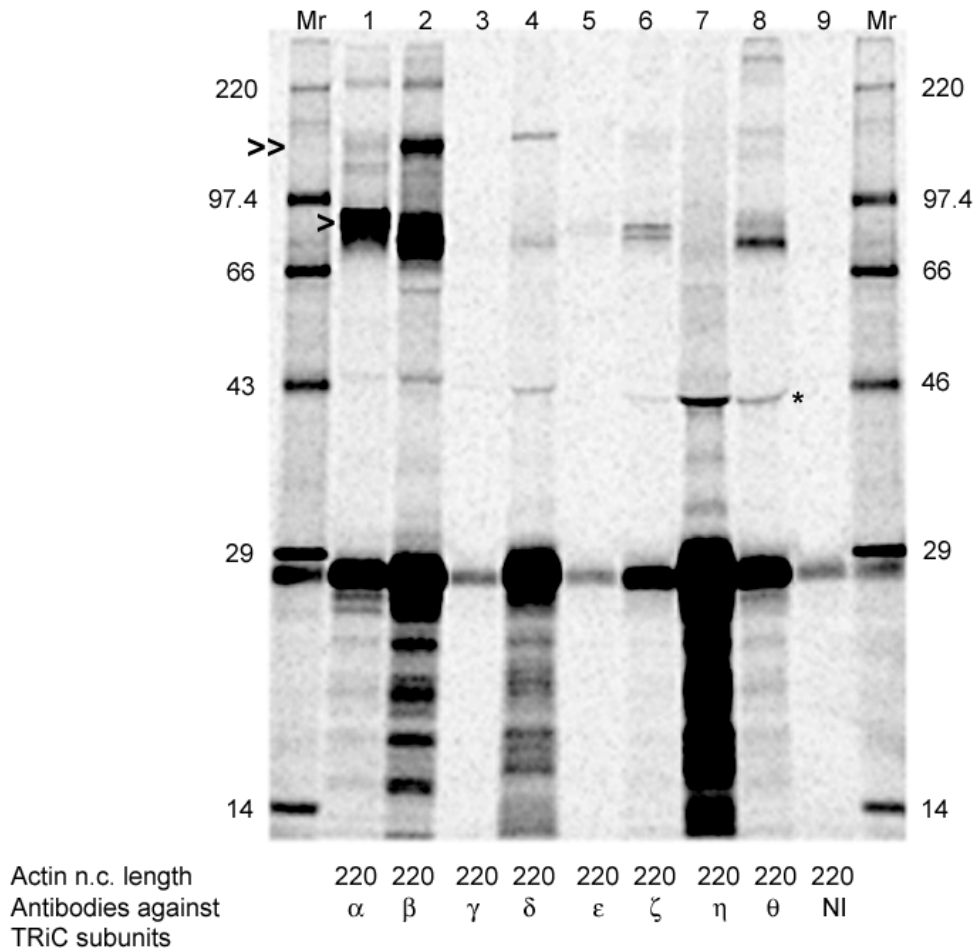
Figure 15. Photocrosslinking of Actin 220mer Nascent Chains to TRiC

The actin 220mer nascent chain was photocrosslinked to different subunits of TRiC and the photoadducts were detected by immunoprecipitation with antibodies specific for each subunit (identified by the single arrowhead). Photoadducts between Actin 220mer and TRiC α were detected (lane 1 single arrowhead), TRiC β (lane 2), TRiC δ (lane 4), TRiC ε (lane 5), TRiC ζ (lane 6) and TRiC θ (lane 8). No photoadducts were detected in lane 3, 7 or lane 9 which also acted as the negative control since it was immunoprecipitated with non-immune serum (NI). Some lanes show a band around 46 kDa that is marked with an asterisk (*). This band represents from radioactive material washed ahead of the IgG heavy chain. Also, higher molecular mass photoadducts that are marked with a double arrowhead are seen in lanes 1, 2, 4 and 8.

Length Dependence of Photocrosslinking of

Actin Nascent Chains to the TRiC β Subunit

Having shown that an actin nascent chain of 220 amino acids photocrosslinks to the TRiC β subunit, I next investigated the nascent chain length dependence of the photocrosslinking of actin to the β subunit. To address this issue, photocrosslinking experiments followed by immunoprecipitations with antibodies against the β subunit of TRiC were performed. Figure 16 shows that the actin nascent chain was in adjacent to the TRiC β subunit when nascent chains were as short at 133 amino acids and as long as 371 amino acids (lanes 2-5, indicated with arrowheads adjacent to lanes 2 and 5). This is the same length dependence that was observed for actin nascent chains with the whole TRiC complex (McCallum et al., 2000).

Photocrosslinking of Actin Nascent Chains to

Individual Subunits of TRiC in the Absence and Presence of Apyrase

The subunits of chaperonins such as the thermosome, TRiC, and GroEL are known to be ATPases (Gutsche et al., 2000b; Meyer et al., 2003; Rye et al., 1999) and cryo-EM studies have shown that nucleotide-dependent conformational changes occur within each subunit (Llorca et al., 1998; Rye et al., 1999). Thus, it is possible that the proximity of the actin nascent chain to a particular subunit of TRiC may vary depending upon whether the subunit is
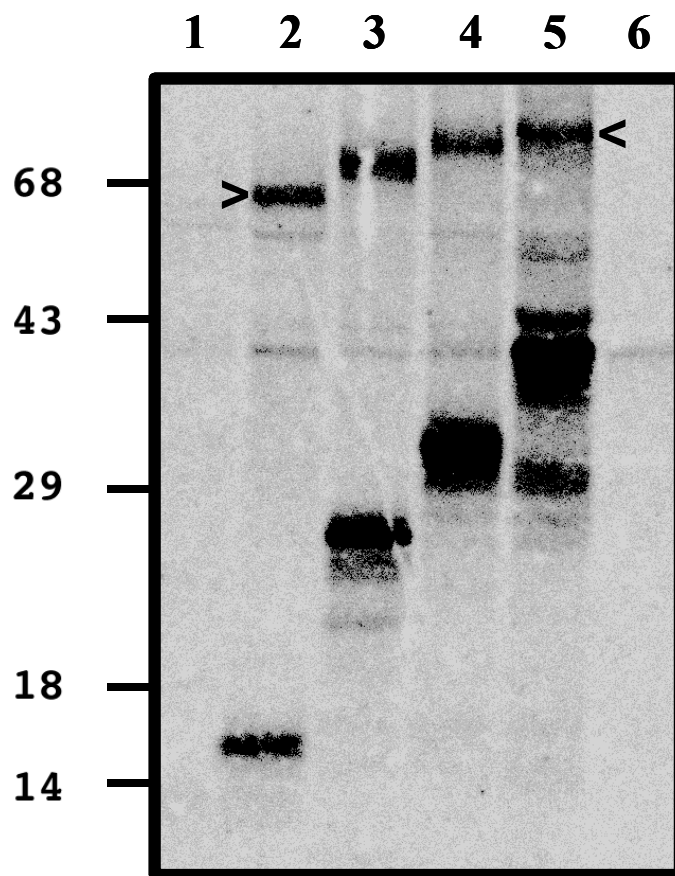
Figure 16. Nascent Chain Length Dependence of Photocrosslinking Between Actin and the TRiC β Subunit

Photoadducts between actin and the TRiC β subunit were detected by immunoprecipitation with antibodies raised against the TRiC β subunit and are identified by the arrowheads adjacent to lanes 2 and 5. Nascent chain lengths were 84 residues in lane 1; 133 in lane 2; 220 in lane 3; 303 in lane 4; 371 in lanes 5 and 6. Non-immune serum was used for the immunoprecipitation in lane 6.

bound to ATP, ADP, or no nucleotide. In order to examine this, photocrosslinking samples were split following translation and either mock-treated or treated with apyrase, an enzyme that hydrolyzes ATP. After photolysis, samples were immunoprecipitated with antibodies raised against each of the TRiC subunits. It is not possible to translate in the absence of ATP, so for this reason samples were treated with apyrase following translation, but prior to photocrosslinking to allow any conformational changes to occur as the ATP bound TRiC was converted to ADP-bound TRiC.

Figure 17 shows that photocrosslinking between the actin nascent chain and the TRiC ε subunit occurred with nascent chains as short as 133 and as long as 371 amino acids. Furthermore, the length dependence was not changed in the presence or absence of apyrase. What is striking is the difference in the intensity of the photoadducts in lanes 3 and 9 of figure 17 since the only difference between the treatments of these two samples was the addition of apyrase for 5 minutes after translation, but prior to photolysis. One explanation of this result might be that a conformational change occurred such that the probe that was crosslinking to the TRiC ε subunit in lane 3 is now closer in proximity to the subunit, or a portion of the subunit is exposed which has greater photocrosslinking efficiency than was accessible before. Does this pattern that was observed for photocrosslinking to the TRiC ε subunit hold true for photocrosslinking to other subunits?
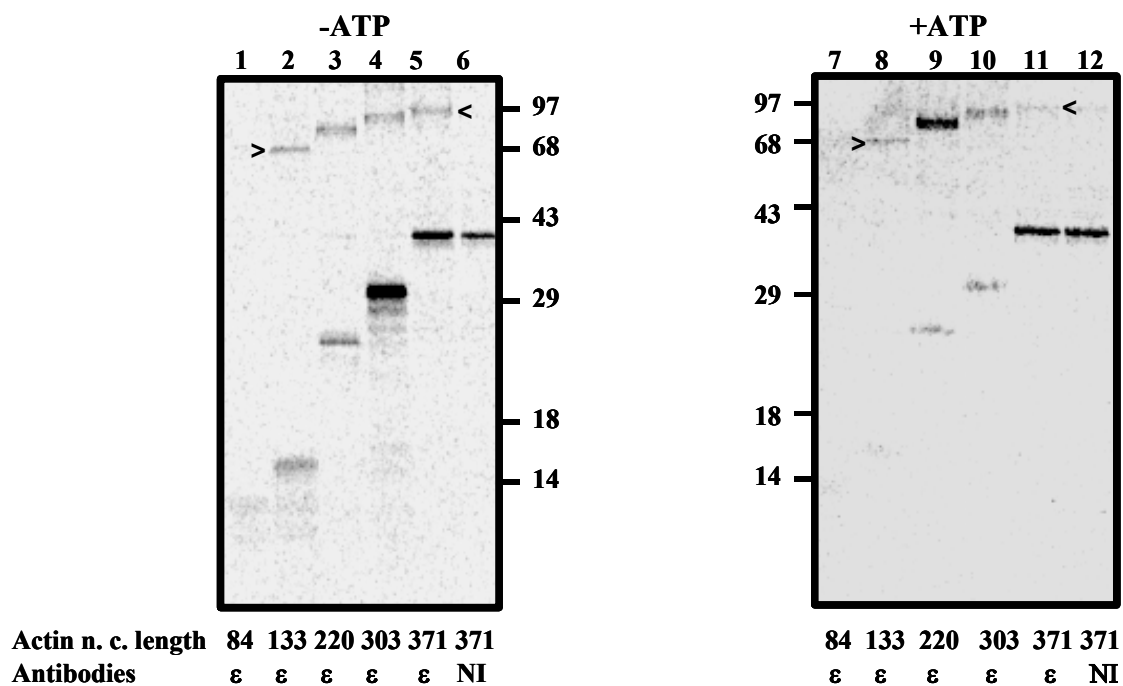
Figure 17. ATP and Length Dependence of Photocrosslinking of Actin Nascent Chains to the TRiC ε Subunit

Photoadducts between actin nascent chains and TRiC ε subunits were detected by immunoprecipitation with antibodies against the TRiC ε subunit and are identified by the arrowheads adjacent to lanes 2, 5, 8 and 11. Nascent chain lengths were 84 residues in lanes 1 and 7; 133 in lanes 2 and 8; 220 in lanes 3 and 9; 303 in lanes 4 and 10; 371 in lanes 5, 6, 11 and 12. Non-immune serum was used for the immunoprecipitations in lanes 6 and 12. Lanes 1 to 6 were treated with apyrase while lanes 7 to 12 were mock treated.

Figure 18 shows the length dependence of photocrosslinking actin nascent chains to the TRiC δ subunit. Photoadducts are observed to actin nascent chains as short as 133 amino acids and as long as 371 amino acids (figure 18, photoadducts are identified with an arrowhead adjacent to lanes 3 and 10). Thus, nascent chain the length dependence of photocrosslinking to the TRiC δ subunit is the same as it was for the β and ε subunits. However, the nascent chain length dependence of the photoadducts that appear to contain two TRiC subunits (one of which is presumably δ since this is an immunoprecipitation with δ-specific antibodies) is different. Actin nascent chains as short as 220 amino acids and as long as 371amino acids photocrosslink to two TRiC subunits (figure 18, photoadducts are identified with double arrowheads adjacent to lanes 5 and 10). This is very interesting as it suggests that a certain number of amino acids must be translated and inserted into the chaperonin before the actin nascent chain can simultaneously (or nearly so) crosslink to two TRiC subunits.

Examination of the ATP dependence of actin photocrosslinking to the TRiC δ subunit shows that the presence or absence of apyrase does not affect the length dependence of photocrosslinking, but does affect the intensity of the photoadducts that are
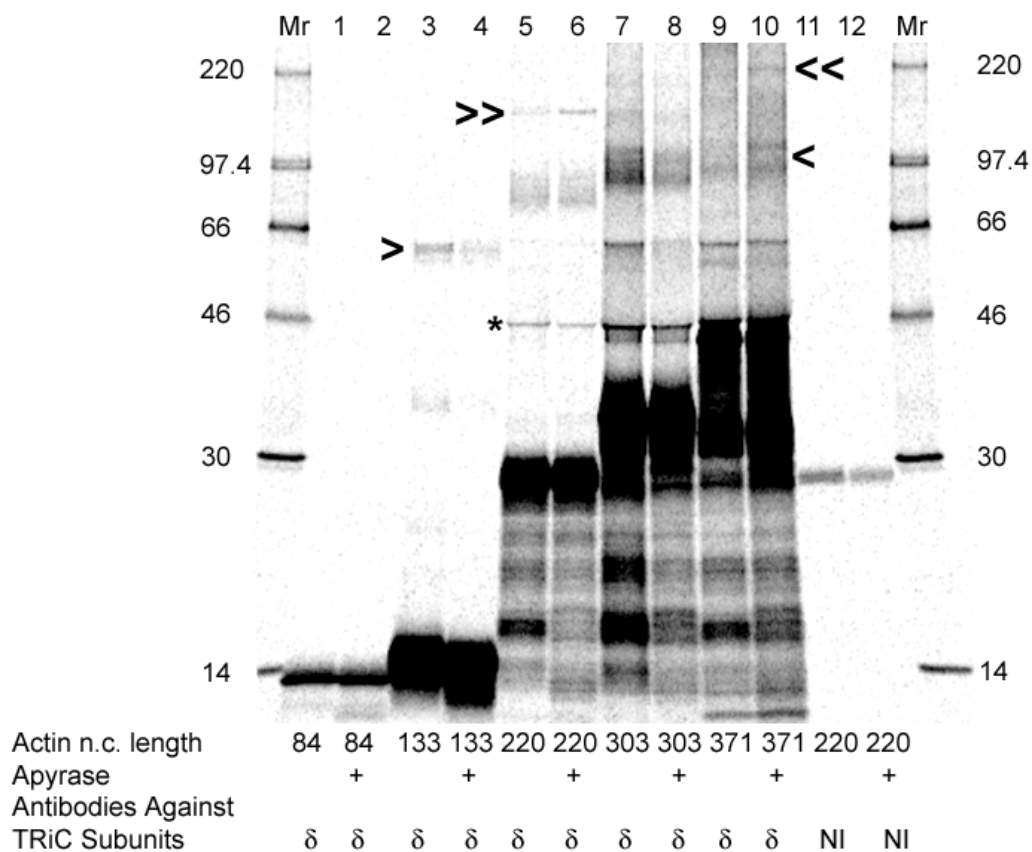
Figure 18. Nascent Chain Length and ATP Dependence of Actin Photocrosslinking to the TRiC δ Subunit

Photoadducts between actin and TRiC δ subunits were detected by immunoprecipitation with antibodies raised against the TRiC δ subunit and are identified by the arrowheads adjacent to lanes 3 and 10. Photoadducts between actin and two subunits of TRiC are indicated with a double arrowhead adjacent to lanes 5 and 10. Nascent chain lengths were 84 residues in lanes 1 and 2; 133 in lanes 3 and 4; 220 in lanes 5, 6, 11 and 12; 303 in lanes 7 and 8; 371 in lanes 9 and 10. Non-immune serum was used for the immunoprecipitations in lanes 11 and 12. Lanes that were treated with apyrase are indicated with a + sign all other lanes were mock treated. The asterisk indicates the leading edge of the IgG heavy chain band.

observed. This is shown by the more intense band of the photoadduct observed in lane 3 of figure 18 (marked with the single arrowhead) than in lane 4. This was also true for the photoadducts in lanes 7 and 8 (figure 18). In both of these cases, the lane that did not receive apyrase prior to photolysis showed more intense photoadduct formation. This agrees with what was observed for photocrosslinking to the TRiC ε subunit when actin was 220 amino acids in length (figure 17). However, at other lengths, the photoadduct bands appear to have similar intensities.

Examination of the length dependence of actin photocrosslinking to a third subunit of TRiC, the θ subunit, shows a different length dependence than was observed for the TRiC ε and δ subunits. Figure 19 shows photoadducts (identified by the single arrowhead next to lanes 5 and 10) to actin nascent chains as short as 220 amino acids and as long as 371 amino acids. In addition, the photoadducts between actin nascent chains and two TRiC subunits (one presumably θ: figure 19, identified with double arrowheads adjacent to lanes 5 and 10) have the same length dependence as the photoadducts containing a single TRiC θ subunit. This differs from what was observed for the length dependence of the single and double photoadducts to the TRiC δ subunit (figure 18), where photoadducts to the TRiC δ subunit alone were observed with nascent chains as short as 133 amino acids.
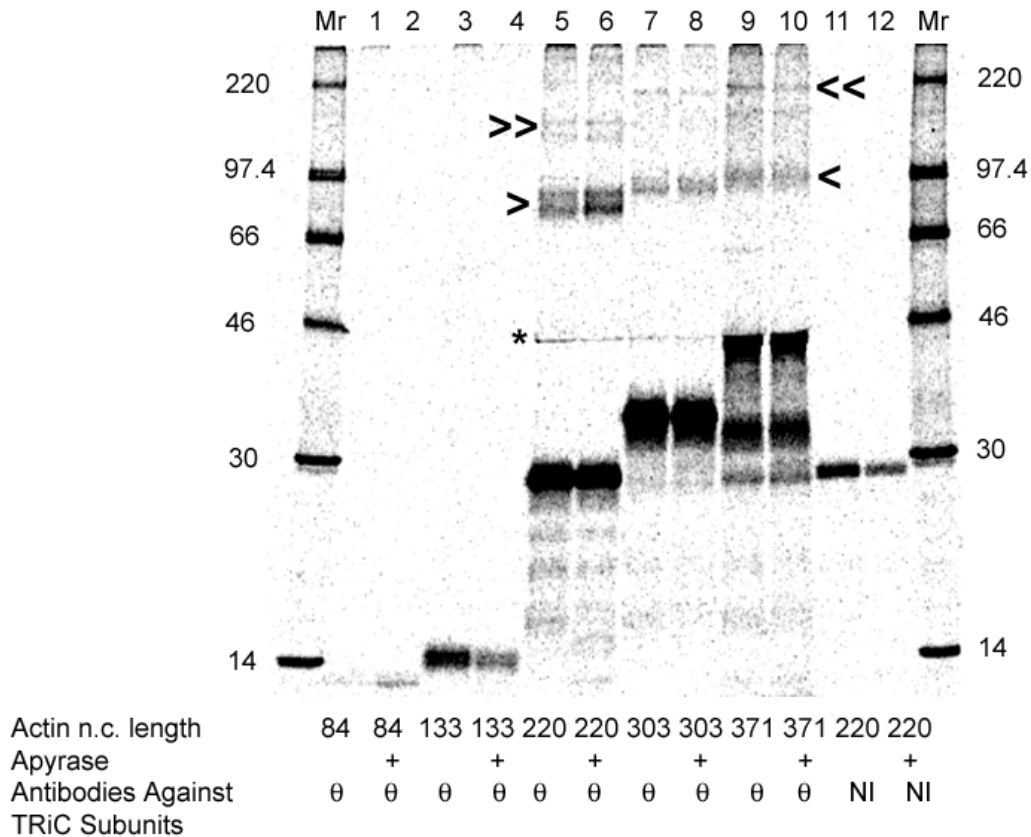
Figure 19. Nascent Chain Length and ATP Dependence of Actin Photocrosslinking to the TRiC θ Subunit

Photoadducts between actin and single TRiC θ subunits were detected by immunoprecipitation with antibodies raised against the TRiC θ subunit and are identified by the arrowheads adjacent to lanes 5 and 10. Photoadducts between actin and two subunits of TRiC are indicated with a double arrowhead adjacent to lanes 5 and 10. Nascent chain lengths were 84 residues in lanes 1 and 2; 133 in lanes 3 and 4; 220 in lanes 5, 6, 11 and 12; 303 in lanes 7 and 8; 371 in lanes 9 and 10. Non-immune serum was used for the immunoprecipitations in lanes 11 and 12. Lanes that were treated with apyrase are indicated with a + sign; all other lanes were mock treated. The asterisk indicates the leading edge of the IgG heavy chain band.

The ATP dependence of actin nascent chain photocrosslinking to the TRiC θ subunit is also different from that to TRiC ε and δ because when one compares the intensity of the photoadducts (identified with an arrowhead adjacent to lanes 5 and 10) in lanes 5 and 6 of figure 19, the photoadduct band in lane 6 is more intense than the photoadduct band in lane 5. Thus, in this case the sample treated with apyrase photocrosslinks more frequently to the TRiC θ subunit than does the sample that was mock treated. This is the reverse of what was observed for the ε subunit at this length of 220 amino acids (figure 17).

Table 4 contains a summary of actin nascent chain photocrosslinking to each of the eight TRiC subunits in the presence of apyrase, while table 5 presents a similar summary of actin photocrosslinks to each TRiC subunit in the absence of apyrase. This summary reveals that the nascent chain length dependence of photocrosslinking to the TRiC α, β, δ and ε subunits was the same in the presence or absence of apyrase, while a different length dependence was observed for photocrosslinking to the θ, η and ζ subunits of TRiC. No photocrosslinks were ever observed to the γ subunit of TRiC.

Several note-worthy points can be made about these results. First, the actin nascent chain is exposed to 7 of the 8 subunits of TRiC soon after emerging from the ribosome. Second, there is some variation in nascent chain exposure to TRiC subunits as a function of length. Third, the photocrosslinking of actin nascent chains to some TRiC subunits is ATP-dependent, suggesting that nascent chain exposure to and/or interaction with some subunits is altered

Table 4. Summary of Photocrosslinking Results with Actin Nascent Chains in the Presence of Apyrase

Actin n.c. Length	α	β	γ	δ	ε	ζ	η	θ
84	- n=2	- n=3	- n=1	- n=1	- n=1	- n=1	- n=1	- n=2
133	+ n=2	+ n=3	- n=2	+ n=2	+ n=3	- n=2	- n=1	- n=2
220	+ n=11	+ n=8	- n=4	+ n=4	+ n=5	+ n=2	- n=2	+ n=13
303	+ n=3	+ n=4	- n=1	+ n=3	+ n=4	- n=2	+ n=1	+ n=1
371	+ n=3	+ n=5	- n=2	+ n=4	+ n=4	- n=2	- n=2	+ n=1

n= number of times the experiment was repeated

Table 5. Summary of Photocrosslinking Results with Actin Nascent Chains in the Absence of Apyrase

Actin n.c. length	α	β	γ	δ	ε	ζ	η	θ
84	- n=1	- n=2	- n=1	- n=1	- n=1	- n=1	- n=1	- n=2
133	+ n=1	+ n=2	- n=1	+ n=2	+ n=1	- n=1	- n=1	- n=2
220	+ n=1	+ n=2	- n=1	+ n=2	+ n=1	- n=1	- n=1	+ n=1
303	+ n=1	+ n=2	- n=1	+ n=2	+ n=1	- n=1	+ n=1	+ n=1
371	+ n=1	+ n=2	- n=1	+ n=2	+ n=1	- n=1	- n=1	+ n=2

n=number of times the experiment was repeated

by ATP-dependent changes in their conformation or topography. A general pattern that emerges from these tables is that as actin gets longer, more TRiC subunits photocrosslink until the nascent chain reaches about 303 amino acids and then photocrosslinks to one less TRiC subunit is observed. This is interesting and represents a first look at the proximity of the actin nascent chain to each TRiC subunit as actin emerges from the ribosome. Thus the picture actins environment as it leaves the ribosomal tunnel is becoming clearer.

Luciferase

In order to ascertain if a different nascent chain would exhibit the same photocrosslinking properties as actin, in terms of nascent chain length and the presence of ATP, luciferase was examined. Previous work by McCallum and colleagues showed that luciferase can photocrosslink to TRiC in in vitro translation experiments (McCallum et al., 2000). Luciferase is a 551 amino acid enzyme that has been used for many years as a reporter gene because of the ease with which its functional assay can be performed. As was outlined in chapter I, luciferase can fold in a co-translational manner and the N-terminal subdomain that consists of amino acids 1-190 folds first in vitro (Frydman et al., 1999). For this reason luciferase nascent chains similar to those used in by McCallum and coworkers were employed here (McCallum et al., 2000). Figure 20 shows the position of every lysine residue in the wild type luciferase protein
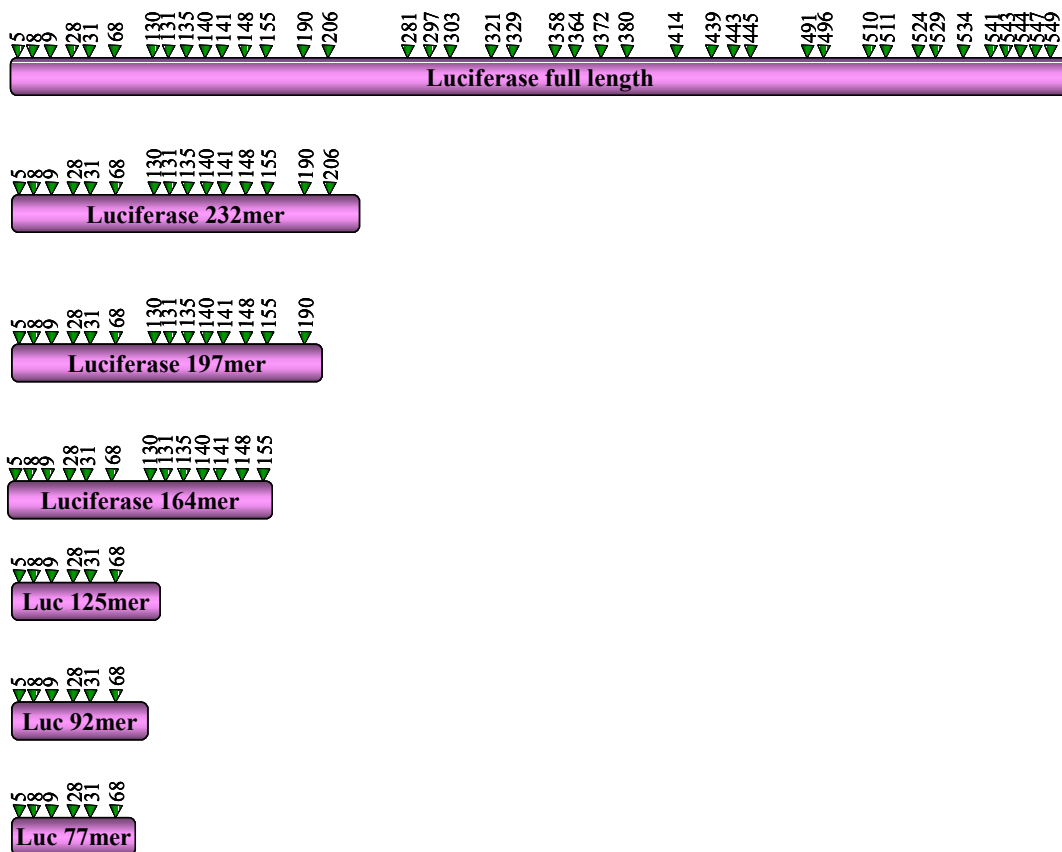
Figure 20. Luciferase Nascent Chains

Full length luciferase and luciferase nascent chains are shown above as purple rods. The length in amino acids is indicated in the center of each rod. A green arrowhead marks the position of each lysine residue and the number above refers to the number of that amino acid in the protein sequence, with the N-terminal methionine being labeled number 1.

and in each of the nascent chains used, identified by an arrowhead and number corresponding to the position of the lysine residue in the sequence, with the N-terminal methionine being number 1.

Photocrosslinking of Luciferase 197mer to the TRiC α, β, δ and θ Subunits

In order to determine to which subunits of TRiC the luciferase nascent chain photocrosslinked, experiments were performed as before with the actin nascent chain. Briefly, luciferase 197mer nascent chains were translated, photolyzed, split into 9 equal aliquots, and then immunoprecipitated with antibodies against each of the eight TRiC subunits. Figure 21 shows the results of this experiment. Photoadducts to luciferase nascent chains are identified with arrowheads adjacent to lanes 1 and 8. Photoadducts of luciferase to the TRiC α, β, δ and θ subunits can be observed in lanes 1, 2, 4 and 8 of figure 21. What is striking is the difference in intensity of the photoadduct bands. The photoadduct bands containing the TRiC β subunit are much stronger than those of the other photoadducts. Furthermore, the β photoadducts appear as a doublet and not as a singlet like the other subunits. A doublet can occur if two populations of luciferase nascent chain-TRiC β subunit covalently complexes occur that have different electrophoretic mobilities. Such populations can arise because the crosslinks occur at different locations in the nascent chain (there are multiple probes per nascent chain) and hence give rise to two distinct photoadducts on the gel. Another possibility is that the luciferase nascent chain
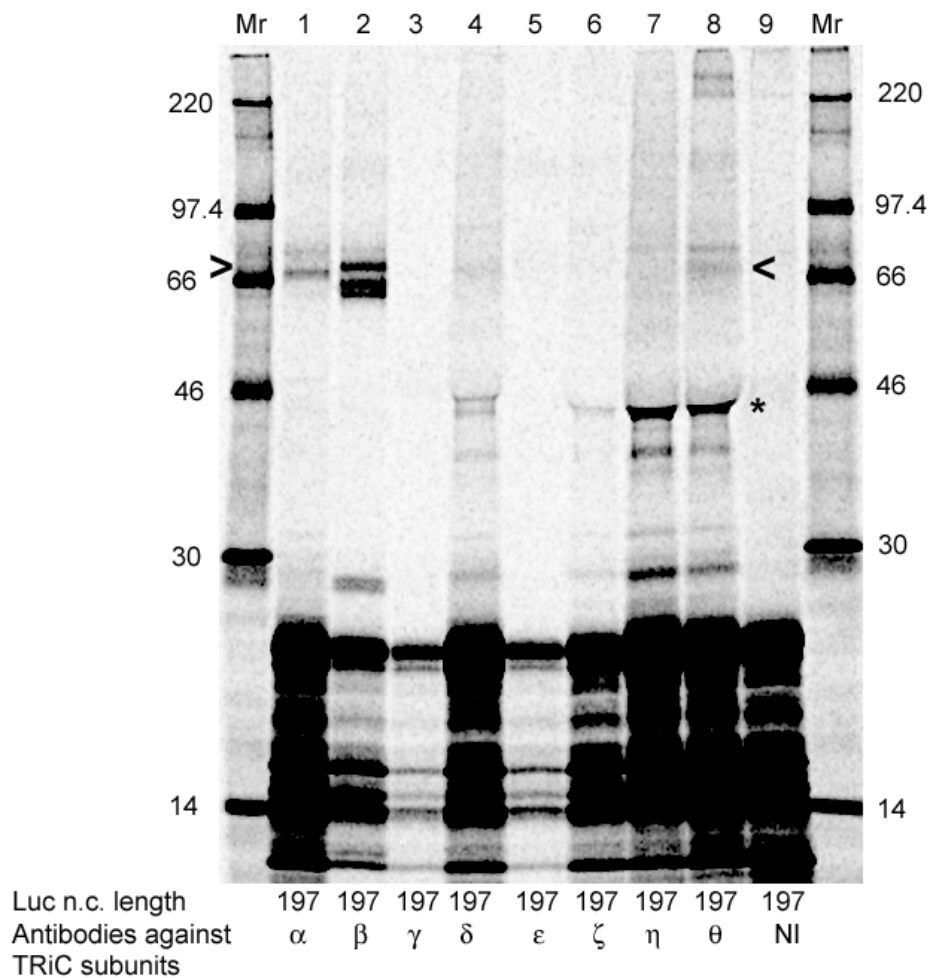
Figure 21. Photocrosslinking of Luciferase 197mer Nascent Chains to TRiC Subunits

The luciferase 197mer nascent chain photocrosslinked to different subunits of TRiC and the photoadducts were detected by immunoprecipitation with antibodies specific for each subunit (identified by the single arrowhead). Photoadducts were detected between luciferase 197mer and TRiC α were detected (lane 1 single arrowhead), TRiC β (lane 2), TRiC δ (lane 4), TRiC ε (lane 5) and TRiC θ (lane 8). Even upon prolonged exposure of this gel to the phosphorimager screen, no photoadducts were detected in lanes 3, 7 or lane 9, which also acted as the negative control since it was immunoprecipitated with non-immune serum (NI). Some lanes show a band around 46 kDa that is marked with an asterisk (*). This band represents radioactive material washed ahead of the IgG heavy chain band.

photocrosslinks to two distinct sites on the β subunit of TRiC and this yield two photoadducts with different electrophoretic mobilities. There is precedence of this effect in photocrosslinking studies involving Sec61α (Plath and Rapoport, 2000).

As was stated earlier in this chapter, the β subunit of TRiC is smaller than the α subunit of TRiC. It is therefore somewhat of a surprise to see a band in lane 2 of figure 21 migrates more slowly than the photoadduct to the TRiC α subunit (lane 1). However, the photoadduct to the TRiC θ subunit migrates at about the same molecular mass as the photoadduct to the TRiC α subunit even though θ is smaller than α. Thus, since it is not known where on the TRiC α subunit the luciferase nascent chain is photocrosslinking, the slower migration of that photoadduct is likely a result of where the covalent bond between the two proteins occurs. However since an abnormal mobility was not observed for the actin-TRiC α subunit photoadduct, it is possible that luciferase is interacting with the α subunit of TRiC in a different manner and/or place than actin did. Alternatively, it could mean that a probe at a different location in the luciferase nascent chain photocrosslinks to the α subunit of TRiC.

Nascent Chain Length and ATP Dependence of Luciferase

Photocrosslinking to TRiC θ

To determine if luciferase has the same nascent chain length dependence of photocrosslinking to the θ subunit as was observed for the actin nascent chain, immunoprecipitation experiments were performed as before. The length dependence of luciferase nascent chains photocrosslinking to the TRiC θ subunit shows that nascent chains as short as 92 amino acids and as long as 232 amino acids photocrosslink to TRiC θ (figure 22, photoadducts are identified with arrowheads adjacent to lanes 3 and 12). The photoadducts are most intense for the 125mer of luciferase, and become much weaker in intensity as the nascent chain lengthens (figure 22, lane 6). No photoadducts appear to the TRiC ζ subunit (figure 22, lanes 15 and 16).

The length dependence for photocrosslinking to the TRiC θ subunit for actin was different from that seen for luciferase. In the case of actin, photoadducts were observed with nascent chains as short as 220 amino acids and as long as 371 amino acids. This difference could be due to the difference in the natural positions of the lysine residues and hence the photoreactive probes in the nascent chain or it could be the result of a different recognition sequence for TRiC on the luciferase nascent chain.
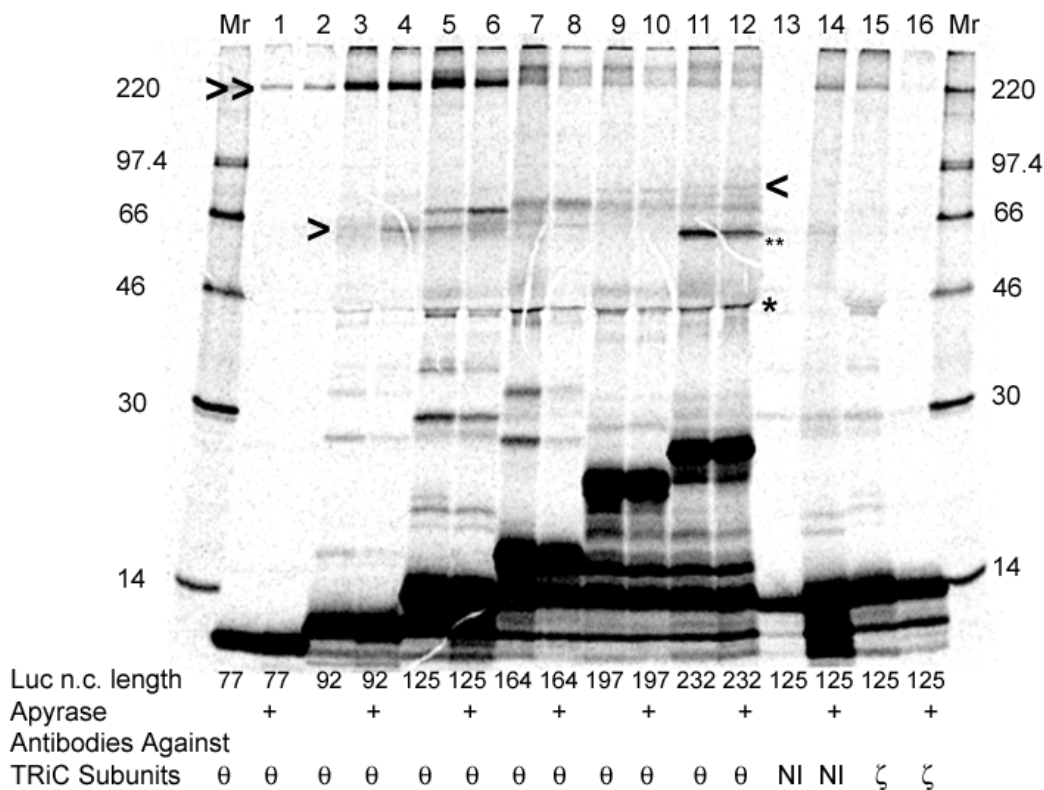
Figure 22. Photocrosslinking of TRiC θ and ζ to Luciferase Nascent Chains

Photoadducts between Luciferase and single TRiC θ subunits were detected by immunoprecipitation with antibodies specific for the TRiC θ subunit and are identified by the arrowheads adjacent to lanes 3 and 12. An unidentified high molecular mass species is indicated with a double arrowhead adjacent to lane 1, a low molecular mass species is identified by the double asterisk, and the leading edge of the immunoglobulin band is identified with a single asterisk. Nascent chain lengths were 77 residues in lanes 1 and 2; 92 in lanes 3 and 4; 125 in lanes 5-6 and 13-16; 164 in lanes 7 and 8; 197 in lanes 9 and 10; and 232 in lanes 11 and 12. Non-immune serum was used for the immunoprecipitations in lanes 13 and 14. Lanes that were treated with apyrase are indicated with a + sign; all other lanes were mock treated.

Examination of the ATP dependence of photocrosslinking of luciferase nascent chains to TRiC θ subunits shows that in the presence or absence of apyrase, an enzyme that hydrolyses ATP, photoadducts to TRiC θ were observed at every length of nascent chain tested regardless of the apyrase treatment. However, the intensities of the photoadduct bands containing the luciferase 92mer and the 125mer were stronger in the presence of apyrase than in the mock-treated samples (figure 22, lanes 3 verses 4 and lanes 5 verses 6). Photoadducts of the TRiC θ subunit to actin nascent chains of 220 amino acids were also more intense in the presence of apyrase than in the absence (figure 19, lanes 5 verses 6). With both the actin and luciferase nascent chains, this difference in the extents of photoadduct formation in the presence or absence of apyrase was observed at the shortest lengths. For longer nascent chains, this difference in photoadduct yield was less apparent.

Nascent Chain Length and ATP-Dependence of Photocrosslinking of Luciferase to TRiC α, β, δ, ε, η and θ Subunits

To examine the nascent chain length and ATP dependence of the photocrosslinking of luciferase translation intermediates to each of the seven remaining TRiC subunits, immunoprecipitation experiments were performed as before. Table 6 shows a summary of these experiments performed in the

Table 6. Summary of Photocrosslinking Results with Luciferase Nascent Chains in the Presence of Apyrase

Luc n.c. Lengths	α	β	γ	δ	ε	ζ	η	θ
77	+ n=1	+ n=1	- n=1	- n=2	+ n=1	- n=2	- n=1	- n=1
92	+ n=1	+ n=2	- n=1	+ n=1	+ n=1	- n=2	- n=1	+ n=1
125	+ n=2	+ n=2	- n=1	+ n=2	+ n=2	- n=3	+ n=1	+ n=3
164	+ n=4	+ n=4	- n=1	+ n=2	+ n=2	- n=2	- n=1	+ n=2
197	+ n=5	+ n=5	- n=2	- n=3	+ n=2	- n=3	- n=2	+ n=4
232	+ n=2	+ n=3	- n=1	- n=3	+ n=2	- n=2	- n=2	+ n=1

n=number of times the experiment was repeated

Table 7. Summary of Photocrosslinking Results of Luciferase Nascent Chains in the Absence of Apyrase

Luc n.c. lengths	α	β	γ	δ	ε	ζ	η	θ
77	+ n=1	+ n=1	- n=1	- n=2	- n=1	- n=1	- n=1	- n=2
92	+ n=1	+ n=1	- n=1	+ n=1	+ n=1	- n=1	- n=1	- n=2
125	+ n=1	+ n=1	- n=1	+ n=2	+ n=1	- n=2	+ n=1	+ n=2
164	+ n=1	+ n=1	- n=1	+ n=1	+ n=1	- n=1	- n=1	+ n=2
197	+ n=1	+ n=1	- n=1	+ n=1	+ n=1	- n=1	- n=1	+ n=2
232	+ n=1	+ n=1	- n=1	- n=2	+ n=1	- n=1	- n=1	+ n=1

n=number of times the experiment was repeated

presence of apyrase, which represents the minus ATP conditions, while table 7 shows the photocrosslinking in the presence of ATP.

The nascent chain length dependencies of photocrosslinking to the TRiC α, β and ε subunits were similar, with photoadducts to nascent chains as short as 77 amino acids and as long as 232 amino acids (table 6). The TRiC δ subunit showed photoadducts to luciferase with nascent chains as short as 92 amino acids and as long as 164 amino acids, which is markedly different from the length dependencies of the TRiC α, β and ε subunits mentioned above. The TRiC θ subunit photocrosslinked to luciferase nascent chains as short as 92 amino acids and as long as 232 amino acids. And finally, the TRiC η subunit was only seen to photocrosslink to luciferase when it was 125 amino acids in length. Photoadducts between luciferase nascent chains in translation intermediates and the TRiC γ and ζ subunits were never observed. The presence or absence of apyrase had little affect on the presence or absence of photoadducts to luciferase nascent chains of different lengths. As was shown, earlier the greatest difference was usually in the intensity of the photoadduct bands.

A general trend that can be observed from tables 6 and 7 is that photoadducts to the greatest number of TRiC subunits were observed at a luciferase nascent chain length of 125 residues, and that fewer TRiC subunits were photocrosslinked as the nascent chain increased in length. This is similar

to the general trend observed for actin, although the lengths at which this trend

was observed for actin are not the same.

CHAPTER IV

PHOTOCROSSLINKING STUDIES OF THE CO-TRANSLATIONAL PROXIMITY OF THE CHAPERONIN TRiC TO SPECIFIC SITES IN ACTIN NASCENT CHAINS

Experimental Design

To determine which lysine residue(s) in the actin nascent chain was/were photocrosslinking to TRiC, several constructs were created with a single amber stop codon at the position of one of the lysine codons. Since photocrosslinking to TRiC was observed with actin nascent chains containing multiple probes when the nascent chain was 133 residues in length (figure 16) and only 5 of the 7 lysine residues had exited the ribosomal tunnel, a probe at position 18, 50, 61, 68, or 84 must be responsible for photocrosslinking to TRiC. Thus, the lysine residue at 18, 50, 61, 68, or 84 was changed by site-directed mutagenesis to an amber stop codon to form five separate constructs named Actin^{18amb}, Actin^{50amb}, Actin^{61amb}, Actin^{68amb}, and Actin^{84amb}, respectively (see figures 10, 23 and Experimental Procedures). Each construct then differed in the location of the single photoreactive probe in each nascent chain. Ribosome-bound actin nascent chains were prepared by in vitro translation as outlined in chapter III and Experimental Procedures, except that εANB-Lys-TRNA^{amb} was added instead of εANB-Lys-tRNA^{Lys}. Thus, a single modified lysine was incorporated into each actin nascent chain that remained ribosome-bound (the
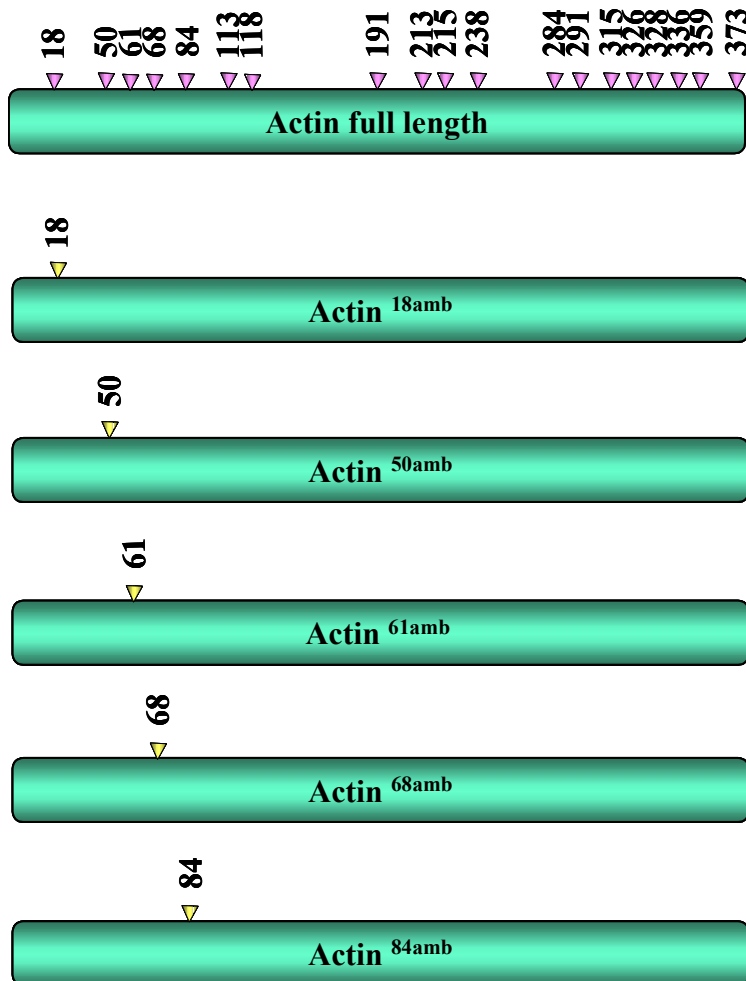
Figure 23. Actin Single Site Amber Suppressor Constructs

The actin protein is represented with an aqua cylinder. The position of each lysine residue in the wild type actin protein (actin full length, 375 amino acids) is marked with a purple arrowhead and the number of that lysine is written above the corresponding arrowhead. Each single site amber suppressor construct is named for the lysine residue that was changed to an amber stop codon. The position of each amber stop codon is marked with a yellow arrowhead and the corresponding amino acid number is shown above the arrowhead.

nascent chains that were terminated at the amber stop codon by the action of the termination factor did not receive a probe were released from the ribosome). Only intermediates that incorporated the modified lysine would have the stop codon suppressed and would continue translation to the correct nascent chain length. All translation products that were not suppressed would be terminated due the amber stop codon and hence would not have incorporated modified lysine. Such nascent chains did not affect the results of the photocrosslinking because they lacked the photoreactive probe. This approach allows one to monitor the proximity of specific nascent chain sites to TRiC. Since the lengths of the nascent chains can be programmed as outlined in chapter III and Experimental Procedures, the length dependence of the photocrosslinking and hence the proximity of a single modified lysine to an individual TRiC subunit can be determined.

Translation and Suppression of Amber Stop Codons in Actin

A construct called actin ^{84amb} that contained an amber stop codon at codon 84 in the actin sequence was constructed by site-directed mutagenesis. Actin^{84amb} was efficiently translated only in the presence of Lys-tRNA^{amb} (figure 24, lanes 2, 4, 6, 8, 10 and 12). The observed molecular mass of each actin^{84amb} nascent chain was in good agreement with the calculated molecular mass of that Actin^{84amb} nascent chain and in good agreement with the corresponding actin wild type nascent chain of the same length. The same type

of experiment was performed for Actin[18amb] 60-371mers inclusive, Actin[50amb] 60-371mers.

Figure 24. In vitro Translation of Actin[84amb] Nascent Chains in Rabbit Reticulocyte Lysate

In vitro translation in RRL of actin [84amb] nascent chains in the presence or absence of Lys-tRNA[amb]. Nascent chain lengths were 133 amino acids in lanes 1 and 2; 177 in lanes 3 and 4; 260 in lanes 5 and 6; 303 in lanes 7 and 8; 337 in lanes 9 and 10; 371 in lanes 11 and 12.
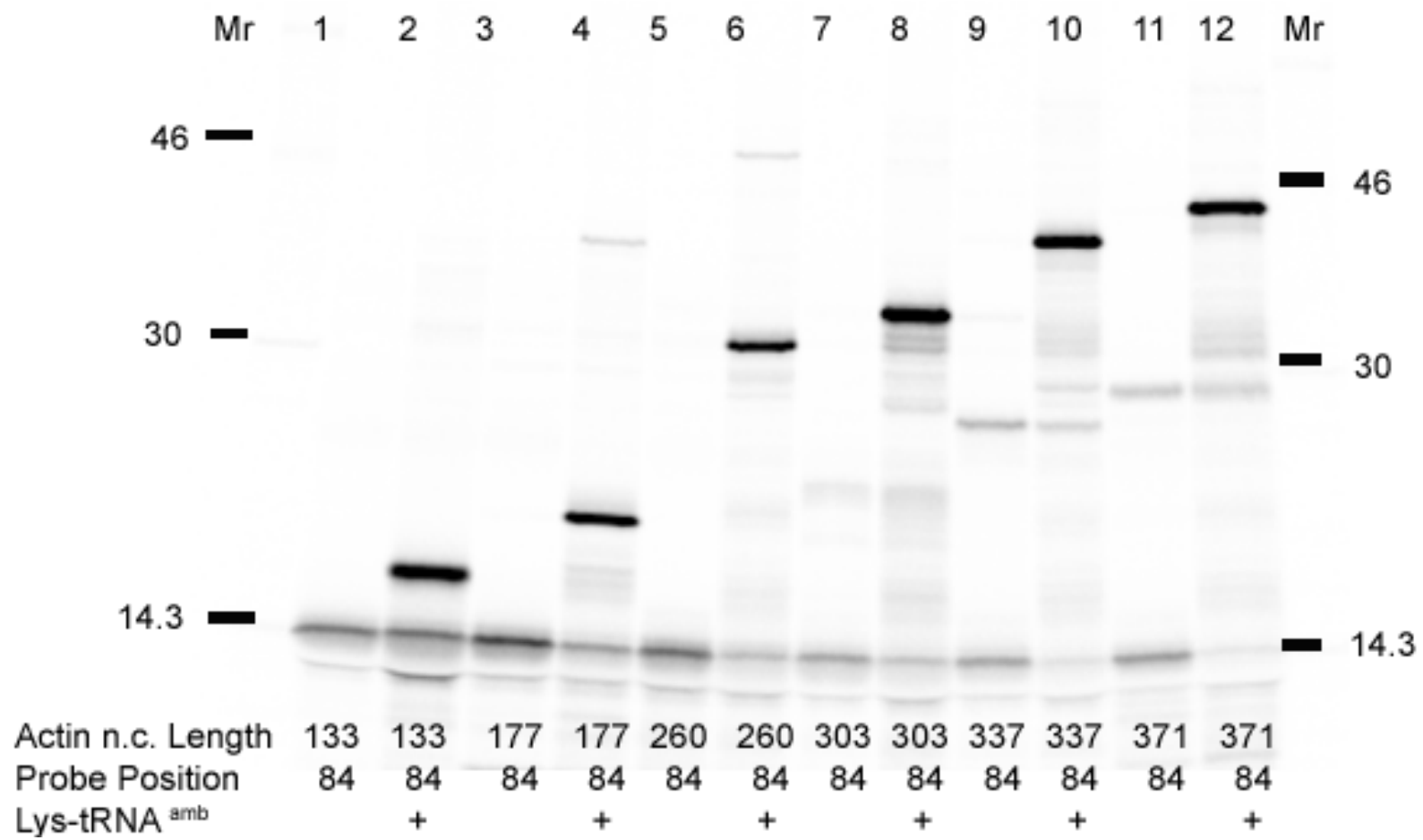
inclusive, Actin[61amb] 84-371mers inclusive and Actin[68amb] 84-371mers inclusive. The results of those experiments all showed that there was suppression of the amber stop codon only in the presence of Lys-tRNA[amb] and the observed molecular masses corresponded well with the calculated nascent chain molecular masses at each nascent chain length (data not shown).

The data shown in figure 24 are particularly noteworthy because they reveal that the efficiency of amber stop codon suppression is exceptionally high in some samples. This is evidenced by the high proportion of nascent chains (>50%) that reach their full truncated lengths instead of being terminated at a length of 84 (e.g., the number of 371-long nascent chains was 8 –fold higher than the number of 84-long nascent chains in lane 12 when the cpm per band was normalized for the number of methionines in each nascent chain).

Incorporation of εANB-Lysine at Amber Stop Codon sites in Actin and Luciferase Single-Site Amber Stop Codon Constructs

Using the actin[61amb] 220mer mRNA, in vitro translation reactions were performed as outlined above with the modification that no [^{35}S]methionine was added to the samples. Thus, the only radioactive component in each sample was the εANB-[^{14}C]Lys-tRNA[amb]. Only nascent chains that are suppressed will have incorporated the modified radiolabeled lysine and hence will be visualized by phosphorimaging. The modified lysine residue was incorporated into the actin[61amb] nascent chain (Figure 25, lane 4). Another observation from this gel is

| Mr | 1 | 2 | 3 | 4 | 5 | 6 | 7 | 8 | Mr |

Actin n.c. length	220	220	220	220					
Luc n.c. length					232	232	232	232	
Probe position	All	61	61	61	All	68	68	68	
εANB-Lys-tRNA Lys	60				60				pmoles
εANB-Lys-tRNA amb		40	60	80		40	60	80	pmoles
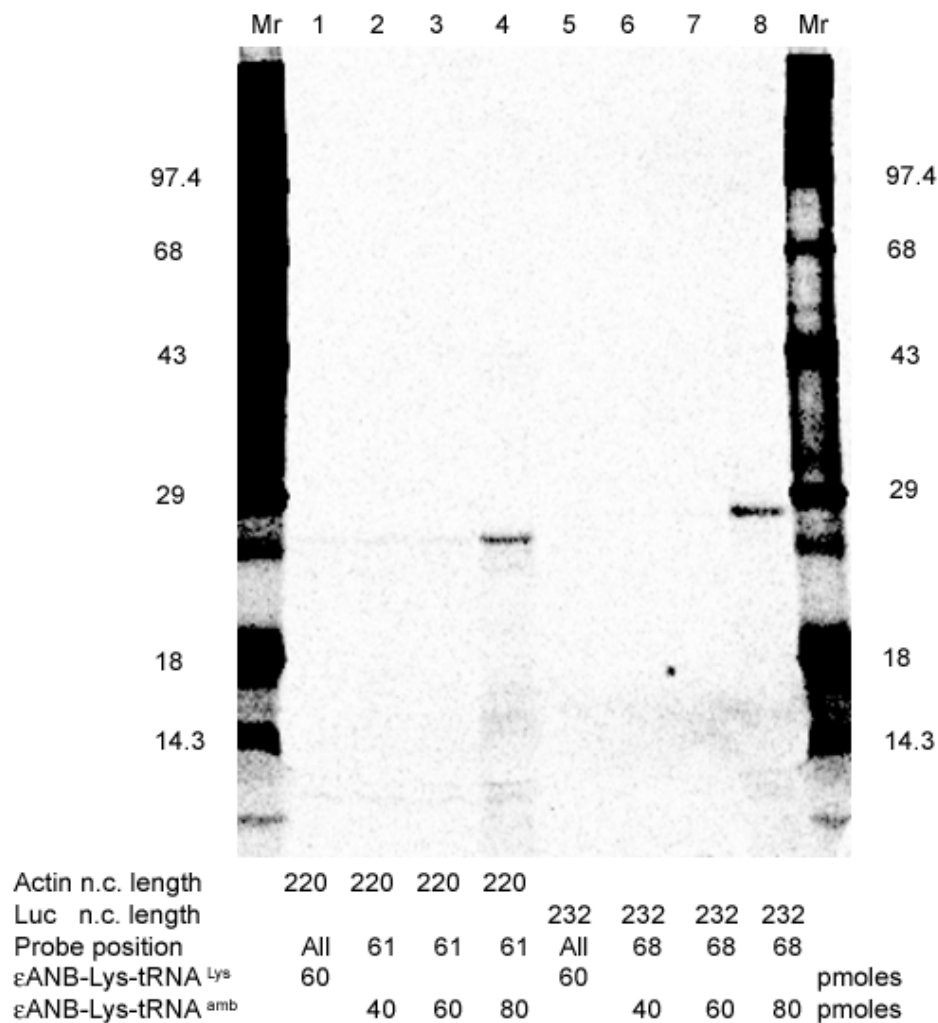
Figure 25. Incorporation of εANB-[^{14}C]Lysine During in vitro Translation of Actin^{61amb} 220mer and Luc^{68amb} 232mer Nascent Chains

Nascent chains were prepared as before except that incubations were increased to 100 μl and no [^{35}S]Met was added. A titration of the amount of εANB-Lys-tRNA^{amb} added was performed in lanes 2-4 (Actin^{61amb} 220mer) and lanes 6-8 (Luc^{68amb} 232mer).

that in a 100 μl translation reaction, 80 pmoles of εANB-Lys-tRNA^{amb} are needed to see the 220mer nascent chain or the Luc^{68amb} 232mer nascent chain (figure 25, lane 4 and 8). In lanes 1 and 5, the wild type actin and luciferase with the εANB-Lys-tRNA^{Lys} were examined as controls, but no nascent chains were visualized in this gel because the particular *E. coli* tRNA used here recognized only the AAA lysine codon and, was later shown to be very poor at incorporation into the actin or luciferase nascent chains that were *in vitro* translated in RRL. In the experiment reported in the previous chapter, the incorporation of εANB-Lys was much higher because I used εANB-Lys-tRNA^{Lys} that was purified from brewer's yeast containing isoacceptors that recognized both the AAA and AAG lysine codons. Importantly, though, the data in figure 25 reveal that a modified lysine can be incorporated efficiently into actin nascent chains during *in vitro* translation in RRL using amber suppressor tRNAs, just as the modified lysine residues were incorporated into the actin wild type constructs during *in vitro* translation in RRL using εANB-Lys-tRNA^{Lys}.

Photocrosslinking of Actin$^{18-84amb}$ 220mers to the TRiC β Subunit

To determine which probe locations in nascent actin can photocrosslink to the TRiC β subunit, constructs of actin which can incorporate a photoreactive probe at only one position along the nascent chain were *in* vitro translated, photolyzed, and immunoprecipitated with antibodies against the TRiC β subunit.

Photocrosslinking showed that Actin[61amb] 220mer was adjacent to the TRiC β

subunit (figure 26, lane 3). In addition, photocrosslinking showed that probes at

positions 18, 50, 68 and 84 of the 220mer nascent chains were also adjacent to

the TRiC β subunit. Crosslinking was observed previously between the TRiC β

subunit and multiply-labeled actin 220mer nascent chains (figures 15 and 16).

Thus, the new observation that a single probe at any one of these 5 positions is

adjacent to the TRiC β subunit is consistent with the previous findings.

Nascent Chain Length Dependence of Actin [18, 50, 61, 68 and 84amb]
Photocrosslinking to the TRiC β Subunit

To determine the nascent chain length dependence of probes located at

positions 18, 50, 61, 68, or 84 being adjacent to the TRiC β subunit,

photocrosslinking experiments and subsequent immunoprecipitations were

performed as above with actin[18, 50, 61, 68 and 84amb] nascent chains of different

lengths. Photocrosslinking showed that the TRiC β subunit was adjacent to the

probe at position 18 when the nascent chain length was at least 84 amino acids

in length (figure 27, lane 2). Position 18 continued to be adjacent to the TRiC β

subunit until almost the entire actin protein had been synthesized (figure 27,

lanes 3-9). Although the translations shown in lanes 2 and 5 in this particular

gel were sub-optimal, the photoadducts were still immunoprecipitated and were

clearly visible at longer exposure times.
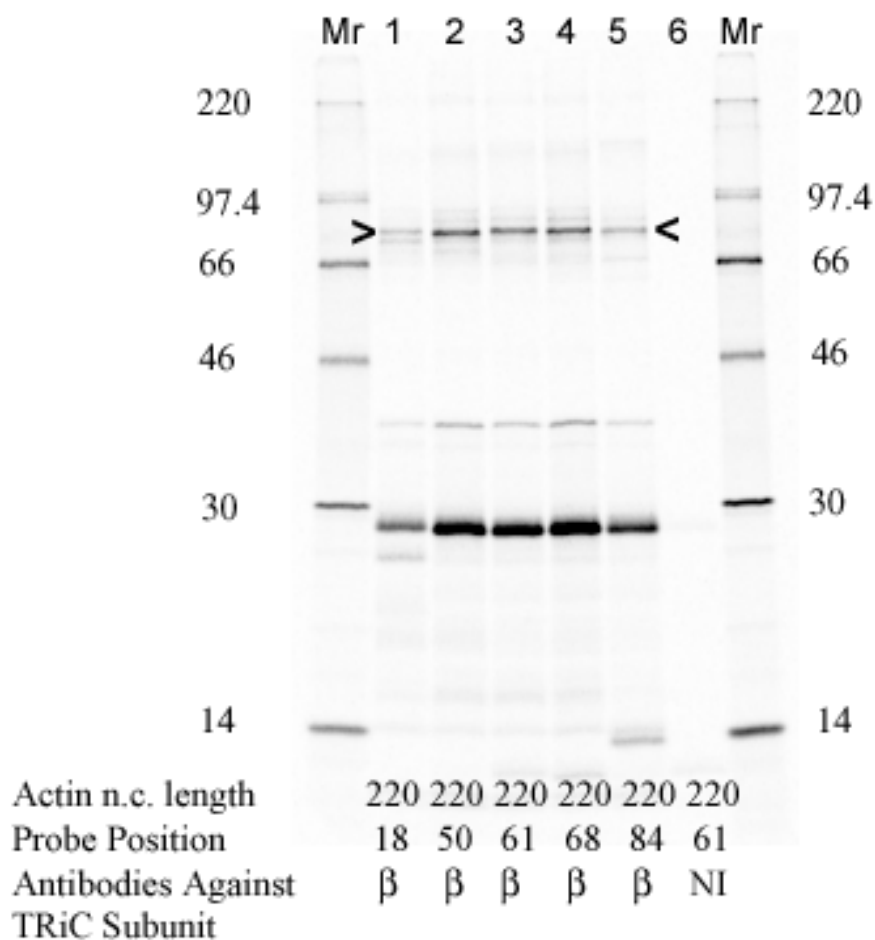
Figure 26. Photocrosslinking of TRiC β Subunit and Actin[18-84amb] 220mer Nascent Chains

The actin[18-84amb] 220mer nascent chains photocrosslinked to the TRiC β subunit, and the photoadducts were detected by immunoprecipitation using antibodies against the TRiC β subunit (identified by the arrowheads next to lanes 1 and 5). No photoadduct was immunoprecipitated with a sample containing an Actin[61amb] 220mer nascent chain when non-immune serum was used (lane 6).
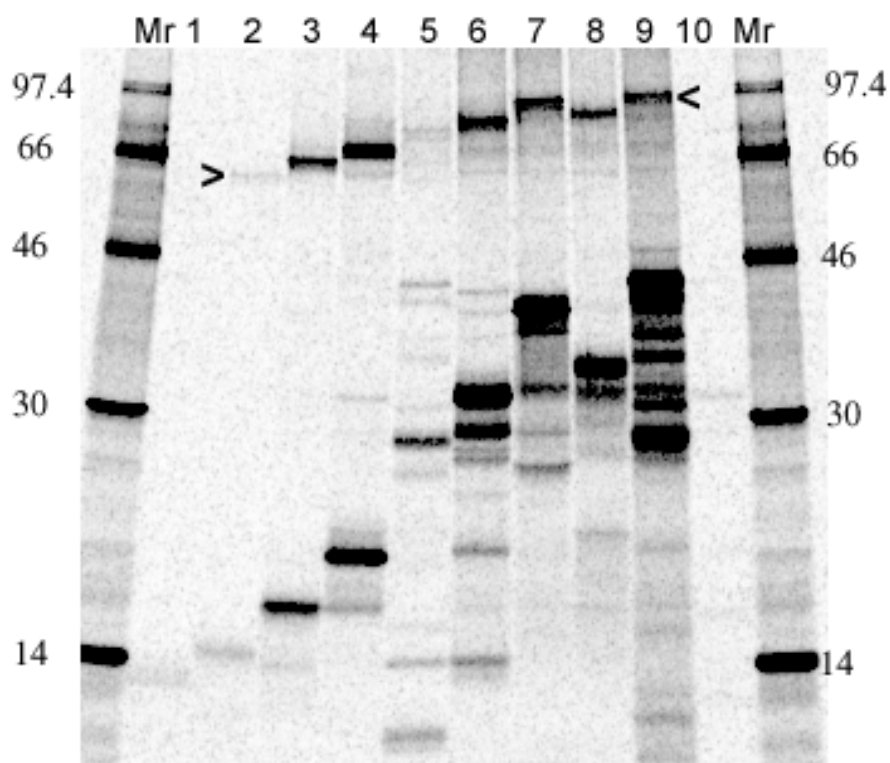
Actin n.c. length	60	84	133	177	220	260	337	303	371	260
Probe position	18	18	18	18	18	18	18	18	18	18
Antibodies to Individual TRiC subunit	β	β	β	β	β	β	β	β	β	NI

Figure 27. Nascent Chain Length Dependence of Photocrosslinking of the TRiC β Subunit to Actin[18amb] Nascent Chains

Photoadducts were detected by immunoprecipitation with affinity-purified antibodies raised against the TRiC β subunit and are identified by the arrowheads adjacent to lanes 2 and 9. Nascent chain lengths were 60 residues in lane1; 84 in lane 2; 133 in lane 3; 177 in lane 4; 220 in lane 5; 260 in lanes 6 and 10; 337 in lane 7; 303 in lane 8; 371 in lane 9. Non-immune serum was used for the immunoprecipitation in lane 10.

When constructs with the amber stop codon (and hence the photoreactive probe) at position 50 were examined, the shortest nascent chain length that formed a photoadduct was 133 amino acids (figure 28, lane 2). The probe at position 50 was still adjacent to the TRiC β subunit when the actin nascent chain was 371 amino acids in length (figure 28, lane 8). No photoadduct contained nascent chains as short as 84 amino acids (figure 28, lane 1). This is not a surprise, since the probe at position 50 is only 34 amino acids from the P-site of the ribosome in the actin 84mer and since the ribosomal tunnel is thought to contain 35-40 residues of the nascent chain (Blobel and Sabatini, 1970; Malkin and Rich, 1967). Hence, the probe at position 50 in the actin 84mer may not have exited the ribosomal tunnel yet, and hence would not be adjacent to TRiC.

The data in figures 27 and 28 are also interesting because the efficiency of photoadduct formation from position 18 does not appear to vary much as the nascent chain length increased (figure 27), while there is considerable variation in the photocrosslinking via position 50 in nascent chains of different lengths (figure 28). This suggests that the exposure of actin 50 to the TRiC β subunit and /or the interaction of actin near residue 50 with β varies as nascent chain folding proceeds.

To ascertain over what lengths of nascent chain the probe at position 61 is adjacent to the TRiC β subunit, photocrosslinking and immunoprecipitation experiments similar to those in figures 27 and 28 were performed.

Figure 28. Nascent Chain Length Dependence of Photocrosslinking of the TRiC β Subunit to Actin^{50amb} Nascent Chains

Photoadducts were detected by immunoprecipitation with affinity-purified antibodies raised against the TRiC β subunit and are identified by the arrowheads adjacent to lanes 2 and 7. Nascent chain lengths were 84 residues in lane1; 133 in lane 2; 177 in lane 3; 260 in lanes 4 and 8; 303 in lane 5; 337 in lane 6; 371 in lane 7. Non-immune serum was used for the immunoprecipitation in lane 8.
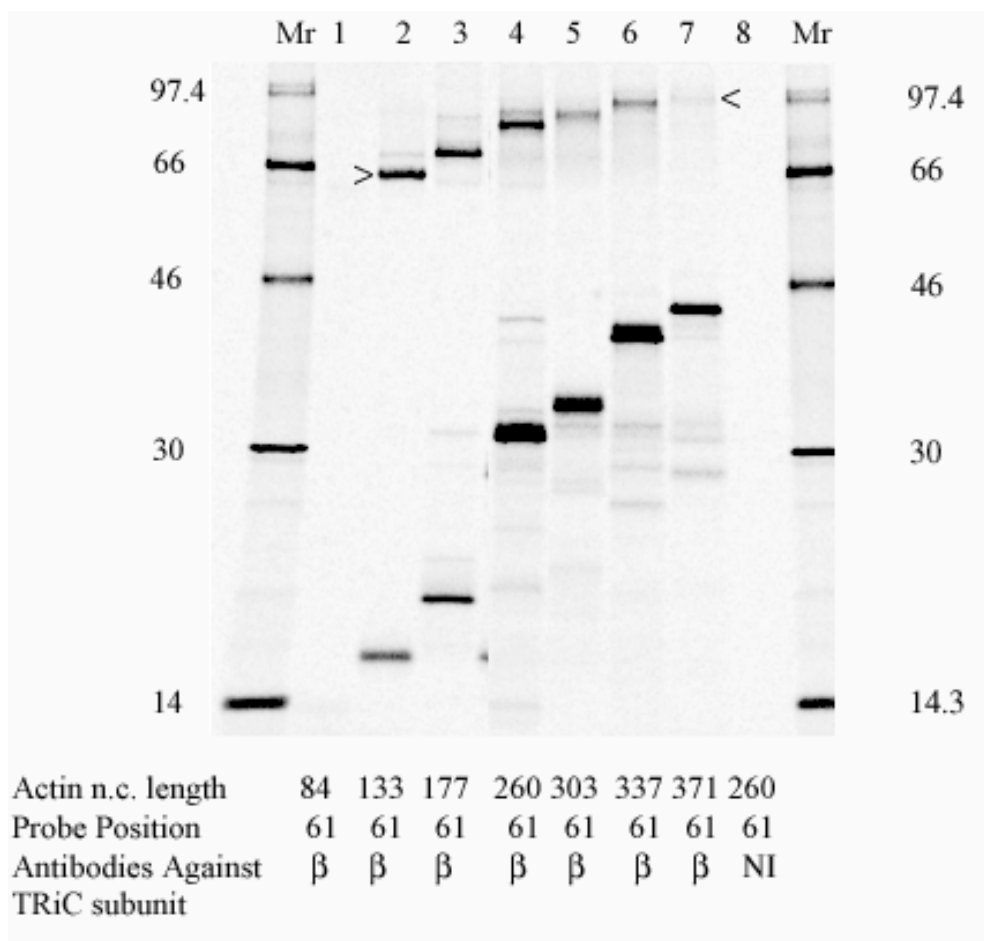
Figure 29. Nascent Chain Length Dependence of Photocrosslinking of the TRiC β Subunit to Actin[61amb] Nascent Chains

Photoadducts were detected by immunoprecipitation with affinity-purified antibodies raised against the TRiC β subunit and are identified by the arrowheads adjacent to lanes 2 and 7. Nascent chain lengths were 84 residues in lane1; 133 in lane 2; 177 in lane 3; 260 in lanes 4 and 8; 303 in lane 5; 337 in lane 6; 371 in lane 7. Non-immune serum was used for the immunoprecipitation in lane 8.

Photocrosslinking showed the same length dependence for probes at position 61 as position 50 (figure 28 verses figure 29). Specifically, we see photoadducts to nascent chains as short as 133 amino acids (figure 29, lane 2) and these photoadducts continue until the nascent chains is 371 amino acids in length (figure 29, lane 8). As a general trend, probes at positions 50 and 61 seem to have lower crosslinking efficiencies as the nascent chain gets longer.

Examination of the nascent chain length dependence of photocrosslinking between Actin[68amb] and the TRiC β subunit showed the following results. Photoadducts were observed to nascent chains as short as 133 amino acids in length and as long as 371 amino acids in length (figure 30, lanes 1-7). This is the same length dependence as was seen for probes at positions 50 and 61 (figure 26, lanes 7 and 8). An examination of the nascent chain length dependence of photocrosslinking between actin nascent chains with a probe at position 84 and the TRiC β subunit revealed that photoadducts were detected to nascent chains as short as 133 amino acids and as long as 371 amino acids (figure 31, lanes 1-6).

Table 8 shows a summary of the results of photocrosslinking of each of the actin[18-84amb] nascent chains to the TRiC β subunit. The pattern that emerges is that positions 50-84 are adjacent to the β subunit of TRiC from a length as short as 133mer until almost full length actin at 371mer. Only probes at position 18 are adjacent to the β subunit of TRiC at nascent chains as short as 84, and this proximity continues through the 371mer.
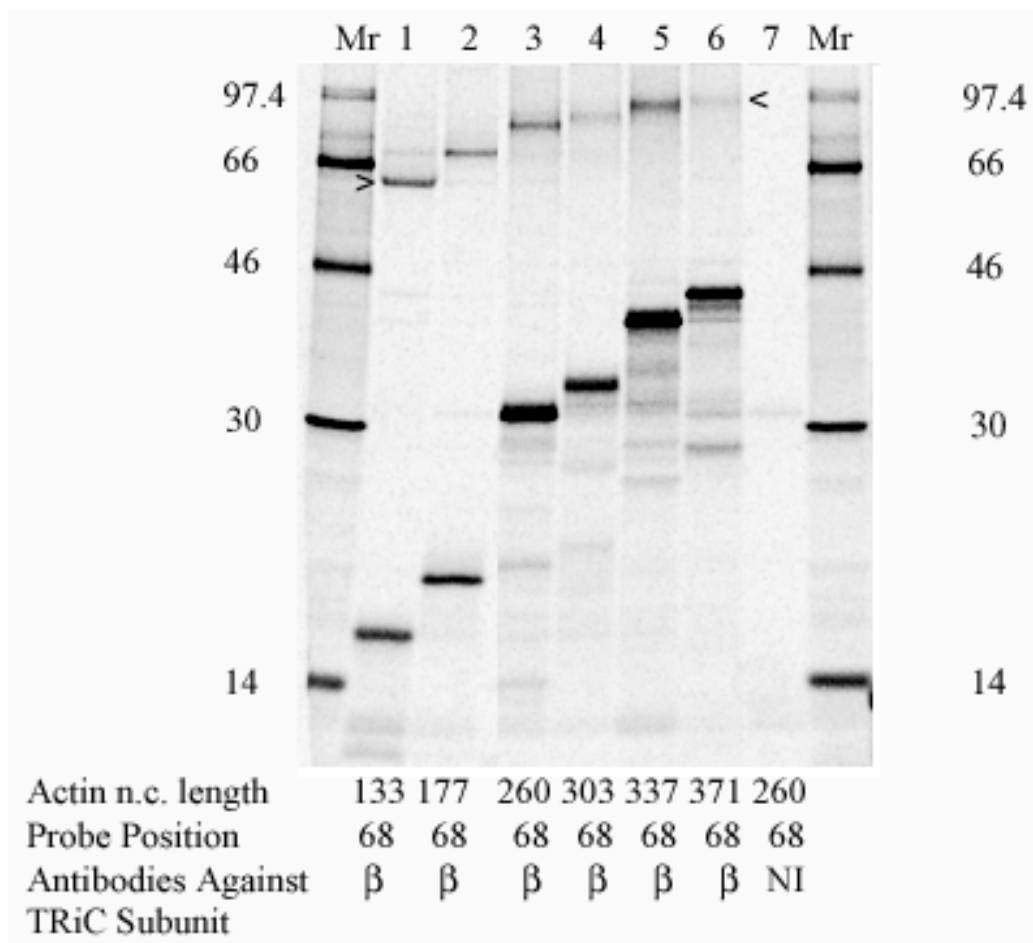
Figure 30. Nascent Chain Length Dependence of Photocrosslinking of the TRiC β Subunit to Actin[68amb] Nascent Chains

Photoadducts were detected by immunoprecipitation with affinity-purified antibodies raised against the TRiC β subunit and are identified by the arrowheads adjacent to lanes 1 and 6. Nascent chain lengths were 133 residues in lane 1; 177 in lane 2; 260 in lane 3 and 7; 303 in lane 4; 337 in lane 5; 371 in lane 6. Non-immune serum was used for the immunoprecipitation in lane 7.
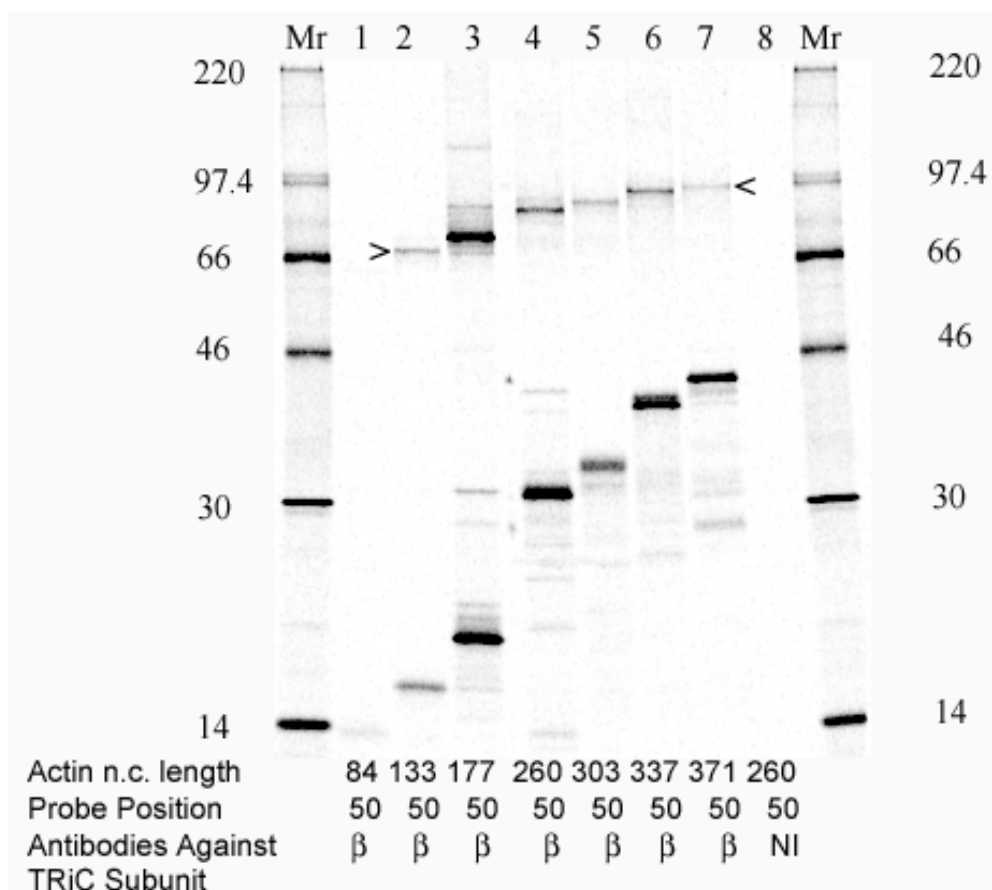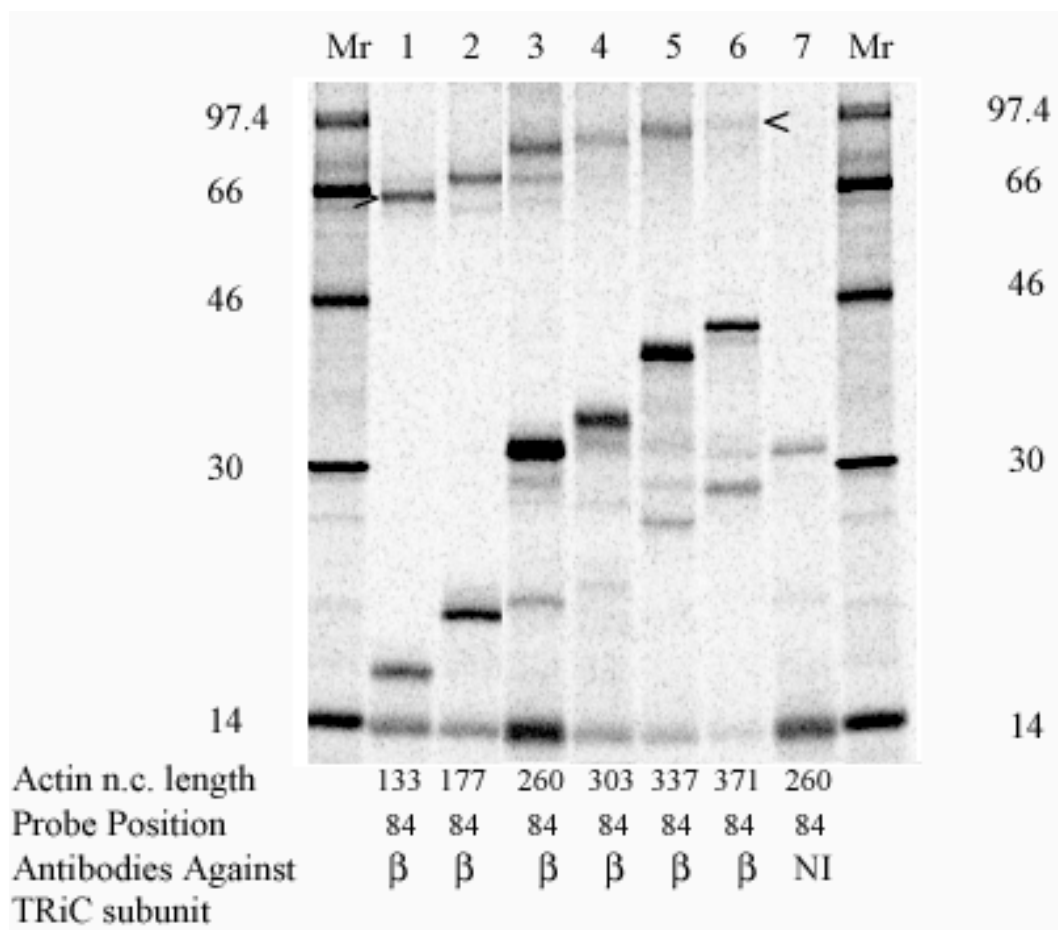
Figure 31. Nascent Chain Length Dependence of Photocrosslinking of the TRiC β Subunit to Actin[84amb] Nascent Chains

Photoadducts were detected by immunoprecipitation with affinity-purified antibodies raised against the TRiC β subunit and are identified by the arrowheads adjacent to lanes 1 and 6. Nascent chain lengths were 133 residues in lane 1; 177 in lane 2; 260 in lane 3 and 7; 303 in lanes 4; 337 in lane 5; 371 in lane 6. Non-immune serum was used for the immunoprecipitation in lane 7.

Table 8. Summary of Photocrosslinking of Actin [18-84amb] to the TRiC β Subunit

Actin n.c. Length	Probe Position 18	50	61	68	84
60	- n=1	n.d.	------------	-----------	-------------
84	+ n=1	- n=1	- n=1	n.d.	-------------
133	+ n=1	+ n=1	+ n=3	+ n=1	+ n=1
177	+ n=1	+ n=1	+ n=4	+ n=1	+ n=1
220	+ n=3	+ n=4	+ n=13	+ n=2	+ n=2
260	+ n=2	+ n=2	+ n=3	+ n=1	+ n=1
303	+ n=1	+ n=1	+ n=2	+ n=1	+ n=1
337	+ n=1	+ n=1	+ n=3	+ n=1	+ n=1
371	+ n=1	+ n=1	+ n=5	+ n=2	+ n=1

n= represents the number of times the experiment was repeated.
n.d.= no data

Photocrosslinking of Actin[61amb] 220mer to TRiC α, β and ϵ Subunits

In chapter III it was demonstrated that actin 220mer nascent chains photocrosslinked to the TRiC α, β and ϵ subunits. In order to ascertain whether the α and ϵ subunits of TRiC were also adjacent to the probe at position 61, an *in vitro* translation reaction followed by photocrosslinking and immunoprecipitation was performed as before.

The photocrosslinking data in figure 32 demonstrated that the probe at position 61 in the actin 220mer is adjacent to the α, β and ϵ subunits of TRiC.

The photoadducts to the TRiC β subunit had a lower apparent molecular mass than the photoadducts to the ϵ subunit of TRiC, and the ϵ photoadduct had a lower apparent molecular mass than the photoadducts containing the α subunit of TRiC (figure 32, compare lanes 1, 2 with lanes 3-5 with lanes 6 and 7). The molecular masses and protein sequences of the rabbit TRiC subunits are not known, except that the ζ subunit was determined to be 97% identical to the mouse ζ subunit (Schwartz et al., 2000) . Since the molecular masses and sequences of the TRiC subunits in mouse are known, if we compare the relative sizes of the α, β and ϵ subunits, we find that the TRiC β subunit is smaller in molecular mass (57 kDa) than the TRiC ϵ subunit (59.6 kDa) and the TRiC α subunit (60.5 kDa) (Kubota et al., 1995a). Given this information about the relative sizes of the TRiC subunits in mice, the observed relative apparent
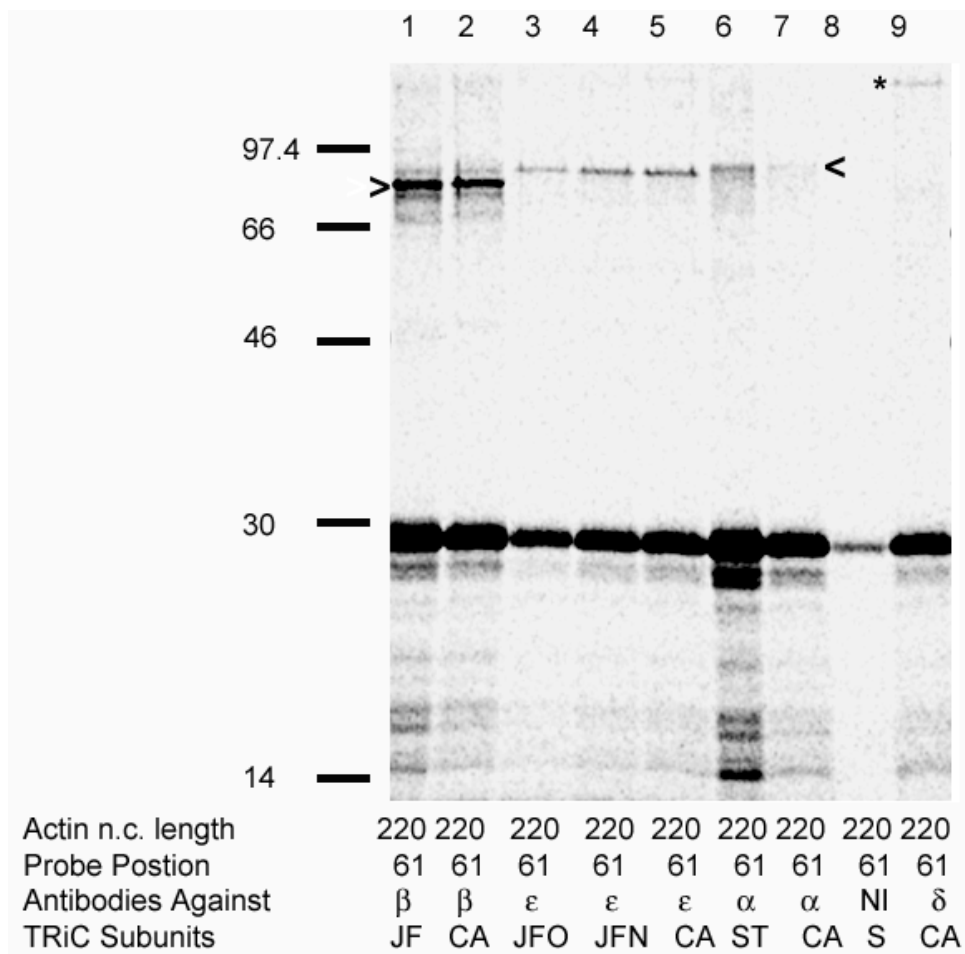
Figure 32. Photocrosslinking of Actin[61amb] 220mer Nascent Chains to TRiC α, β and ε Subunits

Samples containing Actin[61amb] 220mer nascent chains were photolyzed and then split and immunoprecipitated with antibodies raised against the β subunit of TRiC (lanes 1 and 2), the ε subunit of TRiC (lanes 3-5), the α subunit of TRiC (lanes 6 and 7), non-immune serum (lane 8), or the δ subunit of TRiC (lane 9). The photoadducts are identified with white and black arrowheads adjacent to lanes 1 and 7, respectively. The asterisk adjacent to lane 9 identifies an unknown band that consistently appears when the delta antibody is used but is not a photoadduct. The initials below the TRiC antibodies used identify the source of the antibodies: JF is Dr. Judith Frydman (Stanford University), CA is Dr. Martin Carden (University of Kent), JFO is an old lot of Dr. Judith Frydman antibodies, JFN is the new lot of antibodies, ST is Stressgen (Victoria, B.C.), and S is Sigma (St. Louis, MO).

molecular masses of the photoadducts in figure 32 are consistent with actin

photocrosslinking to the β, ϵ and α TRiC subunits.

In this experiment, antibodies from different sources were also used to

determine if new antibodies worked as well as the ones used in the studies

performed in chapter III that were from the lab of Dr Judith Frydman, Stressgen

or Sigma (see Experimental Procedures, table 3, for a full list of antibodies and

their antigens). From this gel, it can be seen that the antibodies from either Dr

Judith Frydman's lab (figure 32, lanes 1, 3 and 4, identified by the initials JF) or

Dr Martin Carden's lab (lanes 2, 5 and 7, identified by the initials CA) or from

the Stressgen company (lane 6, identified by the initials ST) all

immunoprecipitated the photoadduct that they were raised against. However,

the antibodies raised against the α subunit of TRiC in the lab of Dr Martin

Carden did not immunoprecipitate the photoadduct to the α subunit as well as

the antibodies from Stressgen and hence all further immunoprecipitations were

performed with the antibodies made by Stressgen (figure 32, compare lanes 6

and 7). Also the old lot of antibodies raised against the TRiC ϵ subunit in Dr

Judith Frydman's lab did not immunoprecipitate the photoadduct to the TRiC ϵ

subunit as well as the new lot or the antibodies made in the lab of Dr Martin

Carden (figure 32, compare lanes 3, 4 and 5). Hence, only the latter two were

used for subsequent immunoprecipitations.

Nascent Chain Length Dependence of Actin[61amb]

Photocrosslinking to the TRiC ε Subunit

Having demonstrated that the probe at position 61 is adjacent to the

TRiC ε subunit, the next step was to look at the nascent chain length

dependence of the probe being adjacent to the TRiC ε subunit. Employing the

same experimental technique used in the above figures, nascent chains of

actin[61amb] were prepared as before and immunoprecipitated with antibodies

against the ε subunit of TRiC.

Photocrosslinking of actin[61amb] nascent chains to the TRiC ε subunit were

observed with nascent chain lengths as short as 133 amino acids and

continued until the nascent chains were 371 amino acids in length (figure 33,

lanes 2-8). This is the same length dependence that was observed for

photocrosslinking between a probe at position 61 of actin and the TRiC β

subunit.

Examination of the length dependence of photocrosslinking of the TRiC ε

subunit to Actin [18, 50, 68 and 84amb] nascent chains were performed as outlined

above and the results of these experiments are summarized in table 9.

What is observed here is a pattern very similar to the photocrosslinking

pattern observed between actin nascent chains and the TRiC β subunit.

Photocrosslinks to actin nascent chains as short as 133 amino acids and as

long as 371 amino acids are observed with probes at all five positions. This

length dependence for actin nascent chains with a single probe
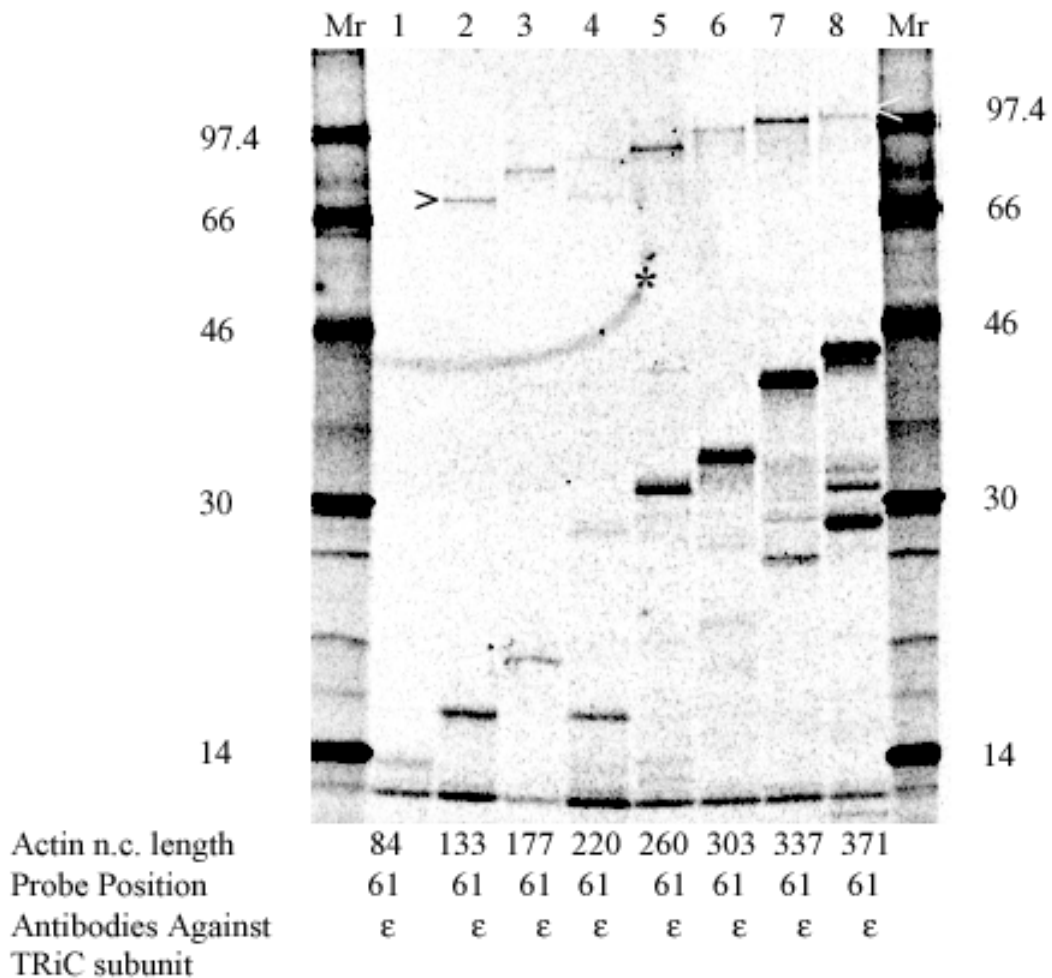
Figure 33. Nascent Chain Length Dependence of Photocrosslinking of the TRiC ε Subunit to Actin[61amb] Nascent Chains

Photoadducts were detected by immunoprecipitation with affinity-purified antibodies raised against the TRiC ε subunit and are identified by the black and white arrowheads adjacent to lanes 2 and 8 respectively. Nascent chain lengths were 84 amino acids in lane1; 133 in lane 2; 177 in lane 3; 220 in lane 4; 260 in lanes 5; 303 in lane 6; 337 in lane 7; 371 in lane 8. A circular mark from the gel dryer is identified with an asterisk.

Table 9. Summary of Photocrosslinking of Actin [18-84amb] to the TRiC ε Subunit

Actin n.c. Length	Probe Position 18	50	61	68	84
60	- n=1	n.d.	------------	------------	-----------
84	- n=1	- n=1	- n=2	- n=2	-----------
133	+ n=3	+ n=2	+ n=3	+ n=3	+ n=2
177	+ n=2	+ n=2	+ n=2	+ n=2	+ n=1
220	+ n=1	+ n=4	+ n=6	+ n=1	n.d.
260	+ n=1	n.d.	+ n=2	+ n=1	n.d.
303	n.d.	+ n=1	+ n=1	+ n=1	n.d.
337	n.d.	n.d.	+ n=1	+ n=1	n.d.
371	+ n=1	+ n=1	+ n=4	+ n=1	+ n=1

n= represents the number of times the experiment was repeated.
n.d.= no data

photocrosslinking to the TRiC ε subunit is the same as the actin nascent chain length dependence of photocrosslinking to the TRiC ε subunit when lysines were placed at multiple probe positions (table 4, chapter III). Thus it can be concluded that probes at each of the five positions between 18 and 84 contributed to the photocrosslinking to the TRiC ε subunit that was observed when multiple lysine probes were present.

Nascent Chain Length Dependence of Photocrosslinking

of the Actin ¹⁸⁻⁸⁴ᵃᵐᵇ Nascent Chains to the TRiC α Subunit

Figure 32 demonstrated that a probe at position 61 in an actin nascent chain of 220 amino acids was adjacent to the TRiC α subunit. To determine the nascent chain length dependence of the proximity of various actin residues to the TRiC α subunit, experiments similar to those employed above were performed. A representative gel with the probe at position 50 is shown in figure 34. In figure 34 we observe that the probe at position 50 is adjacent to the TRiC α subunit when the actin nascent chains are as short as 133 amino acids and as long as 371 amino acids (lanes 3-9). This pattern is the same as was observed for the TRiC β and ε subunits when a probe was placed at position 50 in the actin nascent chain.

Examinations of the length dependencies of photocrosslinking of actin nascent chains to the TRiC α subunit with a probes at positions 18, 61, 68, or 84 revealed photocrosslinks to actin nascent chains as short at 133 amino acids
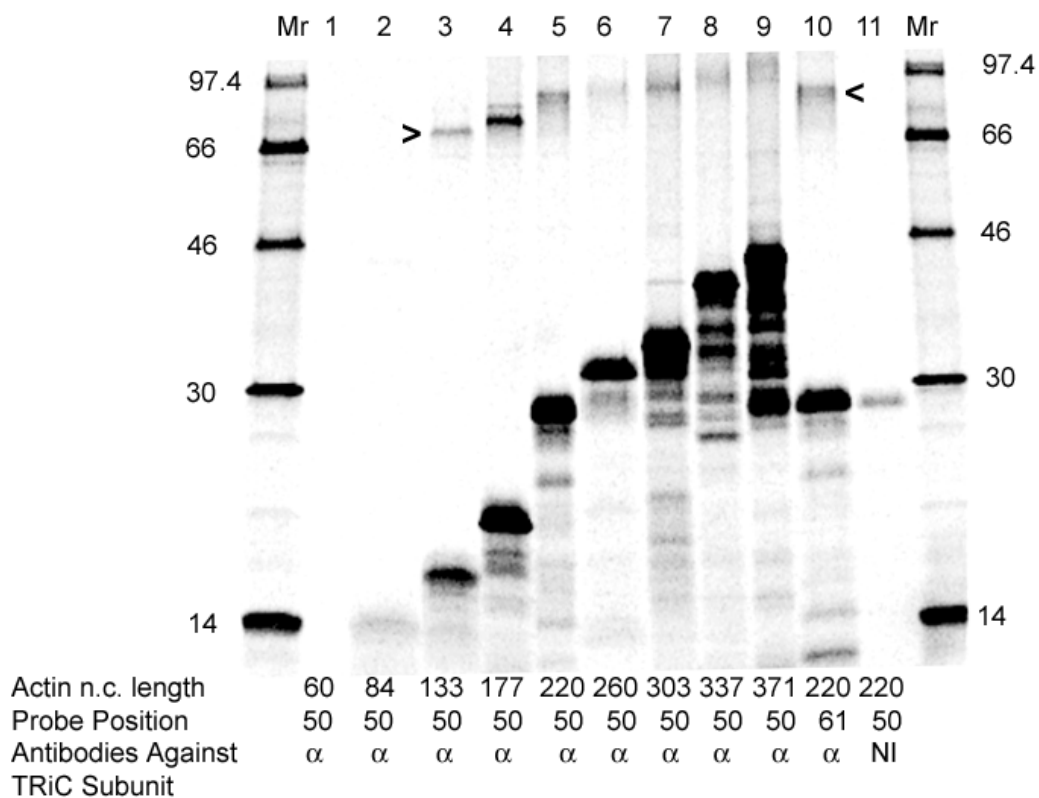
Figure 34. Nascent Chain Length Dependence of Photocrosslinking of the TRiC α subunit to Actin[50amb] Nascent Chains

Photoadducts were detected by immunoprecipitation with monoclonal antibodies raised against the TRiC α subunit and are identified by the arrowheads adjacent to lanes 3 and 10. Nascent chain lengths were 60 amino acids in lane 1; 84 in lane 2; 133 in lane 3; 177 in lane 4; 220 in lane 5; 260 in lanes 6, 10 and 11; 303 in lane 7; 337 in lane 8; 371 in lane 9. Non-immune serum was used for the immunoprecipitation in lane 11.

and as long as 371 amino acids (table 10). This pattern is the same as was observed for the TRiC β and ε subunits (tables 8 and 9), and mirrors what was observed in actin nascent chains with multiple probes per nascent chain (see table 4, chapter III).

Proximity of TRiC to the P-site in the Ribosome

As was previously shown and summarized in tables 1-3, probes at positions 50, 61, 68 and 84 in actin were adjacent to the TRiC α, β and ε subunit when the nascent chains were as short as 133 residues. When a probe was placed at position 18, photocrosslinking to nascent chains as short as 84 amino acids was observed, but only with the β subunit of TRiC and not with α or ε. When a probe is at position 18 and the actin nascent chain length is 84 amino acids, the probe is 66 amino acids from the P-site and therefore outside of the ribosomal tunnel. When a probe is placed at position 84 in an actin nascent chain of 133 amino acids, the probe is 49 residues from the P-site in the ribosome. Since the nascent chain tunnel protects 35-40 nascent chain residues from proteolytic digestion (Blobel and Sabatini, 1970; Malkin and Rich, 1967) TRiC is very close to the ribosomal exit site since TRiC subunits α, β and ε were all observed to photocrosslink to a probe at position 84 in a 133-residue actin nascent chain. Figure 35 shows that all five probe positions in actin nascent chains of length 133 and 177 photocrosslink to the TRiC ε subunit (lanes 1-10).

Table 10. Summary of Photocrosslinking of Actin [18-84amb] to the TRiC α Subunit

Actin n.c. Length	Probe Position 18	50	61	68	84
60	- n=1	- n=1	------------	-----------	-----------
84	- n=1	- n=1	- n=1	- n=1	-----------
133	+ n=1	+ n=1	+ n=1	+ n=1	+ n=1
177	+ n=1	+ n=1	+ n=1	+ n=1	+ n=1
220	+ n=1	+ n=1	+ n=5	+ n=1	+ n=1
260	+ n=1	+ n=1	+ n=2	+ n=1	+ n=1
303	+ n=1	+ n=1	+ n=1	+ n=1	+ n=1
337	+ n=1	+ n=1	+ n=1	+ n=1	+ n=1
371	+ n=1	+ n=1	+ n=1	+ n=1	+ n=1

n= represents the number of times the experiment was repeated.
n.d.= no data
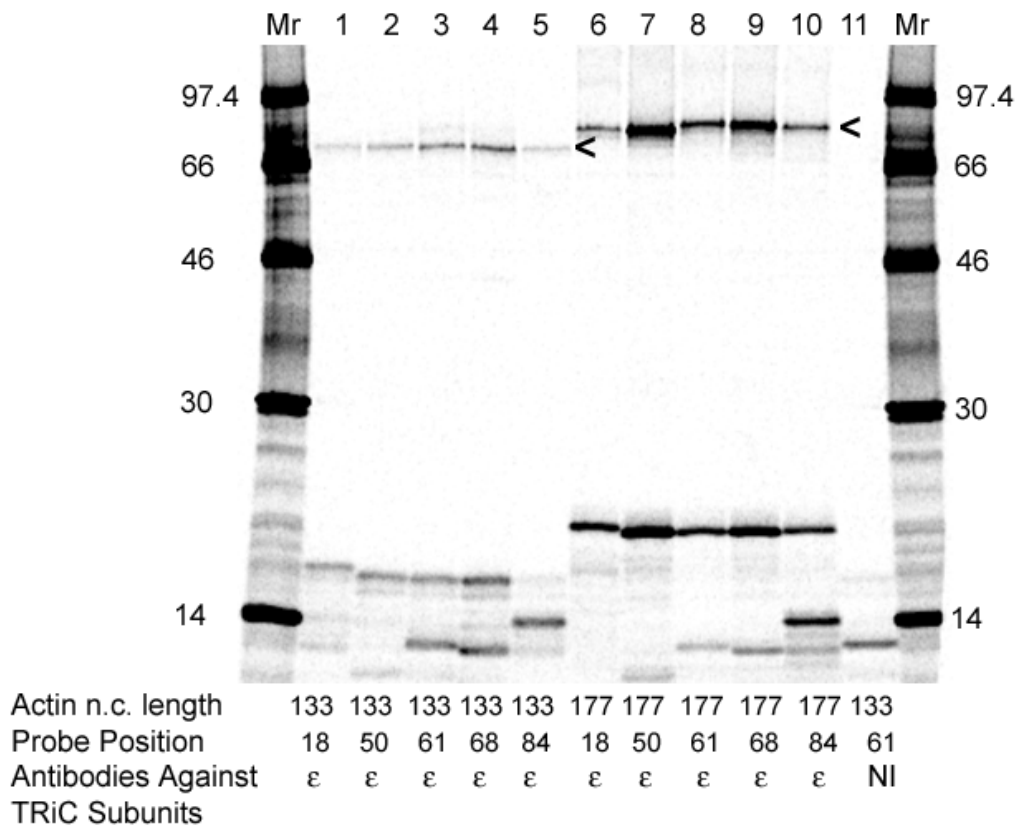
Figure 35. Photocrosslinking of the TRiC ε Subunit to Actin[18-84amb] 133mer and 177mer Nascent Chains

The 133mer and 177mer nascent chains, with probes at positions 18, 50, 61, 68 or 84, photocrosslinked to the TRiC ε subunit (bands identified with the two arrowheads adjacent to lanes 5 and 10 respectively), as demonstrated by immunoprecipitation using an antiserum specific for TRiC ε. No photoadduct was observed when non-immune serum as used for the immunoprecipitation (lane 11).

CHAPTER V

PHOTOCROSSLINKING STUDIES OF THE

CO-TRANSLATIONAL PROXIMITY OF THE

ACTIN NASCENT CHAIN TO THE

CHAPERONIN PREFOLDIN

Experimental Design

Previously, eukaryotic prefoldin was co-purified with actin (Vainberg et al., 1998). It was also shown that ribosome-bound actin nascent chains photocrosslinked to an unidentified protein of approximately 20 kDa (McCallum et al., 2000). This unidentified photocrosslinking band was co-immunoprecipitated under native conditions with antibodies raised against the TRiC α subunit. In the paper, the authors suggested that this photoadduct may include one of the prefoldin subunits. To determine whether this is the case, co-immunoprecipitation experiments similar to those performed by McCallum and colleagues were performed using antibodies raised against the prefoldin 3 subunit (McCallum et al., 2000). In brief, photoreactive probes were incorporated into half the sample and the other half of the sample was mock treated (received Lys-tRNA$^{\text{Lys}}$). The samples were then spun down in the dark
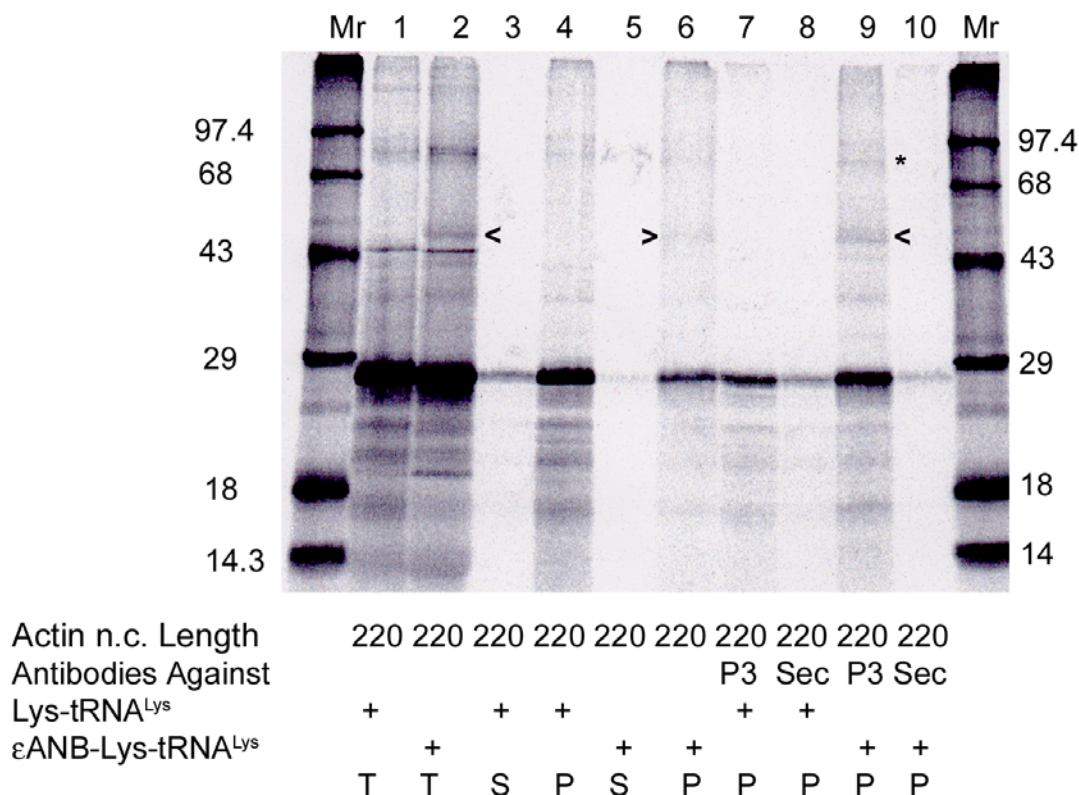
Figure 36. Photocrosslinking and Native Immunoprecipitation of Actin to Prefoldin

An actin 220mer nascent chain was photocrosslinked to prefoldin 3. Immunoprecipitation using antibodies raised against prefoldin 3 (P3) were used to detect the photoadduct (identified by the arrowhead in lane 9). No photoadduct was immunoprecipitated in lane 7 that contained actin intermediates with no incorporated photoprobes and hence served as a negative control. When antibodies against Sec 61α were used in lane 10 ("Sec"), no photoadduct was immunoprecipitated. T stands for totals, S stands for supernatant and P stands for pellets. The photoadduct marked with the asterisk contains the TRiC subunits identified in chapter III.

to pellet the ribosome-bound nascent chains, and after resuspension the samples were photolyzed. Following this, each of the two samples was split again and immunoprecipitated with antibodies against either prefoldin 3 or as a control, Sec 61α. In figure 36 we see a probe-dependent photocrosslink to a 20 kDa protein (compare lanes 1 and 2). In lanes 3-6 we see that the photocrosslinked band is in the pellet after a centrifugation step to pellet the ribosome-bound nascent chains. In lanes 7-10, the immunoprecipitation of the pellets from lanes 4 and 6 and reveal that the 20 kDa crosslink is immunoprecipitated in lane 9 with the anti-prefoldin 3 antibodies, but not with an antibody specific for the Sec 61α complex (lane 10). Thus, prefoldin photocrosslinks to actin nascent chains. Furthermore, since this photoadduct can be co-immunoprecipitated with antibodies against a TRiC α subunit under native conditions (McCallum et al., 2000), and TRiC also photocrosslinks to actin nascent chains, TRiC and prefoldin appear to associate simultaneously with the actin nascent chain. Recently, a cryo-EM structure of a TRiC-prefoldin complex was published (Martin-Benito et al., 2002) which showed that these two large complexes can associate.

The sequences of the rabbit prefoldin subunits are not yet known, but mouse and human prefoldin sequences are known. An examination of the amino acid sequence of subunit 2 for both mouse and human showed only 2 different amino acids in the entire 154 amino acid sequence. Thus, it is reasonable to assume that the rabbit prefoldin sequences will be very similar to

the human and mouse sequences. The following are the lengths of the human

prefoldin subunits: prefoldin 1 is 122 amino acids, prefoldin 2 is 154 aa,

prefoldin 3 is 197 aa, prefoldin 4 is 134 aa, prefoldin 5 is 154 aa and prefoldin 6

is 129 aa. Since the photocrosslinked band contains an approximately 20 kDa

protein, the actin nascent chain has most likely photocrosslinked to prefoldin 2,

3, or 5, which have calculated molecular masses of 16.9, 20.4, and 16.9 kDa,

respectively. Without antibodies against the other subunits, it is not possible at

this point to know exactly to which subunit of prefoldin the actin nascent chains

is photocrosslinking.

Photocrosslinking of Actin $^{61-84amb}$ 220mer to Prefoldin, but Not Actin^{50amb} 220mer

Having shown that prefoldin photocrosslinked to actin nascent chains of

220 amino acids, the next step was to determine which lysine residue(s) was

(were) involved in that crosslinking. Using the actin single-site suppressor

constructs of 220 amino acids shown earlier, probe-dependent photocrosslinks

to prefoldin were observed at positions 61 and 68 (numbering is from the N-

terminus). Clearly, position 68 has a much higher efficiency of photocrosslinking

than position 61 (figure 37). There is also a radioactive band with the expected

apparent molecular weight of a prefoldin photoadduct in lane 8, but since this

band is also visible in lane 7, it does not appear to be a probe-dependent

photocrosslink. Thus, only a limited number of nascent chains residues are adjacent to prefoldin in the translation intermediate.

Length Dependence of Actin Nascent Chain
Photocrosslinking to Prefoldin

Since there was a strong photoadduct when the probe was located at position 68 in the actin 220 amino acid nascent chain, the next step was to determine the length dependence of this photocrosslinking at position 68. Photocrosslinks to prefoldin were observed with actin nascent chains as short as 177 amino acids and as long as 371 amino acids (figure 38). It is interesting that actin nascent chains with the probe at position 68 photocrosslink to TRiC when the nascent chains are as short as 133 amino acids, but the same nascent chains do not photocrosslink to prefoldin until the nascent chain is 177 amino acids in length. The prefoldin photoadduct bands are also less intense than the TRiC photoadduct bands observed at 220 amino acids.

Since a probe located at position 68 in an actin 220mer can photocrosslink either to prefoldin (figures 37 and 38) or to at least 3 different TRiC subunits (figure 26, tables 9 and 10), the origin of this heterogeneity must be considered. Do the actin translation intermediates bind either prefoldin or TRiC? Or do prefoldin and TRiC bind simultaneously to the same actin nascent chain? If the latter, the heterogeneity in photocrosslinking target presumably results from a dynamic nascent chain interaction with the chaperonins that exposes position
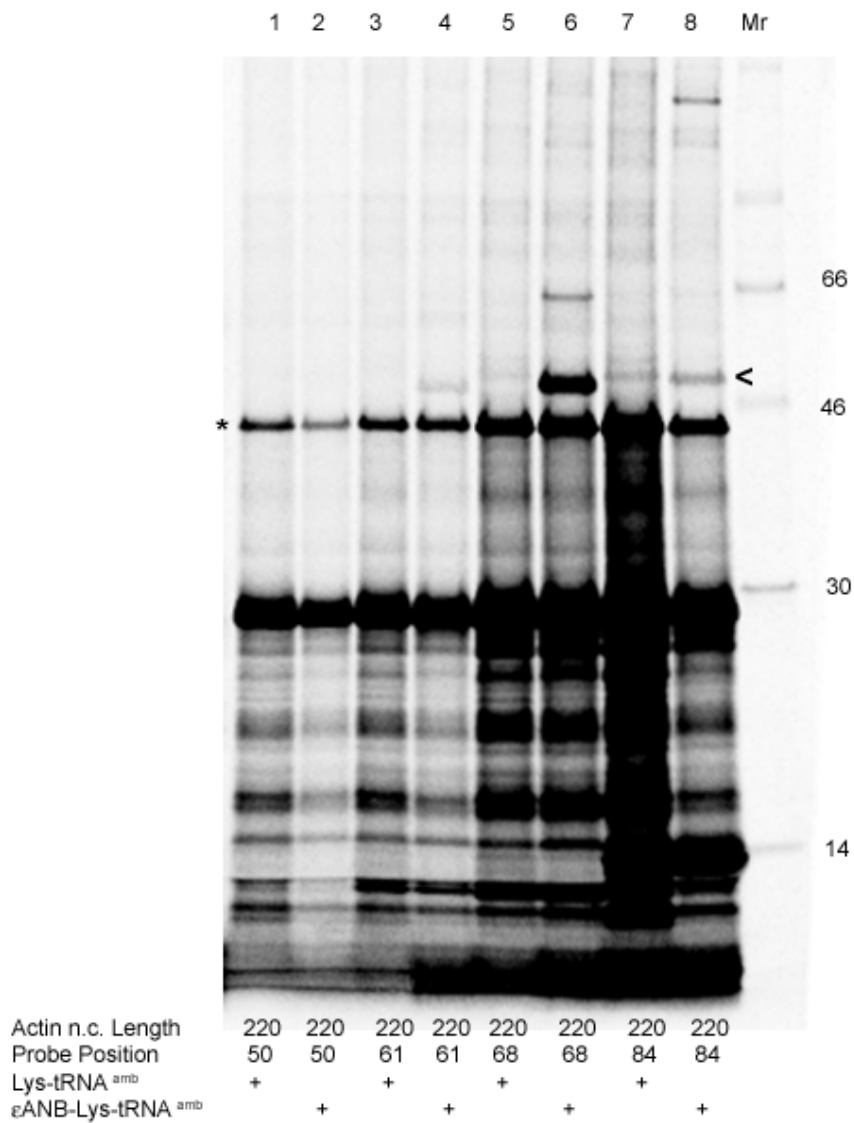
Figure 37. Photocrosslinking of Actin[50-84amb] 220mer to Prefoldin

Actin[50-84amb] 220mer nascent chains were *in vitro* translated and photolyzed, then ribosome-bound nascent chains were sedimented and analyzed by SDS-PAGE. Photoadducts to prefoldin were observed in lanes 4, 6 and 8 (identified with an arrowhead adjacent to lane 8). The nascent chains attached to tRNA are marked with an asterisk (*). No photoadducts were seen with actin[50amb] 220mer or in the odd-numbered lanes that lacked photoreactive probes.
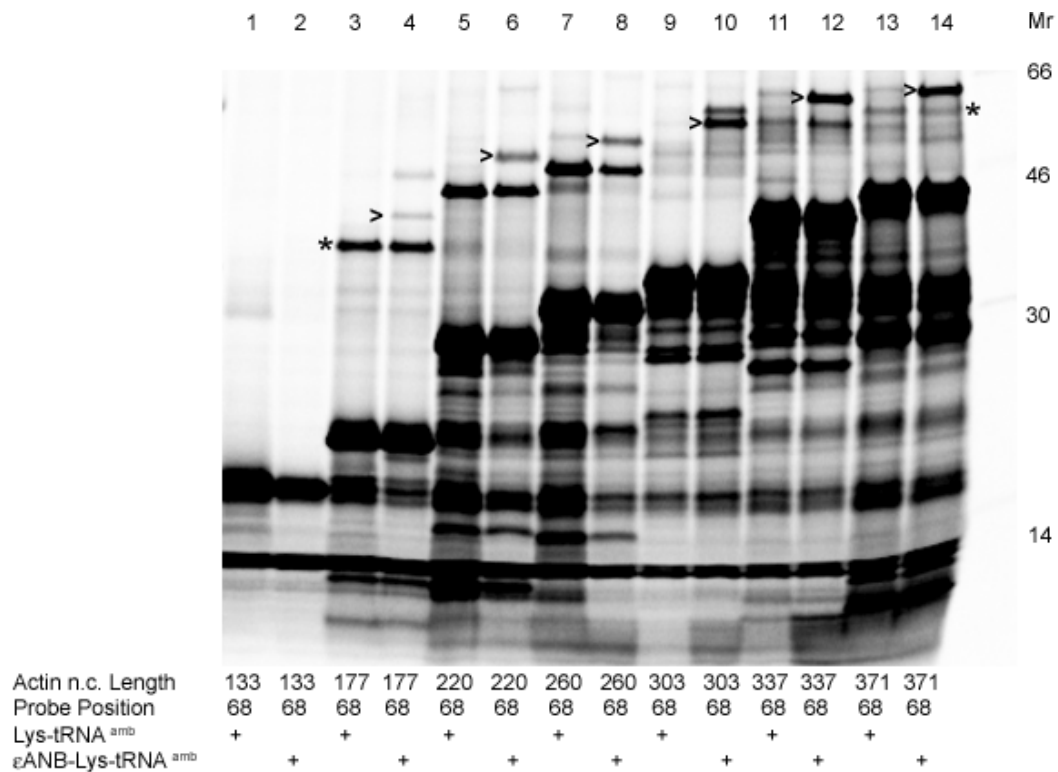
Figure 38. Length Dependence of Photocrosslinking of Actin[68amb] Nascent Chains to Prefoldin

Actin[68amb] nascent chains were generated by *in vitro* translation in RRL. The samples were photolyzed and the ribosome-bound nascent chain complexes were purified by sedimentation before analysis by SDS-PAGE. The 177mer, 220mer, 260mer, 337mer and 371mer photocrosslinked to a 20 kDa protein (identified with an arrowhead adjacent to lanes 4, 6, 8, 12, and 14 respectively). The 303mer was photocrosslinked to 20 and 22 kDa proteins (identified with an arrowhead adjacent to the 20 kDa protein in lane 10). No photoadducts were detected in the odd numbered lanes since no photoprobe was incorporated. The bands with apparent molecular weights slightly less than the photoadducts are due to tRNA-bound nascent chains (asterisk).

68 to a variety of different proteins and environments. Since nascent chain-bound prefoldin and TRiC are co-immunoprecipitated under native conditions (figure 36), it is clear that the observed heterogeneity in nascent chain-chaperonin photocrosslinking reflects primarily a heterogeneity in nascent chain alignment and/or folding with in the ribosome-chaperonin complex.

CHAPTER VI

PHOTOCROSSLINKS OF SINGLY-LABELED

LUCIFERASE NASCENT CHAINS TO

AN UNKNOWN 105 kDa PROTEIN

Experimental Design

To determine the location of the nascent chain lysine residue(s) that resulted in the photoadduct between luciferase and TRiC outlined in chapter III, constructs were made as outlined in the Experimental Procedure that contained a single amber stop codon at lysine residues 5, 8, 9, 28, 31, or 68, respectively. Each of these constructs had a single amber stop codon in place of one of the lysine residues. Nascent chains were prepared as before, but this time εANB-Lys-tRNA^{amb} was added instead of εANB-Lys-tRNA^{Lys}. If the modified lysine group were incorporated into the nascent chain, then the truncated mRNA would be translated to its end, yielding a nascent chain with a defined and known length. If the modified lysine were not incorporated, then the nascent chain would be terminated at the stop codon and released from the ribosome. Thus all translation intermediates containing a modified lysine have the same length. This approach allows one to determine which of the above-mentioned lysines were involved in the formation of the photoadduct. What was very surprising in these experiments was that the crosslinking to TRiC was very

weak, while a much stronger photoadduct appeared. I will therefore focus on this photoadduct for the remainder of this chapter.

Photocrosslinking of Luc[31amb] Nascent Chains

Using the Luc[31amb] construct that has an amber stop codon in place of a lysine at residue 31 from the N-terminus, the following nascent chains were generated: 60mer, 77mer, 92mer, 125mer, 164mer, 197mer, 232mer, 280mer, 337mer, and 371mer. Each nascent chain was in vitro translated as described in the Experimental Procedures, and subsequently photolyzed. Photocrosslinking showed a photoadduct of 115 kDa (figure 39, lane 3). When the molecular mass of the luciferase 92mer (~ 10 kDa) is subtracted from the apparent molecular weight of the photoadduct, one is left with a protein with an apparent mass of about 105 kDa. This 105 kDa protein photocrosslinked to luciferase nascent chains of 77, 92 and 125 amino acids (lanes 2-4), but not to nascent chain lengths longer than 125 residues (lanes 5-10). Thus, after 125 amino acids had been translated, the probe at position 31 appears to have changed its location relative to the 105 kDa protein because the photoadduct is no longer observed. When the nascent chain is only 60 residues in length, there is no photocrosslinking to the 105 kDa protein (figure 39, lane 1), presumably because the probe at position 31 is not yet out of the ribosomal tunnel.
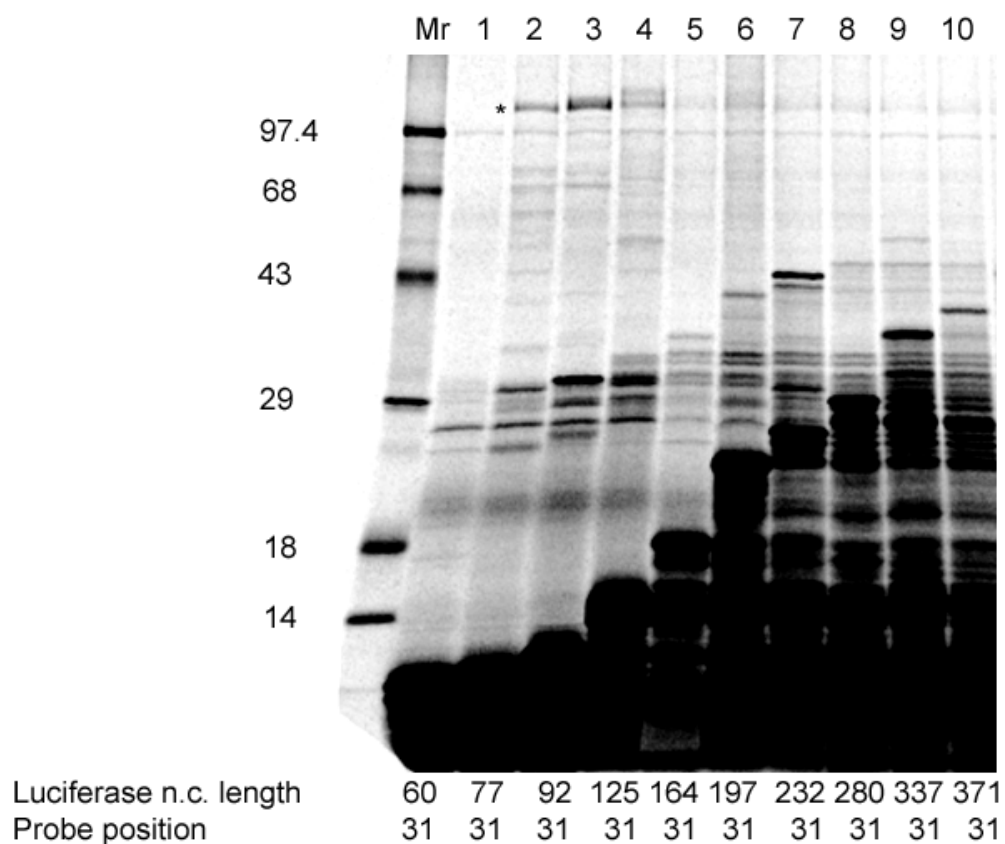
Figure 39. Photocrosslinking of Luciferase Nascent Chains to an Unknown Protein

Samples containing Luc[31amb] truncated mRNAs were translated and subsequently photolyzed for 15 min. The ribosome-bound nascent chains complexes were then pelleted through a sucrose cushion and the resulting pellet was resuspended in SDS-PAGE sample buffer and the samples were analyzed by SDS-PAGE. A 105 kDa photoadduct was observed in lane 2 and is identified by an asterisk (*). In lanes 3 and 4, we also see 105 kDa photoadducts, but in lane 6 we do not see with photoadduct.

Photocrosslinking of Luc [5-68amb] 77mer, 92mer and 125mer

Nascent Chains to a 105 kDa Protein

To ascertain if the 105 kDa protein photocrosslinked to any of the other

lysine residues around position 31 of luciferase, nascent chains of 77, 92 and

125 amino acids of the constructs Luc^{5amb}, Luc^{8amb}, Luc^{9amb}, Luc^{28amb}, Luc^{31amb}

and Luc^{68amb} were in vitro translated and photolyzed. The 105 kDa protein was

observed to be photocrosslinked to luciferase nascent chains that had probes in

positions 5, 9, 28 or 31, but not 8 or 68 (figure 40). It is very striking that

photocrosslinking is seen at position 9, but not at position 8, since these two

amino acids are adjacent to one another in the nascent chain. In the crystal

structure of luciferase, the two lysine side chains are oriented in directions

differing by about 100° on an α-helix, but given that lysine has a flexible side

chain it is difficult to assess exactly where the probes at 8 and 9 are located.

Still, it is surprising that position 8 and 9 differ so much in accessibility to the

105 kDa protein. Perhaps the 105 kDa protein is binding to one face of the α-

helix, but not to the other, and the photoprobe at position 8 is directed away

from the 105 kDa protein so that no photocrosslinks can be
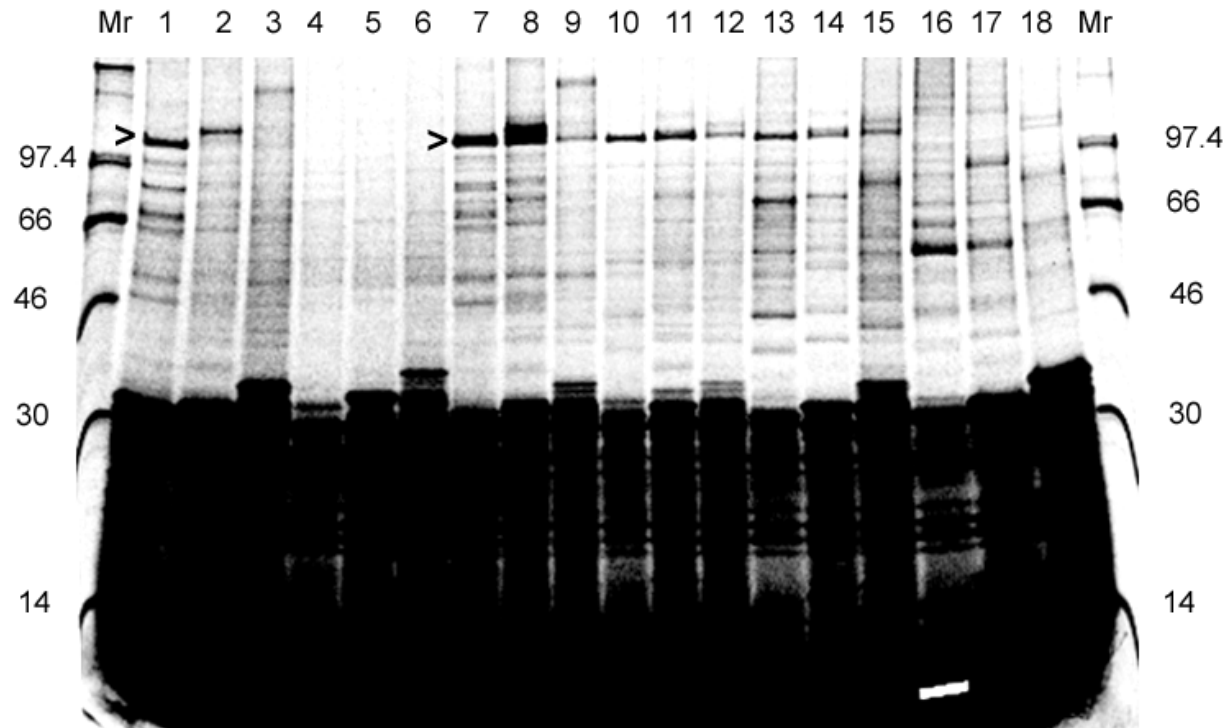
Figure 40. Photocrosslinking of Luc$^{5-68amb}$ 77mer, 92mer and 125mer Nascent Chains to a 105 kDa Protein

Luc$^{5-68amb}$ nascent chains were translated as outlined in the Experimental Procedures, photolyzed, and then sedimented prior to analysis by SDS-PAGE. Nascent chains were 77 amino acids in lanes 1, 4, 7. 10, 13 and 16; 92 amino acids in lanes 2, 5, 8, 11, 14 and 17; and 125 amino acids in lanes 3, 6, 9, 12, 15 and 18. Probes were incorporated at positions 5 (lanes 1-3); 8 (lanes 4-6); 9 (lanes 7-9); 28 (lanes 10-12); 31 (lanes 13-15); and 68 (lanes 16-18). An arrowhead adjacent to lanes 1 and 7 identifies photoadducts to the 105 kDa protein.
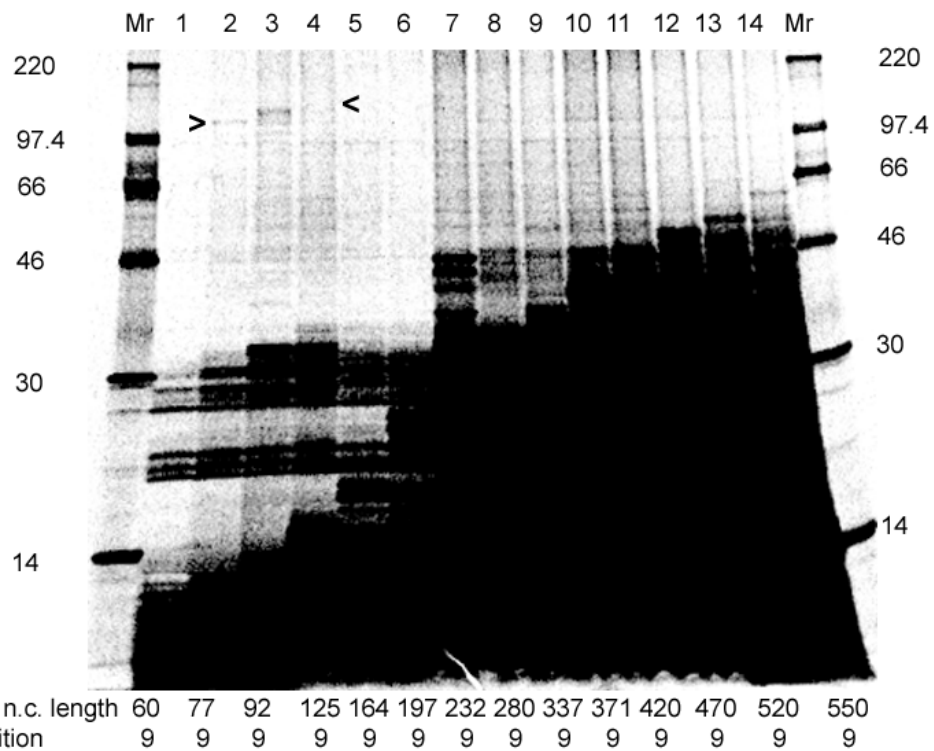
Figure 41. Length Dependence of Photocrosslinking of Luc[9amb] Nascent Chains to the 105 kDa Protein

Luc[9amb] nascent chains were translated, photolyzed, sedimented and analyzed as outlined in the Experimental Procedures. Nascent chain lengths were 60 amino acids in lane 1; 77 in lane 2; 92 in lane 3; 125 in lane 4; 164 in lane 5; 197 in lane 6; 232 in lane 7; 280 in lane 8; 337 in lane 9; 371 in lane 10; 420 in lane 11; 470 in lane 12; 520 in lane 13; and 550 in lane 14. Photoadducts to the 105 kDa protein are identified with the arrowheads adjacent to lanes 2 and 4.

formed. These photoadducts showed the same length dependence as was observed for Luc[31amb] (figure 39, lanes 2-4). To confirm that this length dependence was similar over shorter and longer nascent chains than tested in figure 2, Luc[9amb] nascent chains were in vitro translated and photolyzed. The same length dependence of the photoadduct was observed (figure 41, lanes 2-4). Thus, the binding of the 105 kDa protein to nascent luciferase appears to be transient, lasting only while the first 22% of luciferase is emerging from the ribosome.

It has been shown that Hsp110 interacts with luciferase in the cytosol to keep the protein in a refoldable conformation during heat shock (Oh et al., 1997; Oh et al., 1999). In an attempt to determine if the photoadduct contained Hsp 110, antibodies raised against Hsp110 a generous gift from Dr Subjeck at Roswell Park Cancer Institute, Buffalo, NY (Oh et al., 1997) were used in immunoprecipitation experiments. However, the photoadduct was never immunoprecipitated with these antibodies (data not shown). Since there was a possibility that the probe formed a covalent bond to Hsp 110 in a region where the antibody also recognized Hsp 110, purified Sse1 (a yeast homologue of Hsp110) which had a his-Tag at its C-terminus was added to in vitro translation reactions prior to photolysis and subsequently Ni-NTA beads were used to purify any possible photoadducts. Once again, the photoadduct to the 105 kDa protein was not retained on the column. Thus, the unidentified 105 kDa protein does not appear to be Hsp 110.

Other candidates for the identity of the 105 kDa protein were the N-acetyl transferases (Nat1p and Nat3p), which have been shown to acetylate the N-terminal amino groups of proteins co-translationally when only 20-50 residues are outside of the ribosomal tunnel (Polevoda and Sherman, 2000). The first five amino acids of luciferase are Met-Glu-Asp-Ala-Lys, and it has been shown that Nat3p acetylates chains that start with Met-Glu. Nat1p is 854 amino acids in length in yeast, which gives a predicted molecular mass of about 94 kDa that is a little too small to be the photoadduct, but the sequences of rabbit Nat1p or Nat3p are not known. The reason for considering Nat as a possible candidate for the 105 kDa protein is that we observe photocrosslinking to the 105 kDa protein only from probe locations near the N-terminus (5, 9, 28, 31 but not 68), and only when the nascent chains are between 77 and 125 amino acids in length (which represents only 14-20% of the protein's full length of 551 amino acids). It might be expected that a protein whose function is to add an acetyl group to the N-terminal methionine would interact with a nascent chain very close to the N-terminus. But since, to my knowledge no antibodies to rabbit Nat1p or Nat3p are available, no conclusions can be drawn about the identity of the 105 kDa protein. Instead, further experiments need to be done to establish its identity. However, this work has shown that there is a length dependence of nascent chain photocrosslinking to the 105 kDa protein, and that photocrosslinks can be seen when the probe is placed at amino acids 5, 9, 28 and 31, but not 8 and 68.

CHAPTER VII

DISCUSSION AND SUMMARY

Six aspects of the environment of the actin nascent chain as it emerges from the ribosome are revealed by experiments performed in this dissertation. First, it was found that the actin and luciferase nascent chains were adjacent to more than one TRiC subunit at different stages of folding. Second, widely-spaced, site-specific probe locations in the actin nascent chain reveal that multiple sequences of the nascent chain are adjacent to the same 3 subunits at different stages of translation. Third, subunit exposure to different nascent chains varies with the length of the nascent chain. Fourth, prefoldin photocrosslinks to actin nascent chains and co-immunoprecipitates with photoadduct bands containing TRiC and actin nascent chains, suggesting that prefoldin and TRiC form a complex on the actin nascent chain. Fifth, TRiC is in very close proximity to the exit site of the ribosomal tunnel. Sixth, the presence and absence of ATP influences the photocrosslinking yields which suggests that ATP alters either the conformation of the subunit and/or their affinity for the nascent chain.

First, it was that found both the luciferase and actin nascent chains were adjacent to six and seven out of the eight subunits of TRiC respectively, at different stages of co-translational folding. Since, TRiC has eight unique subunits, it has been proposed that each subunit might have a substrate

specialized function. Therefore, it was surprising to see nascent chains adjacent to almost all of the TRiC subunits.

Given that our experiments revealed that during translation, the actin nascent chain was adjacent to all but the TRiC γ subunit and that luciferase was adjacent to all but the γ and ζ subunits. This suggests several possibilities. The first possibility to explain the above results would be that TRiC does not contain all the subunits in each ring or is not in a ring when actin or luciferase nascent chains are photocrosslinking. This possibility is highly unlikely given the following results by other labs and in this dissertation. Purification of TRiC from either RRL or bovine testis folded by HPLC of the complexes revealed the presence of eight subunits (Rommelaere et al., 1993). Co-immunoprecipitation studies with actin-TRiC complexes that were isolated in the 20 S peak of a sucrose gradient showed that all eight subunits were present (Hynes and Willison, 2000). This experiment was performed with antibodies made in the same way as those used in this dissertation. *In vitro* translation experiments with radiolabeled actin containing photoreactive probes analyzed on Native-PAGE showed actin comigrating with TRiC complexes (McCallum et al., 2000). Also, the cryo-EM structure of actin in complex with TRiC and an antibody against the δ subunit of TRiC shows the antibody next to only one of the subunits in the ring (Llorca et al., 1999a). In addition, the deletion of any of the eight subunits in yeast is lethal and over-expression of any subunit has not been shown to compensate for a lack of another subunit (Ursic et al., 1994).

Thus there is previous evidence that TRiC contains all eight of the subunits mentioned and that actin interacts with this TRiC complex. Therefore, the possibility that actin is seeing TRiC which does not contain all eight subunits per ring is not very probable.

The second possibility is that there may be some redundancy in the function of the TRiC subunits during early interactions with the nascent chain. If this were true, then why could the overexpression of one subunit of similar function not compensate for a lack of another as was state above (Ursic et al., 1994).Thus, this second possibility seems unlikely, but cannot be ruled out because the subunits might still be functionally redundant when it comes to folding substrates, but not when it comes to assembly of the complex.

A third possibility is that the nascent chain samples the different binding surfaces of each subunit as it emerges from the ribosome and presumably starts to fold. If this is true, it would suggest that the nascent chain does not bind tightly to any one subunit. It would also suggest that the nascent chain spends more time not bound to the subunits than bound, and that the nascent chain is possibly moving quickly between folding intermediates. This would make sense in light of the fact that the function of TRiC is to help the nascent chain fold into its native structure and presumably increase the rate at which that structure is reached. If a section of nascent chain bound tightly to any one of the TRiC subunits, that might hinder the rate of folding if for example that

section of the nascent chain were located in the interior of the protein's native structure.

From our photocrosslinking results, it cannot be determined if the nascent chains are adjacent to the outer surface or the inner surface of TRiC subunits. Cryo-EM and SAXS (small angle x-ray scattering) experiments with actin have shown actin to reside inside the ring (Llorca et al., 1999a; Meyer et al., 2003). This is also true for cryo-EM studies and crystal structures of GroEL with peptides (Chen and Sigler, 1999). From these cryo-EM structures, the authors have suggested that there is a septum between the two rings that prevents substrates from occupying both rings at once by spanning the entire cavity (Llorca et al., 1999b). Since, purified actin has been shown to be located inside the ring of TRiC subunits (Llorca et al., 1999a; Meyer et al., 2003), it seems highly likely that actin nascent chains would also be located within the TRiC cavity.

Given the high probability that there is only one of each type of subunit per ring and that actin nascent chains cannot cross from the top ring to the bottom ring of TRiC, it seems very likely that photoadduct bands of the correct molecular mass to contain two subunits and the actin nascent chain are to two different TRiC subunits in the same ring. Photocrosslinks between actin nascent chains and two TRiC subunits were observed for TRiC subunits α, β, δ and θ (figure 15, lanes 1, 2, 4 and 8). There is evidence for actin to be adjacent to the δ and β subunits simultaneously in the cryo-EM structure of purified actin

and TRiC (Llorca et al., 1999a). Thus, the photoadduct bands that contain actin nascent chains and two TRiC subunits are most likely adjacent to two different TRiC subunits within the same ring.

Summing up all of these ideas, it seems that actin and luciferase nascent chains are adjacent to more than one different TRiC subunit within the cavity of the ring closest to the ribosomal exit site at different stages of folding.

Second, widely-spaced, site-specific probe locations in the actin nascent chain are adjacent to the same three subunits at different stages of translation. Experiments using singly-labeled actin nascent chains revealed that the N-terminus of the actin nascent chain was adjacent to the α, β and ε subunits of TRiC when the actin nascent chains were as short as 133 amino acids and as long as 371 amino acids. Photoadducts were observed for each of these actin nascent chain lengths to each of the three TRiC subunits at each of the 5 probe locations tested (positions 18, 50, 61, 68 and 84). Since a probe at position 61 can photocrosslink and hence be adjacent to either the α, β or ε subunits when the nascent chain is 177 amino acids, there maybe three or more populations of partially-folded actin nascent chains inside the cavity with a percentage of the nascent chains adjacent to each of the three subunits. Alternatively, the nascent chain maybe moving very rapidly within the cavity, not bound to any specific subunit, and photolysis may simply reflect transient proximity to individual subunits as the nascent chain samples different conformations within the TRiC cavity. But the hypothesis that a single TRiC subunit binds stably to a single

sequence or conformation of the actin nascent chain has been ruled out by my experiments. If that were true, a single probe would reproducibly photocrosslink only to one, or at most two, TRiC subunits at each stage (i.e., nascent chain length) of actin folding.

Another way to view these results is to note that single probes in actin separated by 66 residues (231Å of fully extended polypeptide) each photocrosslink to α, β, and ε (figure 32) at multiple lengths of actin nascent chains (tables 8, 9 and 10). If nascent chains bind to specific sites in the TRiC cavity and have sufficient binding affinity to occupy those binding sites for a prolonged time, then it seems surprising that each of those sites would localize probes at positions 18, 50, 61, 68 and 84 next to each site. Although one cannot rule out such a possibility, it seems unlikely and highly coincidental. Hence, similar photocrosslinking results from widely different probe locations suggest instead that the actin nascent chain spends the bulk of its time within the TRiC cavity and not bound to TRiC subunits.

One can imagine a variety of mechanisms by which TRiC interacts with the nascent chain and facilitates nascent chain folding. For example, one possibility is that once a probe at a certain position in the nascent chain sequence is adjacent to a TRiC subunit, it remains adjacent to that subunit as the nascent chain lengthens. Another scenario is that a probe at a certain nascent chain location, is positioned next to the α subunit of TRiC when the nascent chain is 133 amino acids in length, but moves next to the β subunit

when the nascent chain is 177 amino acids in length. In this second scenario, there could be many possible combinations of the order of subunits that a certain probe is adjacent to as the nascent chain lengthens. Our current data cannot distinguish between these two possibilities. The experiments performed with actin nascent chains containing a single probe, raise many questions, but these results demonstrate that the actin nascent chain does not occupy a specific binding site within the TRiC cavity.

Third, subunit exposure to different nascent chains varies with the length of the nascent chain. This suggests that the nascent chain is initially exposed to only some of the TRiC subunits. However, it is not clear whether this results from the nascent chain being unable to reach some subunits soon after entering the TRiC cavity or whether some subunits preferentially bind to the short nascent chains.

There seems to be a core of subunits (TRiC α, β, and ϵ) that is adjacent to actin nascent chains as short as 133 amino acids and as long as 371 amino acids. While the TRiC δ subunit is also adjacent to the actin nascent chain at the same lengths as the core subunits, it does not follow the photocrosslinking pattern of the core subunits with respect to the luciferase nascent chain. The other three subunits (TRiC θ, η and ζ) were not adjacent to actin nascent chains as short as 133 residues and/or were not adjacent to actin nascent chains as long as 371 residues. Although it has previously been shown that actin nascent chains as short as 133 amino acids and as long as 371 amino acids interact

with TRiC, this was done under denaturing immunoprecipitation conditions which were designed to keep the subunit of TRiC in a complex (McCallum et al., 2000). Here, for the first time, we looked at each individual subunit.

The ζ subunit of TRiC has only been observed to photocrosslink to actin nascent chains of 220 amino acids and not longer chains, this means that the probe in the actin nascent chain which forms the photocrosslink when the nascent chain is 220 amino acids in length must move relative to the surface of the TRiC ζ subunit since the photocrosslinking is not observed at longer lengths. This suggests that the nascent chains is moving relative to the surface of certain subunits as it emerges from the ribosome. This movement might be due to the nascent chain folding in a domain-wise fashion. However, the only actin domain that can fold when the nascent chain is 220 amino acids is domain 2, and it can have variable structures depending on its nucleotide occupancy, which at this length of nascent chain is not possible.

The η subunit of TRiC photocrosslinks to nascent chains at a length of 303 amino acids, but then disappears as the nascent chain lengthens to 371 amino acids. However, since these experiments were not performed more than once, the length dependence studies of this subunit need further repetition to confirm that this pattern is repeatable.

The θ subunit of TRiC is adjacent to actin nascent chains as short as 220 amino acids and as long as 371 amino acids. It is not adjacent to the actin nascent chain as early as the core subunits, but occurs at a longer chain length.

This might suggest that the actin nascent chain either moves close to the

θ subunit of TRiC as the nascent chain elongates or that it moves along the

surface of the subunit to a site where photocrosslinking to the θ subunit is

favorable. This also suggests that the actin nascent chain is moving or folding

between the lengths of 133 amino acids and 220 amino acids.

Both similarities and differences were found when the photocrosslinking

of actin and luciferase nascent chains to TRiC were compared. For example,

both nascent chains exhibited length dependencies in their photocrosslinking

targets, but the lengths at which photocrosslinking occurred to individual TRiC

subunits were different. Luciferase nascent chains photocrosslinked to TRiC

when the nascent chain was only 77 amino acids in length, while

photocrosslinks to actin nascent chains were not observed until the nascent

chain was 133 amino acids. Luciferase nascent chains as short as 77 amino

acids and as long as 232 amino acids were adjacent to the α, β and ϵ subunits

of TRiC (the core subunits). Photocrosslinking to the core subunits over almost

the entire length of the nascent chain and or nascent chain sub-domain was

observed for both actin and luciferase. Photocrosslinking of luciferase nascent

chains to the δ subunit of TRiC occurred at a nascent chain length of 92 amino

acids. The θ subunit of TRiC was also photocrosslinked at the luciferase

nascent chain length of 92 amino acids and continued until the nascent chain

was 232 amino acids in length. This suggests that as the nascent chain

lengthens from 77 to 92 amino acids, it moves adjacent to the δ and θ subunits

of TRiC and remains there until 164 and 232 amino acids have been synthesized, respectively.

The η subunit of TRiC is adjacent to the luciferase nascent chain when it is 125 amino acids in length, but moves away when the nascent chain lengthens to 164 amino acids. Photoadducts to the γ and ζ subunits were never observed. This suggests that the luciferase nascent chain either is not located near the γ or ζ subunit or that the interaction with these subunits is too fast to be detected with the experimental technique that was used. However, since actin nascent chains of 220 amino acids in length were observed to photocrosslink to the ζ subunit the later explanation seems unlikely. The difference in the length dependence of luciferase nascent chain photocrosslinking to different TRiC subunits reveals that the nascent chain must move relative to the subunits as the nascent chain elongates.

Fourth, prefoldin photocrosslinks to actin nascent chains, and co-immunoprecipitates with photoadduct bands containing TRiC and actin nascent chains. This suggests that prefoldin and TRiC form a complex on the actin nascent chain. Coimmunoprecipitation experiments performed with antibodies specific either for prefoldin 3 (figure 36) or the TRiC α subunit (McCallum et al., 2000) revealed that photoadduct bands containing actin nascent chains and prefoldin or actin nascent chains and TRiC subunits were recognized and bound by both antibodies, thereby indicating that prefoldin and TRiC were bound to the same actin nascent chain. Since a probe at position 68 in actin

nascent chains could photocrosslink to either prefoldin or TRiC (α, β and ϵ subunits), the possibility of TRiC and prefoldin competing for binding to the same nascent chain must be considered. As discussed in chapter V, the coimmunoprecipitation data strongly indicate that the nascent chain associates with two chaperonins simultaneously, and this in turn leads to several questions centered around both how and why.

When the length dependence of this interaction was observed it was found that prefoldin was adjacent to actin nascent chains as short as 177 amino acids and as long as 371 amino acids, while TRiC was adjacent to actin[68amb] when the nascent chain was only 133 amino acids in length. This result suggests that prefoldin interacts with the nascent chain after TRiC. While a lack of photocrosslinking does not demonstrate that prefoldin is absent, the close proximity of TRiC to the ribosomal tunnel exit site does create doubt about whether there is sufficient room for prefoldin to also bind. This order of interactions is the reverse of the model proposed by Vainberg and colleagues based on native gel analysis of radiolabeled actin being transferred from the complex shown to be prefoldin to the complex shown to be TRiC (Vainberg et al., 1998). When actin is 177 amino acids in length and a probe is at position 84, there is photocrosslinking to the TRiC α, β and ϵ subunits and there are 93 amino acids from the probe to the P-site in the ribosome. If TRiC were to move further way from the ribosome at this point, then there might be room for prefoldin to associate with the nascent chain between the ribosomal exit site

and TRiC. Since the crystal structure of archaeal prefoldin shows that it is about 85 Å high (Siegert et al., 2000), it seems that there is very little space for prefoldin to fit in between TRiC and the ribosome. In addition, evidence presented in the introduction suggested that the tips of the coiled-coils of the β-subunits of archaeal prefoldin are involved in folding the substrates that were tested (Siegert et al., 2000). For this reason one might expect that the tips of the coiled-coils would face towards the nascent chain and since the probe at position 68 can photocrosslink to either TRiC or prefoldin, prefoldin might be oriented with the tips of the coiled-coils near TRiC. A recent study with purified TRiC and purified prefoldin showed the formation of a complex with one TRiC complex capped by two prefoldin complexes to form a football shaped structure (Martin-Benito et al., 2002). Thus the formation of a complex between TRiC and prefoldin on actin nascent chain may prove to be somewhat like GroEL/ES forming a chamber for folding their substrate, but this is different in the sense that it is occurring co-translationally instead of post-translationally. In the cryo-EM structure of the TRiC/prefoldin complex there are two channels by which the nascent chain could be threaded through prefoldin and into the TRiC cavity (Martin-Benito, 2002). Thus, it seems very likely that prefoldin and TRiC are forming a complex on the actin nascent chain.

Fifth, TRiC is in very close proximity to the exit site of the ribosomal nascent chain tunnel. Actin nascent chains were observed to crosslink to the α, β and ε subunits of TRiC when a single probe was placed at position 84 in a

133-residue nascent chain. In this case there are only 49 amino acids between the probe and the P-site in the ribosome. Since the ribosomal nascent chain tunnel holds between 35-40 residues (Blobel and Sabatini, 1970; Malkin and Rich, 1967) the probe is located only 9-14 amino acids from the exit site of the ribosome. If the assumption is made that the 9-14 amino acids are in a fully-extended conformation with 3.5 Å between residues, then the probe is a maximum of 32-49 Å from the ribosome. (This distance may be significantly less because I have not done a high resolution mapping of all of the nascent chain lengths between 84 and 133 to determine when the probe at position 84 first photocrosslinks to a TRiC subunit.) Thus, TRiC is located close to the ribosomal exit site, especially if the probe at 84 is crosslinking to a TRiC subunit from inside the TRiC cavity. In fact, this close proximity raises the possibility that the TRiC entry site contacts the ribosomal exit site during co-translational folding of the nascent chain. Whether TRiC remains close to the ribosome as the nascent chain elongates is not known, but it will be interesting to see in future experiments.

A very interesting observation using the singly-labeled actin nascent chains was the lack of photocrosslinking observed at nascent chains shorter than 133 amino acids in length, even when the probe was positioned at residue 18. When the probe is located at position 18 of a 84mer actin nascent chain, there are 66 amino acids from the probe to the P-site of the ribosome. If we estimate conservatively that the C-terminal 40 amino acids are in the nascent

chain tunnel, there are 26 amino acids from the exit of the ribosomal tunnel to the probe (91Å of fully-extended polypeptide). Yet only the β subunit of TRiC was photocrosslinked to the actin 84 mer with a probe at residue 18. When the actin nascent chain was lengthened to 133 amino acids, then all 5 probe positions were found to crosslink to α, β and ε subunit of TRiC, even though the probe at position 84 was much closer (9 residues) to the exit site of the ribosome than was the probe at position 18 in the 84 mer. This suggests that the initial binding of TRiC to nascent actin requires a longer nascent chain than does TRiC binding later in the processing of actin. One possible explanation of this observation is that a specific sequence must emerge from the ribosome and be exposed to TRiC before TRiC will stably associate with the ribosome-bound nascent chain. Thus, we can conclude from these findings that TRiC is closely located to the exit site of the ribosome nascent chain tunnel.

Sixth, the presence or absence of ATP influences the photocrosslinking yields which, suggests that the ATP alters either the conformation of the subunits and /or their affinity for the nascent chain. Since it has been observed by cryo-EM and SAXS that TRiC (which has ATPase activity in each subunit (Kafri et al., 2001)) has a different conformation in the presence of ADP than in the presence of ATP (Llorca et al., 1998; Meyer et al., 2003), I investigated whether such a conformational change might affect photocrosslinking. After a 40 min translation, a time point when it was determined that the actin nascent chain of 371 amino acids had been synthesized (data not shown), apyrase was

added and a 5 min incubation was performed prior to photocrosslinking. While it was not determined chemically if all of the ATP had been hydrolyzed during this incubation, it can be assumed that a good portion of the ATP was hydrolyzed since differences in photocrosslinking were observed in identical samples that were split prior to apyrase addition or mock treatment.

We also do not know the nucleotide binding state of each of the TRiC subunits when photocrosslinking occurs. The apyrase addition was an attempt to shift all of the TRiC to the nucleotide-free state. Since there is a suggestion of negative cooperativity between the cis and trans ring of TRiC (Kafri et al., 2001), all the subunits of one ring might have ADP bound in each of the eight binding sites, while the other ring might have ATP bound in each of the sites. Recent SAXS experiments suggest that the apical loop which is thought to act as a lid closes when the trigonal-bipyramidal transition state analogue of ATP is bound and this confers an asymmetric shape to TRiC (Meyer et al., 2003). If this were the case, then the addition of apyrase would decrease the pool of free ATP such that ATP hydrolysis by the subunits of the chaperonin TRiC would then not lead to replacement with fresh ATP, but would leave the subunits in the nucleotide-free state.

The extent of actin nascent chain 220 mer photocrosslinking to the ε subunit of TRiC was much stronger in the absence of apyrase than in the presence, while 220 mer photocrosslinking to the θ subunit was more frequent in the presence of apyrase and there was no difference in photocrosslinking to

the δ subunit. However, there were differences observed for the δ subunit of TRiC at actin nascent chain lengths of 133 amino acids and 303 amino acids, and in both cases the intensity of the photoadduct band increased in the absence of apyrase. There are at least two different possible explanations for this variation in the dependence of photocrosslinking on ATP. One is that the subunit changes conformation in response to nucleotide binding and hence the actin nascent chain (and its photoreactive probe) has moved relative to that subunit. Alternatively, other chaperones with ATPase domains (such as Hsp 70 and Hsp 40) may interact with the nascent chains in an ATP-dependent manner and move the nascent chain within TRiC. However, in view of the close proximity of TRiC to the ribosome, I do not think that this second possibility is very likely. Although actin can bind ATP, examination of the actin crystal structure (figure 7) shows that ATP binds in the cleft that is formed by amino acids that have not yet been synthesized in a 220 mer and for this reason actin's nucleotide binding state was not taken into account. Therefore, subunits of TRiC photocrosslink to actin nascent chains to different extents in the presence or absence of apyrase. The exposure of actin nascent chains to, or their interaction with, individual TRiC subunits is therefore ATP-dependent.

The presence or absence of apyrase has a similar effect on the TRiC photocrosslinking to luciferase nascent chains because apyrase did not effect the presence or absence of photoadducts to a particular TRiC subunits, only the extent of photoadduct formation. Photoadducts were observed in the presence

or absence of apyrase, but only at luciferase nascent chain lengths of 92 and 125 was there a difference in the intensity of the photoadducts and in these cases, the photoadducts in the presence of apyrase were more intense than in the absence which argues that there must be movement be either the θ subunit of TRiC or the nascent chain.

An as-yet unidentified 105 kDa protein was found to be adjacent to and presumably bind to luciferase nascent chains as short as 77 amino acids and as long as 125 amino acids. This 105 kDa protein was photocrosslinked to the nascent chain by probes located at amino acids 5, 9, 28 and 31. It is therefore particularly interesting that no photocrosslinking was observed when probes were located at position 8. Thus, the 105 kDa protein must occupy a very precise position relative to the luciferase nascent chain and/or the N-terminal end of the nascent chain must fold into a specific conformation when it associates with the 105 kDa protein.

A model that incorporates all of the data presented here with regards to the actin nascent chain is shown in figure 42. The actin nascent chain when it is 133 amino acids in length is adjacent to the α, β, δ, and ϵ subunits of TRiC. As the nascent chain lengthens to 177 amino acids, prefoldin is now adjacent to amino acid 68 and stays there until the entire protein has been synthesized. At 220 amino acids in length, the nascent chain is now adjacent to two addition TRiC subunits (ζ and θ) and as the nascent chain lengthens to 303 amino acids, it is no longer near the ζ subunit but near the η subunit. Finally, when all but the

last four amino acids of actin have been synthesized, the nascent chain is no longer adjacent to the η subunit. Following the completion of translation, actin may remain bound to TRiC while folding is completed before the final native structure is completed. However, the steps between the release of actin from the ribosome and its folding into a native proteins are still largely unknown.

Figure 42. Model of the Environment Adjacent to the Actin Nascent Chain As It Emerges From the Ribosomal Tunnel.

In this cartoon model, the ribosome is represented in green and with the actin nascent chain is represented in blue. TRiC is represented by the labeled subunits that are either white (not adjacent to the actin nascent chain), yellow (adjacent to the actin nascent chain) or red (the core subunits adjacent to the actin nascent chain). Prefoldin is represented by the multi-colored coil structure and mRNA is represented with the pink line. When the actin nascent chain is 133 amino acids in length, it is adjacent to the α, β, ε and δ subunits of TRiC. At a nascent chain length of 177, prefoldin is now adjacent to the actin nascent chain. In this cartoon, prefoldin is not placed on top of the TRiC ring closest to the ribosomal exit site in order that the subunits that are adjacent to the actin nascent chain can be more easily visualized. At a length of 220 amino acids, the actin nascent chain is adjacent to every TRiC subunit except γ and η. As the nascent chain grows to 303 amino acids, the nascent chain is no longer adjacent to the ζ subunit of TRiC, but is adjacent to the η subunit. Finally, at 371 amino acids (4 amino acids short of full-length actin), only TRiC α, β, δ, ε and θ are adjacent to the actin nascent chain. Following completion of translation of actin and its folding to the native conformation, it is released from TRiC/prefoldin. The order of subunits in the TRiC ring is assumed to be the same as that proposed by Liou and coworkers (Liou, 1997).

Actin 133mer **Prefoldin** **Actin 177mer** **Actin 220mer**

Actin 303mer **Actin 371mer**
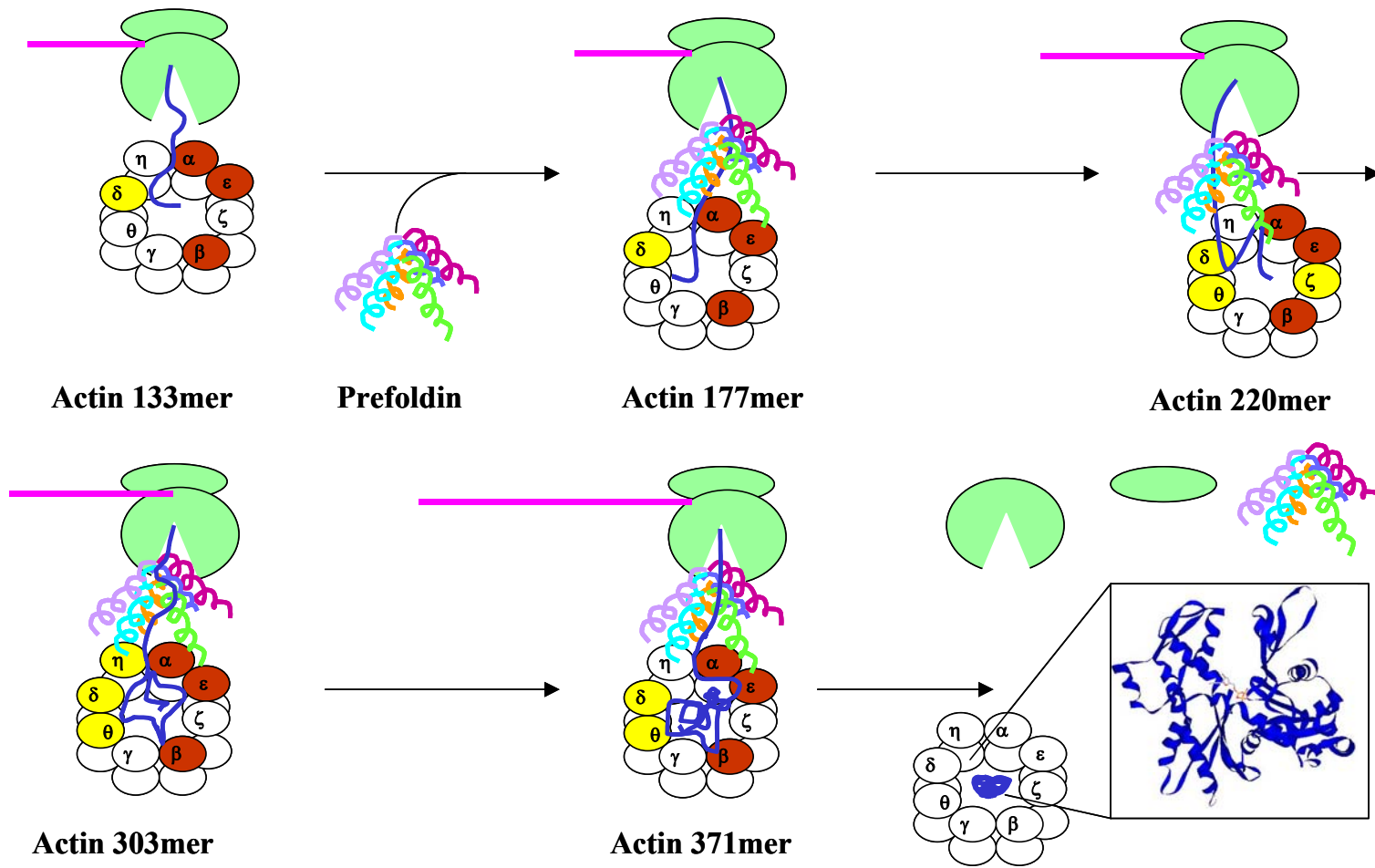
A model for the environment adjacent to the luciferase nascent chain as it emerges from the ribosomal tunnel is shown in figure 43. At a length of 77 amino acids, the nascent chain is adjacent to a 105 kDa protein and/or the α, β and ϵ subunits of TRiC. It remains to be determined whether the 105 kDa protein and TRiC bind to the nascent chain simultaneously or separately. However, in the cartoon (figure 43), I have arbitrarily chosen to shown TRiC and the 105 kDa protein interacting with the same nascent chain. As the nascent chain lengthens to 92 amino acids, the nascent chain is also adjacent to the δ and θ subunit of TRiC, and at 125 amino acids the nascent chain is adjacent to the η subunit as well. When the nascent chain reaches 164 amino acids in length, photocrosslinking to both the 105 kDa protein and the η subunit of TRiC disappear. When the luciferase nascent chain reaches 197 amino acids in length, the photoadducts to the δ subunit are no longer present. At 232 amino acids in length, only photoadducts to the core TRiC subunits are observed.

Figure 43. Model of the Environment Adjacent to the N-terminal Subdomain of the Luciferase Nascent Chain As It Emerges from the Ribosome

In this cartoon model, the ribosome is represented in green, and the luciferase nascent chain is shown in blue. TRiC is represented by the labeled subunits that are either white (not adjacent to the luciferase nascent chain), yellow (adjacent to the luciferase nascent chain) or red (the core subunits adjacent to the luciferase nascent chain). The 105 kDa protein is represented by the orange horseshoe shaped structure and mRNA is represented with the pink line. When the luciferase nascent chain is 77 amino acids, in length it is adjacent to the α, β, and ε subunits of TRiC. At a nascent chain length of 92 amino acids, the δ and θ subunits of TRiC are also now adjacent to the nascent chain. In this cartoon, the 105 kDa protein is not drawn on top of the TRiC ring closest to the ribosomal exit site in order that the subunits that are adjacent to the luciferase nascent chain can be more easily visualized. I have arbitrarily chosen the draw the 105 kDa protein on the same nascent chains as TRiC, but there is no evidence to show that this is or is not the case. At a length of 125 amino acids, the luciferase nascent chain is adjacent to every TRiC subunit except γ and ζ. When the nascent chain length reaches 164 amino acids, the nascent chain is no longer adjacent to the η subunit of TRiC and the 105 kDa protein is no longer adjacent to the luciferase nascent chain. At 197 amino acids in length, the luciferase nascent chain is no longer adjacent to the δ subunit of TRiC. Finally, at 232 amino acids, only TRiC α, β and ε are adjacent to the actin nascent chain. Following completion of translation of the first 232 amino acids, the N-terminal domain folds into a protease-resistant structure. The first 191 amino acids from the luciferase crystal structure (Conti et al., 1996) are shown in the inset. The order of the subunits is the TRiC ring is assumed to be the same as that proposed by Liou and coworkers (Liou, 1997).
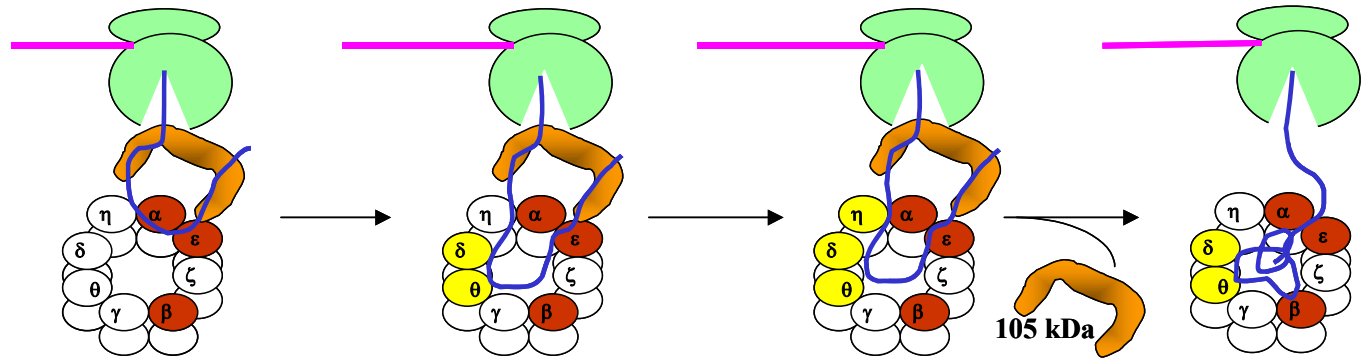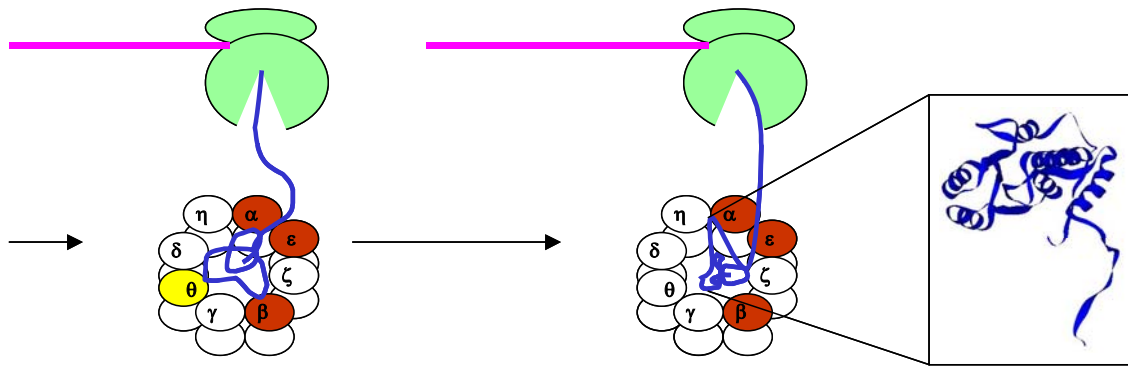
Luciferase 77mer **Luciferase 92mer** **Luciferase 125mer** **Luciferase 164mer**

105 kDa

Luciferase 197mer **Luciferase232mer**

The focus of the work in this dissertation examined actin and luciferase nascent chain interactions with TRiC, prefoldin and an unidentified 105 kDa protein. Placing these finding into the context of the cytosol, the environment that a nascent chain "sees" at it emerges from the ribosomal tunnel is a diverse mixture of proteins and protein complexes (figure 44). A list of some of the known proteins or protein complexes that have been shown to interact with nascent chains are discussed below.

The signal recognition particle (SRP) is known to bind free ribosomes, and to photocrosslink to the signal sequence of secretory proteins (Flanagan et al., 2003). If a ribosome is translating a cytosolic protein does SRP leave that ribosome to look for one that is translating a nascent chain with a signal sequence, or does TRiC or one of the other complexes compete with SRP for binding to the nascent chain? Another possible scenario is the selection of mRNAs that encode secretory proteins by ribosomes with bound SRP. This last possibility would involve a great deal of communication between SRP, the ribosome and the mRNA that it was going to translate and seems unlikely.

The nascent chain associated complex (NAC) has been shown to photocrosslink to cytosolic proteins as they emerge from the ribosomal tunnel (Beatrix et al., 2000). Do TRiC, prefoldin and/or the 105 kDa protein compete with NAC for binding to nascent chains?

Finally, how does Hsp70/Hsp40 fit into this picture? Previous work by Frydman and coworkers showed that Hsp70/Hsp40 interacted with nascent
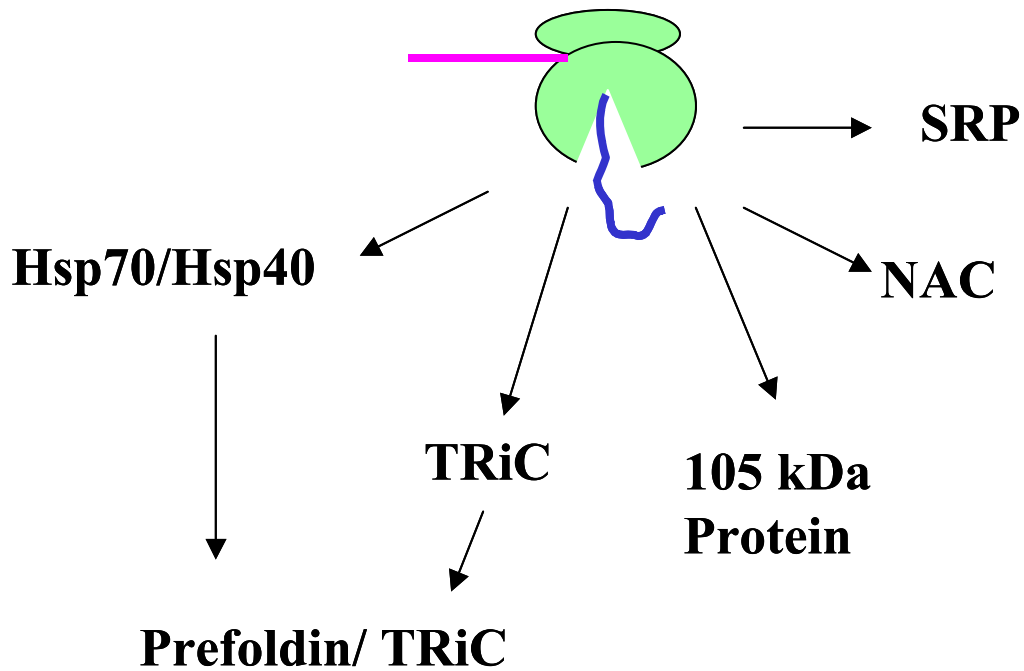
Figure 44. Multiple Options for Nascent Chain Interactions with Cytoplasmic Species

In this cartoon the ribosome is represented in green, with the nascent chain represented in blue. NAC refers to the nascent chain associated complex. SRP refers to the signal recognition particle.

chains prior to TRiC (Frydman et al., 1994). Is this the reason that in actin nascent chains of 84 amino acids in length, photocrosslinking was not observed to the majority of TRiC subunits? Was Hsp70/Hsp40 interacting with the extreme N-terminus of the actin nascent chain until TRiC interacted?

A great many questions arise from examining the results of this dissertation in the context of the whole cytosolic environment. It will be exciting to see what the mechanism(s) for cytosolic protein or protein complex recognition of different nascent chains is/are.

REFERENCES

Anfinsen, C. B. (1973). Principles that govern the folding of protein chains. Science *181*, 223-230.

Ashcroft, A. E., Brinker, A., Coyle, J. E., Weber, F., Kaiser, M., Moroder, L., Parsons, M. R., Jager, J., Hartl, U. F., Hayer-Hartl, M., and Radford, S. E. (2002). Structural plasticity and noncovalent substrate binding in the GroEL apical domain. A study using electrospray ionization mass spectrometry and fluorescence binding studies. J. Biol. Chem. *277*, 33115-33126.

Barraclough, R. A. and Ellis., R. J. (1980). Protein synthesis in chloroplasts IX. Assembly of newly synthesized large subunits into ribulose bisphosphate carboxylase in isolated intact pea chloroplasts. Biochem. Biophys. Acta *608*, 19-31.

Barzilai, A., Zilkha-Falb, R., Daily, D., Stern, N., Offen, D., Ziv, I., Melamed, E., and Shirvan, A. (2000). The molecular mechanism of dopamine-induced apoptosis: identification and characterization of genes that mediate dopamine toxicity. Journal of Neural Transmission Supplementum, 59-76.

Beatrix, B., Sakai, H., and Wiedmann, M. (2000). The alpha and beta subunit of the nascent polypeptide-associated complex have distinct functions. J. Biol. Chem. *275*, 37838-37845.

Blobel, G., and Sabatini, D. D. (1970). Controlled proteolysis of nascent polypeptides in rat liver cell fractions. I. Location of the polypeptides within ribosomes. J. Cell Biol. *45*, 130-145.

Braig, K., Otwinowski, Z., Hegde, R., Boisvert, D. C., Joachimiak, A., Horwich, A. L., and Sigler, P. B. (1994). The crystal structure of the bacterial chaperonin GroEL at 2.8 A. Nature *371*, 578-586.

Brinker, A., Pfeifer, G., Kerner, M.J., Naylor, D.J., Hartl, F.U., and Hayer-Hartl, M. (2001). Dual function of protein confinement in chaperonin-assisted protein folding. Cell *107*, 223-233.

Caspar, D. L. D., and Klug, A. (1962). Physical principles in the construction of regular viruses. Cold Spring Harbor Symp Quant Biol *27*, 1-24.

Chaudhuri, T. K., Farr, G. W., Fenton, W. A., Rospert, S. and Horwich, A. L. (2001). GroEL/GroES-mediated folding of a protein too large to be encapsulated. Cell *107*, 235-246.

Chen, L., and Sigler, P. B. (1999). The crystal structure of a GroEL/peptide complex: plasticity as a basis for substrate diversity. Cell *99*, 757-768.

Chen, S., Roseman, A. M., Hunter, A. S., Wood, S. P., Burston, S. G., Ranson, N. A., Clarke, A. R., and Saibil, H. R. (1994). Location of a folding protein and shape changes in GroEL-GroES complexes imaged by cryo-electron microscopy. Nature *371*, 261-264.

Conti, E., Franks, N. P., and Brick, P. (1996). Crystal structure of firefly luciferase throws light on a superfamily of adenylate-forming enzymes. Structure *4*, 287-298.

Coyle, J. E., Texter, F. L., Ashcroft, A. E., Masselos, D., Robinson, C. V., and Radford, S. E. (1999). GroEL accelerates the refolding of hen lysozyme without changing its folding mechanism. Nat. Struct. Biol. *6*, 683-690.

Crowley, K. S., Liao, S., Worrell, V. E., Reinhart, G. D., and Johnson, A. E. (1994). Secretory proteins move through the endoplasmic reticulum membrane via an aqueous, gated pore. Cell *78*, 461-471.

Crowley, K. S., Reinhart, G. D., and Johnson, A. E. (1993). The signal sequence moves through a ribosomal tunnel into a noncytoplasmic aqueous environment at the ER membrane early in translocation. Cell *73*, 1101-1115.

Ditzel, L., Lowe, J., Stock, D., Stetter, K. O., Huber, H., Huber, R., and Steinbacher, S. (1998). Crystal structure of the thermosome, the archaeal chaperonin and homolog of CCT. Cell *93*, 125-138.

Do, H., Falcone, D., Lin, J., Andrews, D. W. and Johnson, A. E. (1996). The cotranslational integration of membrane proteins into the phospholipid bilayer is a multistep process. Cell *85*, 369-378.

Dobrzynski, J. K., Sternlicht, M. L., Farr, G. W., and Sternlicht, H. (1996). Newly-synthesized beta-tubulin demonstrates domain-specific interactions with the cytosolic chaperonin. Biochemistry *35*, 15870-15882.

Dobrzynski, J. K., Sternlicht, M. L., Peng, I., Farr, G. W., and Sternlicht, H. (2000). Evidence that beta-tubulin induces a conformation change in the cytosolic chaperonin which stabilizes binding: implications for the mechanism of action. Biochemistry *39*, 3988-4003.

Ellis, M. J., Knapp, S., Koeck, P. J. B., Fakoor-Biniaz, Z., Ladenstein, R. and Hebert, H. (1998). Two-dimensional crystallization of the chaperonin TF55 from the hyperthermophilic archaeon Sulfolobus solfaterius. J. Struct. Biol. *123*, 30-36.

Ellis, R. J. (1990a). The molecular chaperone concept. Seminars in Cell Biology *1*, 1-9.

Ellis, R. J. (1990b). Molecular chaperones: the plant connection. Science *250*, 378-379.

Ellis, R. J. (1993). The general concept of molecular chaperones. In "Molecular Chaperones" (R. J. Ellis, R. A. Lasky and G. H. Lorimer, eds.), 1-5 Chapman and Hall, London (published for the Royal Society).

Ellis, R. J., and Hemmingsen, S. M. (1989). Molecular chaperones: proteins essential for the biogenesis of some macromolecular structures. Trends Biochem. Sci. *14*, 339-342.

Feldman, D. E., Thulasiraman, V., Ferreyra, R. G., and Frydman, J. (1999). Formation of the VHL-Elongin BC tumor suppressor complex is mediated by the chaperonin TRiC. Mol. Cell *4*, 1051-1061.

Flanagan, J. J., Chen, J. C., Miao, Y., Shao, Y., Lin, J., Bock, P. E., and Johnson, A. E. (2003). SRP binds to ribosome-bound signal sequences with fluorescence-detected subnanomolar affinity that does not diminish as the nascent chain lengthens. J. Biol. Chem. *278,*18628-18637.

Frydman, J. (2001). Folding of newly translated proteins in vivo: the role of molecular chaperones. Annu. Rev. Biochem. *70*, 603-647.

Frydman, J., Erdjument-Bromage, H., Tempst, P., and Hartl, F. U. (1999). Co-translational domain folding as the structural basis for the rapid de novo folding of firefly luciferase. Nat. Struct. Biol. *6*, 697-705.

Frydman, J., and Hartl, F. U. (1996). Principles of chaperone-assisted protein folding: differences between in vitro and in vivo mechanisms. Science *272*, 1497-1502.

Frydman, J., Nimmesgern, E., Erdjument-Bromage, H., Wall, J. S., Tempst, P., and Hartl, F. U. (1992). Function in protein folding of TRiC, a cytosolic ring complex containing TCP-1 and structurally related subunits. EMBO J. *11*, 4767-4778.

Frydman, J., Nimmesgern, E., Ohtsuka, K., and Hartl, F. U. (1994). Folding of nascent polypeptide chains in a high molecular mass assembly with molecular chaperones. Nature *370*, 111-117.

Gao, Y., Thomas, J. O., Chow, R. L., Lee, G. H., and Cowan, N. J. (1992). A cytoplasmic chaperonin that catalyzes beta-actin folding. Cell *69*, 1043-1050.

Geissler, S., Siegers, K., and Schiebel, E. (1998). A novel protein complex promoting formation of functional alpha- and gamma-tubulin. EMBO J. *17*, 952-966.

Gupta, R. S. (1990). Sequence and structural homology between a mouse T-complex protein TCP-1 and the 'chaperonin' family of bacterial (GroEL, 60-65 kDa heat shock antigen) and eukaryotic proteins. Biochemistry International *20*, 833-841.

Gutsche, I., Holzinger, J., Rossle, M., Heumann, H., Baumeister, W., and May, R. P. (2000a). Conformational rearrangements of an archaeal chaperonin upon ATPase cycling. Curr. Biol. *10*, 405-408.

Gutsche, I., Mihalache, O., and Baumeister, W. (2000b). ATPase cycle of an archaeal chaperonin. J. Mol. Biol. *300*, 187-196.

Hansen, W. J., Cowan, N. J., and Welch, W. J. (1999). Prefoldin-nascent chain complexes in the folding of cytoskeletal proteins. J. Cell Biol. *145*, 265-277.

Hansen, W. J., Ohh, M., Moslehi, J., Kondo, K., Kaelin, W. G., and Welch, W. J. (2002). Diverse effects of mutations in exon II of the von Hippel-Lindau (VHL) tumor suppressor gene on the interaction of pVHL with the cytosolic chaperonin and pVHL-dependent ubiquitin ligase activity. Mol. Cell Biol. *22*, 1947-1960.

Hendrick, J. P., and Hartl, F. U. (1993). Molecular chaperone functions of heat-shock proteins. Annu. Rev. Biochem. *62*, 349-384.

Hong, S., Choi, G., Park, S., Chung, A. S., Hunter, E., and Rhee, S. S. (2001). Type D retrovirus Gag polyprotein interacts with the cytosolic chaperonin TRiC. J. Virology *75*, 2526-2534.

Houry, W. A., Frishman, D., Eckerskorn, C., Lottspeich, F., and Hartl, F. U. (1999). Identification of in vivo substrates of the chaperonin GroEL. Nature *402*, 147-154.

Hynes, G., Sutton, C. W., U, S., and Willison, K. R. (1996). Peptide mass fingerprinting of chaperonin-containing TCP-1 (CCT) and copurifying proteins. FASEB J. *10*, 137-147.

Hynes, G. M., and Willison, K. R. (2000). Individual subunits of the eukaryotic cytosolic chaperonin mediate interactions with binding sites located on subdomains of beta-actin. J. of Biol. Chem. *275*, 18985-18994.

Ivan, M., and Kaelin, W. G., Jr. (2001). The von Hippel-Lindau tumor suppressor protein. Curr. Opin. Genet. Dev. *11*, 27-34.

Jackson, R. J., and Hunt, T. (1983). Preparation and use of nuclease-treated rabbit reticulocyte lysates for the translation of eukaryotic messenger RNA. Methods Enzymol. *96*, 50-74.

Johnson, A. E., Adkins, H. J., Matthews, E. A., and Cantor, C. R. (1982). Distance moved by transfer RNA during translocation from the A site to the P site on the ribosome. J. Mol. Biol. *156*, 113-140.

Johnson, A. E., Woodard, W.R., Hebert, E., and Menninger, J.R. (1976). Nε–acetyllysine transfer ribonucleic acid: a biologically active analog of aminoacyl transfer ribonucleic acids. Biochemistry *15*, 569-575.

Kafri, G., and Horovitz, A. (2003). Transient kinetic analysis of ATP-induced allosteric transitions in the eukaryotic chaperonin containing TCP-1. J. Mol. Biol. *326*, 981-987.

Kafri, G., Willison, K. R., and Horovitz, A. (2001). Nested allosteric interactions in the cytoplasmic chaperonin containing TCP-1. Protein Sci. *10*, 445-449.

Kashuba, E., Pokrovskaja, K., Klein, G., and Szekely, L. (1999). Epstein-Barr virus-encoded nuclear protein EBNA-3 interacts with the epsilon-subunit of the T-complex protein 1 chaperonin complex. J. Hum. Vir. *2*, 33-37.

Klumpp, M., Baumeister, W., and Essen, L. O. (1997). Structure of the substrate binding domain of the thermosome, an archaeal group II chaperonin. Cell *91*, 263-270.

Krieg, U. C., Johnson, A. E. and Walter,P. (1989). Protein translocation across the endoplasmic reticulum membrane: identification by photocross-linking of a 39-kD integral membrane glycoprotein as part of a putative translocation tunnel. J. Cell Biol. *109*, 2033-2043.

Krieg, U. C., Walter, P. and Johnson, A. E. (1986). Photocrosslinking of the signal sequence of nascent preprolactin to the 54-kilodalton polypeptide of the signal recognition particle. Proc.Natl. Acad. Sci. USA *83*, 8604-8608.

Kubota, H., Hynes, G., Carne, A., Ashworth, A., and Willison, K. (1994). Identification of six Tcp-1-related genes encoding divergent subunits of the TCP-1-containing chaperonin. Curr. Biol. *4*, 89-99.

Kubota, H., Hynes, G., and Willison, K. (1995a). The chaperonin containing t-complex polypeptide 1 (TCP-1). Multisubunit machinery assisting in protein folding and assembly in the eukaryotic cytosol. Eur. J. Biochem. *230*, 3-16.

Kubota, H., Hynes, G., and Willison, K. (1995b). The eighth Cct gene, Cctq, encoding the theta subunit of the cytosolic chaperonin containing TCP-1. Gene *154*, 231-236.

Kubota, H., Hynes, G. M., Kerr, S. M., and Willison, K. R. (1997). Tissue-specific subunit of the mouse cytosolic chaperonin-containing TCP-1. FEBS Lett. *402*, 53-56.

Kusmierczyk, A. R. M. J. (2001). Chaperonins-keeping a lid on folding proteins. FEBS Lett. *505*, 343-347.

Large, A. T., Kovacs, E., and Lund, P. A. (2002). Properties of the chaperonin complex from the halophilic archaeon Haloferax volcanii. FEBS Lett. *532*, 309-312.

Leroux, M. R., Fandrich, M., Klunker, D., Siegers, K., Lupas, A. N., Brown, J. R., Schiebel, E., Dobson, C. M., and Hartl, F. U. (1999). MtGimC, a novel archaeal chaperone related to the eukaryotic chaperonin cofactor GimC/prefoldin. EMBO J. *18*, 6730-6743.

Lewis, V. A., Hynes, G. M., Zheng, D., Saibil, H., and Willison, K. (1992). T-complex polypeptide-1 is a subunit of a heteromeric particle in the eukaryotic cytosol. Nature *358*, 249-252.

Liao, S., Lin, J., Do, H. and Johnson A. E. (1997). Both lumenal and cytosolic gating of the aqueous ER translocon pore are regulated from inside the ribosome during membrane protein integration. Cell *90*, 31-41.

Lingappa, J. R., Martin, R. L., Wong, M. L., Ganem, D., Welch, W. J., and Lingappa, V. R. (1994). A eukaryotic cytosolic chaperonin is associated with a high molecular weight intermediate in the assembly of hepatitis B virus capsid, a multimeric particle. J. Cell Biol. *125*, 99-111.

Liou, A. K., and Willison, K.R. (1997). Elucidation of the subunit orientation in CCT (chaperonin containing TCP1) from the subunit composition of CCT micro-complexes. EMBO J. *16*, 4311-4316.

Llorca, O., Martin-Benito, J., Gomez-Puertas, P., Ritco-Vonsovici, M., Willison, K. R., Carrascosa, J. L., and Valpuesta, J. M. (2001). Analysis of the interaction between the eukaryotic chaperonin CCT and its substrates actin and tubulin. J. Struct. Biol. *135*, 205-218.

Llorca, O., Martin-Benito, J., Ritco-Vonsovici, M., Grantham, J., Hynes, G. M., Willison, K. R., Carrascosa, J. L., and Valpuesta, J. M. (2000). Eukaryotic chaperonin CCT stabilizes actin and tubulin folding intermediates in open quasi-native conformations. EMBO J. *19*, 5971-5979.

Llorca, O., McCormack, E. A., Hynes, G., Grantham, J., Cordell, J., Carrascosa, J. L., Willison, K. R., Fernandez, J. J., and Valpuesta, J. M. (1999a). Eukaryotic type II chaperonin CCT interacts with actin through specific subunits. Nature *402*, 693-696.

Llorca, O., Smyth, M. G., Carrascosa, J. L., Willison, K. R., Radermacher, M., Steinbacher, S., and Valpuesta, J. M. (1999b). 3D reconstruction of the ATP-bound form of CCT reveals the asymmetric folding conformation of a type II chaperonin. Nat. Struct. Biol. *6*, 639-642.

Llorca, O., Smyth, M. G., Marco, S., Carrascosa, J. L., Willison, K. R., and Valpuesta, J. M. (1998). ATP binding induces large conformational changes in the apical and equatorial domains of the eukaryotic chaperonin containing TCP-1 complex. J. Biol. Chem. *273*, 10091-10094.

Llorca, O., Martin-Benito, J., Grantham, J., Ritco-Vonsovici, M., Willison, K. R., Carrascosa, J. L. and Valpuesta,J. M. (2001). The 'sequential allosteric ring' mechanism in the eukaryotic chaperonin-assisted folding of actin and tubulin. EMBO J. *20*, 4065-4075.

Malkin, L. I., and Rich, A. (1967). Partial resistance of nascent polypeptide chains to proteolytic digestion due to ribosomal shielding. J. Mol. Biol. *26*, 329-346.

Martin, J., Langer, T., Boteva, R., Schramel, A., Horwich, A. L., and Hartl, F. U. (1991). Chaperonin-mediated protein folding at the surface of groEL through a 'molten globule'-like intermediate. Nature *352*, 36-42.

Martin-Benito, J., Boskovic, J., Gomez-Puertas, P., Carrascosa, J.L., Simons, C. T., Lewis, S. A., Bartolini, F., Cowan, N. J. and Valpuesta J. M. (2002). Structure of eukaryotic prefoldin and of its complexes with unfolded actin and the cytosolic chaperonin CCT. EMBO J. *21*, 6377-6386.

McCallum, C. D., Do, H., Johnson, A. E., and Frydman, J. (2000). The interaction of the chaperonin tailless complex polypeptide 1 (TCP1) ring complex (TRiC) with ribosome-bound nascent chains examined using photo-cross-linking. J. Cell Biol. *149*, 591-602.

McCormack, E. A., Llorca, O., Carrascosa, J. L., Valpuesta, J. M., and Willison, K. R. (2001a). Point mutations in a hinge linking the small and large domains of beta-actin result in trapped folding intermediates bound to cytosolic chaperonin CCT. J. Struct. Biol. *135*, 198-204.

McCormack, E. A., Rohman, M. J., and Willison, K. R. (2001b). Mutational screen identifies critical amino acid residues of beta-actin mediating interaction between its folding intermediates and eukaryotic cytosolic chaperonin CCT. J. Struct. Biol. *135*, 185-197.

McCormick, P. J., Miao, Y., Shao, Y., Lin, J., and Johnson, A. E. (in press). Cotranslational protein integration into the ER membrane is mediated by the binding of nascent chains to translocon protiens. Mol. Cell

Melki, R., and Cowan, N. J. (1994). Facilitated folding of actins and tubulins occurs via a nucleotide-dependent interaction between cytoplasmic chaperonin and distinctive folding intermediates. Mol. Cell. Biol. *14*, 2895-2904.

Melki, R., Vainberg, I. E., Chow, R. L., and Cowan, N. J. (1993). Chaperonin-mediated folding of vertebrate actin-related protein and gamma-tubulin. J. Cell Biol. *122*, 1301-1310.

Meyer, A. S., Gillespie, J. R., Walther, D., Millet, I. S., Doniach, S., and Frydman, J. (2003). Closing the folding chamber of the eukaryotic chaperonin requires the transition state of ATP hydrolysis. Cell *113*, 369-381.

Nimmesgern, E., and Hartl, F. U. (1993). ATP-dependent protein refolding activity in reticulocyte lysate. Evidence for the participation of different chaperone components. FEBS Lett. *331*, 25-30.

Nitsch, M., Klumpp, M., Lupas, A., and Baumeister, W. (1997). The thermosome: alternating alpha and beta-subunits within the chaperonin of the archaeon Thermoplasma acidophilum. J. Mol. Biol. *267*, 142-149.

Oh, H. J., Chen, X., and Subjeck, J. R. (1997). Hsp110 protects heat-denatured proteins and confers cellular thermoresistance. J. Biol. Chem. *272*, 31636-31640.

Oh, H. J., Easton, D., Murawski, M., Kaneko, Y. and Subjeck, J. R. (1999). The chaperoning activity of Hsp110. J. Biol. Chem. *274*, 15712-15718.

Pappenberger, G., Wilsher, J. A., Roe, S. M., Counsell, D. J., Willison, K. R., and Pearl, L. H. (2002). Crystal structure of the CCTgamma apical domain: implications for substrate binding to the eukaryotic cytosolic chaperonin. J. Mol. Biol. *318*, 1367-1379.

Phipps, B. M., Hoffmann, A., Stetter, K. O., and Baumeister, W. (1991). A novel ATPase complex selectively accumulated upon heat shock is a major cellular component of thermophilic archaebacteria. EMBO J. *10*, 1711-1722.

Plath, K., and Rapoport, T. A. (2000). Spontaneous release of cytosolic proteins from posttranslational substrates before their transport into the endoplasmic reticulum. J. Cell Biol. *151*, 167-178.

Polevoda, B., and Sherman, F. (2000). Nalpha -terminal acetylation of eukaryotic proteins. J. Biol. Chem. *275*, 36479-36482.

Ranson, N. A., Farr, G. W., Roseman, A. M., Gowen, B., Fenton, W. Q., Horwich, A L., and Saibil, H. R. (2001). ATP-bound states of GroEL captured by cryo-electron microscopy. Cell *107*, 869-879.

Ritco-Vonsovici, M., and Willison, K. R. (2000). Defining the eukaryotic cytosolic chaperonin-binding sites in human tubulins. J. Mol. Biol. *304*, 81-98.

Rommelaere, H., De Neve, M., Melki, R., Vandekerckhove, J., and Ampe, C. (1999). The cytosolic class II chaperonin CCT recognizes delineated hydrophobic sequences in its target proteins. Biochemistry *38*, 3246-3257.

Rommelaere, H., De Neve, M., Neirynck, K., Peelaers, D., Wterschoot, D., Goethals, M., Fraeyman, N., Vandekerckhove, J. and Ampe, C. (2001). Prefoldin recognition motifs in the nonhomologous proteins of the actin and tubulin families. J. Biol. Chem. *276*, 41023-41028.

Rommelaere, H., Van Troys, M., Gao, Y., Melki, R., Cowan, N. J., Vandekerckhove, J., and Ampe, C. (1993). Eukaryotic cytosolic chaperonin contains t-complex polypeptide 1 and seven related subunits. Proc. Natl. Acad. Sci. USA *90*, 11975-11979.

Roobol, A., Grantham, J., Whitaker, H. C., and Carden, M. J. (1999). Disassembly of the cytosolic chaperonin in mammalian cell extracts at intracellular levels of K+ and ATP. J. Biol. Chem. *274*, 19220-19227.

Roseman, A. M., Chen, S., White, H., Braig, K., and Saibil, H. R. (1996). The chaperonin ATPase cycle: mechanism of allosteric switching and movements of substrate-binding domains in GroEL. Cell *87*, 241-251.

Rye, H. S., Roseman, A. M., Chen, S., Furtak, K., Fenton, W. A., Saibil, H. R., and Horwich, A. L. (1999). GroEL-GroES cycling: ATP and nonnative polypeptide direct alternation of folding-active rings. Cell *97*, 325-338.

Schoehn, G., Hayes, M., Cliff, M., Clarke, A. R., and Saibil, H. R. (2000a). Domain rotations between open, closed and bullet-shaped forms of the thermosome, an archaeal chaperonin. J. Mol. Biol. *301*, 323-332.

Schoehn, G., Quaite-Randall, E., Jimenez, J. L., Joachimiak, A., and Saibil, H. R. (2000b). Three conformations of an archaeal chaperonin, TF55 from Sulfolobus shibatae. J. Mol. Biol. *296*, 813-819.

Schwartz, G. J., Kittelberger, A. M., and Segel, G. B. (2000). Cloning of rabbit Cct6 and the distribution of the Cct complex in mammalian tissues. Experimental Nephrology *8*, 152-160.

Shtilerman, M., Lorimer, G. H., and Englander, S. W. (1999). Chaperonin function: folding by forced unfolding. Science *284*, 822-825.

Siegers, K., Waldmann, T., Leroux, M. R., Grein, K., Shevchenko, A., Schiebel, E., and Hartl, F. U. (1999). Compartmentation of protein folding in vivo: sequestration of non-native polypeptide by the chaperonin-GimC system. EMBO J. *18*, 75-84.

Siegert, R., Leroux, M. R., Scheufler, C., Hartl, F. U., and Moarefi, I. (2000). Structure of the molecular chaperone prefoldin: unique interaction of multiple coiled coil tentacles with unfolded proteins. Cell *103*, 621-632.

Silver, L. M., Artz, K., and Bennett, D. (1979). A major testicular cell protein specified by a mouse T/t complex gene. Cell *17*, 275-284.

Thrift, R. N., Andrews, D. W., Walter, P., and Johnson, A. E. (1991). A nascent membrane protein is located adjacent to ER membrane proteins throughout its integration and translation. J. Cell. Biol. *112*, 809-821.

Tilly, K., Murialdo, H., and Georgopoulos, C. (1981). Identification of a second Escherichia coli groE gene whose product is necessary for bacteriophage morphogenesis. Proc. Natl. Acad. Sci. USA *78*, 1629-1633.

Trent, J. D., Nimmesgern, E., Wall, J. S., Hartl, F. U., and Horwich, A. L. (1991). A molecular chaperone from a thermophilic archaebacterium is related to the eukaryotic protein t-complex polypeptide-1. Nature *354*, 490-493.

Ursic, D., Sedbrook, J. C., Himmel, K. L., and Culbertson, M. R. (1994). The essential yeast Tcp1 protein affects actin and microtubules. Mol. Biol. Cell *5*, 1065-1080.

Vainberg, I. E., Lewis, S. A., Rommelaere, H., Ampe, C., Vandekerckhove, J., Klein, H. L., and Cowan, N. J. (1998). Prefoldin, a chaperone that delivers unfolded proteins to cytosolic chaperonin. Cell *93*, 863-873.

Wang, J. D., and Weissman, J. S. (1999). Thinking outside the box: new insights into the mechanism of GroEL-mediated protein folding. Nat. Struct. Biol. *6*, 597-600.

Weissman, J. S. (2001). The ins and outs of GroEL-mediated protein folding. Mol. Cell, *8,*730-731.

Widmann, M., and Christen, P. (1995). Differential effects of molecular chaperones on refolding of homologous proteins. FEBS Lett. *377*, 481-484.

Yaffe, M. B., Farr, G. W., Miklos, D., Horwich, A. L., Sternlicht, M. L., and Sternlicht, H. (1992). TCP1 complex is a molecular chaperone in tubulin biogenesis. Nature *358*, 245-248.

Yokota, S., Hirata, D., Minota, S., Higashiyama, T., Kurimoto, M., Yanagi, H., Yura, T. and Kubota, H. (2000). Autoantibodies against Chaperonin CCT in human sera with rheumatic autoimmune diseases:comparison with antibodies against other Hsp60 family proteins. Cell Stress & Chaperones *5*, 337-346.

VITA

NAME: Stephanie Anne Etchells

EDUCATION: B.Sc.H. Biochemistry SSP
June 1996
Queen's University
Kingston, Ontario, Canada

Ph.D., Biochemistry
August 2003
Texas A&M University
College, Station, TX

PERMANENT ADDRESS: 721 Wideman Rd
Waterloo, Ontario, Canada
N2J 3Z4

EMAIL ADDRESS: etchells@netcom.ca